

## **General Disclaimer**

### **One or more of the Following Statements may affect this Document**

- This document has been reproduced from the best copy furnished by the organizational source. It is being released in the interest of making available as much information as possible.
- This document may contain data, which exceeds the sheet parameters. It was furnished in this condition by the organizational source and is the best copy available.
- This document may contain tone-on-tone or color graphs, charts and/or pictures, which have been reproduced in black and white.
- This document is paginated as submitted by the original source.
- Portions of this document are not fully legible due to the historical nature of some of the material. However, it is the best reproduction available from the original submission.



# DOCUMENTATION OF PROCEDURES FOR TEXTURAL/SPATIAL PATTERN RECOGNITION TECHNIQUES

NASA CR-

150995

FINAL REPORT

April 15, 1976

RSL Technical Report 278-1

**Robert M. Haralick**

**William F. Bryant**

(NASA-CR-150995) DOCUMENTATION OF  
PROCEDURES FOR TEXTURAL/SPATIAL PATTERN  
RECOGNITION TECHNIQUES Final Report (Kansas  
Univ. Center for Research, Inc.) 219 p HC  
\$7.75

N76-33598

Unclas  
07260

CSCI 02F G3/43

Funded by:

**NASA LYNDON B. JOHNSON SPACE CENTER**

**Contract NAS 9-14453**

**Houston, Texas 77058**



**THE UNIVERSITY OF KANSAS CENTER FOR RESEARCH, INC.**

2291 Irving Hill Drive—Campus West Lawrence, Kansas 66045





**THE UNIVERSITY OF KANSAS CENTER FOR RESEARCH, INC.**

2291 Irving Hill Drive—Campus West Lawrence, Kansas 66045

Documentation of Procedures for Textural/Spatial  
Pattern Recognition Techniques

Final Report

April 15, 1976

RSL Technical Report 278-1

Robert M. Haralick

William F. Bryant

Funded by:

NASA Lyndon B. Johnson Space Center  
Contract NAS 9-14453  
Houston, Texas 77058

## Table of Contents

	Page
List of Figures -----	ii
List of Tables -----	viii
I Introduction-----	1
I.1 Contingency Tables of Classification Results -----	4
II Table Look-Up Decision Rule-----	6
III Texture -----	14
III.1 Optical Processing Methods and Texture -----	15
III.2 Texture and Edges -----	16
III.3 Digital Transform Methods and Texture-----	17
III.4 Spatial Grey Tone Dependence: Co-occurrence-----	18
III.5 A Textural Transform-----	19
IV Spatial Pre-Processing -----	21
V Spatial Post-Processing -----	22
VI Spectral Analysis: Edit 6 -----	27
VII Spectral Analysis: Edit 9 -----	41
VIII Spectral Analysis: Edit 14 -----	53
IX Spectral Analysis: Edit 3 -----	67
X Spectral-Textural Analysis: Edit 6 -----	79
XI Spectral-Textural Analysis: Edit 9 -----	97
XII Spectral-Textural Analysis: Edit 14 -----	118
XIII Spectral-Textural Analysis: Edit 3 -----	123
XIV Conclusions -----	133
References -----	134
Appendix 1 - Textural Transform Programs -----	137

## List of Figures

Figure Number	Title	Page
II.1	Illustrates how quantizing can be done differently for each category.	12
II.2	Illustrates a graph of the number of reserved decisions versus probability threshold alpha.	13
V.1a	Illustrates the 4-neighborhood of a resolution cell.	23
V.1b	Illustrates the 8-neighborhood of a resolution cell.	23
V.2	Illustrates the effect of 4 and 8-filling on a single resolution cell.	24
V.3	Illustrates the relationship between set convexity and regularity.	26
VI.1	The .72 - .76 micrometer band	30
VI.2	The ground truth training data overlaid on the .72 - .76 micrometer band.	30
VI.3	The classification of the best two band pairs for alpha-beta thresholds of .3 and .021.	31
VI.4	The classified image of Figure VI.3 after a complete filling.	31
VI.5	The classified image of Figure VI.3 after 4-fill, 8-fill, 4-shrink, and then complete filling operations.	34
VI.6	The classified image of Figure VI.3 after 4-fill, 8-fill, 4-shrink, 8-shrink, and then complete filling operations.	34
VI.7	The classification of the three best band pairs for alpha-beta thresholds of .6 and .042.	36
VI.8	The classified image of Figure VI.7 after a complete filling.	36
VI.9	The classified image of Figure VI.8 after a 4-shrink operation and then a complete filling.	38
VI.10	The classified image of Figure VI.7 after 4-fill, 8-fill, 4-shrink, 8-shrink and complete filling operations.	38

List of Figures (Continued)

Figure Number	Title	Page
VII.1	The .72 - .76 micrometer band.	43
VII.2	The ground truth training data overlayed on the .72 - .76 micrometer band.	43
VII.3	The classification of the best two band pairs for alpha-beta thresholds of .3 and .021.	45
VII.4	The classified image of Figure VII.3 after a complete filling.	45
VII.5	The classified image of Figure VII.3 after 4-shrink and complete filling operations.	47
VII.6	A plot of the alpha thresholds versus number of reserved decisions.	48
VII.7	The classification of the three best band pairs for alpha-beta thresholds of .6 and .042.	50
VII.8	The classified image of Figure VII.7 after a complete filling.	50
VII.9	The classified image of Figure VII.7 after 4-fill, 8-fill, 4-shrink, 8-shrink and complete filling operations.	52
VIII.1	The .72 - .76 micrometer band.	55
VIII.2	The ground truth training data overlayed on the .72 - .76 micrometer band.	55
VIII.3	The classification of the three best band pairs for alpha-beta thresholds of .62 and .042.	58
VIII.4	The classified image of Figure VIII.3 after a complete filling.	58
VIII.5	The classified image of Figure VIII.4 after a 4-shrink operation.	60
VIII.6	The classified image of Figure VIII.5 after a complete filling.	60
VIII.7	The classified image of Figure VIII.3 after a 4-fill operation.	62
VIII.8	The classified image of Figure VIII.3 after 4- and 8-fill operations.	62

## List of Figures (Continued)

Figure Number	Title	Page
VIII.9	The classified image of Figure VIII.3 after 4-fill, 8-fill, and 4-shrink operations.	64
VIII.10	The classified image of Figure VIII.3 after 4-fill, 8-fill, 4-shrink and 8-shrink operations.	64
VIII.11	The classified image of Figure VIII.3 after 4-fill, 8-fill, 4-shrink, 8-shrink and complete filling operations.	66
IX.1	The .72 - .76 micrometer band.	69
IX.2	The ground truth training data overlayed on the .72 - .76 micrometer band.	69
IX.3	Number of reserved decisions as a function of probability threshold alpha for best 2 band pairs, spectral only for edit #3.	70
IX.4	Number of reserved decisions as a function of probability threshold alpha for best 3 band pairs, spectral only for edit #3.	73
IX.5	The classification of the three best band pairs for alpha-beta thresholds of .5 and .035.	75
IX.6	The classified image of Figure IX.5 after 4-fill and 8-fill operations.	75
IX.7	The classified image of Figure IX.5 after 4-fill, 8-fill, and 4-shrink operations.	77
IX.8	The classified image of Figure IX.5 after 4-fill, 8-fill, 4-shrink, 8-shrink and complete filling operations.	77
X.1	The classification of the best 2 band pairs for alpha-beta thresholds of .3 and .021.	84
X.2	The classified image of Figure X.1 after a complete filling.	84
X.3	The classified image of Figure X.1 after complete filling, 4-shrink, and complete filling operations.	86
X.4	The classified image of Figure X.1 after 4-fill, 8-fill, 4-shrink, 8-shrink and complete filling operations.	86

### List of Figures (Continued)

Figure Number	Title	Page
X.5	The classified image of Figure X.1 after 4-fill, 8-fill, 4-shrink, 8-shrink, 4-shrink, 8-shrink and complete filling operations.	88
X.6	The classification of the best 2 band pairs for alpha-beta thresholds of .5 and .035.	88
X.7	The classified image of Figure X.6 after a complete filling.	90
X.8	The classified image of Figure X.6 after complete filling, 4-shrink and complete filling operations.	90
X.9	The classified image of Figure X.6 after 4-fill, 8-fill, 4-shrink, 8-shrink, and complete filling operations.	92
X.10	The classified image of Figure X.6 after 4-fill, 8-fill, 4-shrink and complete filling operations.	92
X.11	The classification of the best 3 band pairs for alpha-beta thresholds of .7 and .049 after complete filling, 4-shrink, and complete filling operations.	95
X.12	The classification of the best 3 band pairs for alpha-beta thresholds of .7 and .049 after 4-fill, 8-fill, 4-shrink, 8-shrink, and complete filling operations.	95
XI.1	The .82 - .88 micrometer band used for the texture transform.	100
XI.2	Shows Figure XI.1 after a 2x2 rectangular convolution.	100
XI.3	Shows Figure XI.1 after a 3x3 rectangular convolution.	101
XI.4	The texture transform of Figure XI.1	101
XI.5	The texture transform of Figure XI.2	102
XI.6	The texture transform of Figure XI.3	102
XI.7	Shows Figure XI.4 after a 2x2 rectangular convolution.	103
XI.8	Shows Figure XI.5 after a 2x2 rectangular convolution.	103
XI.9	Shows Figure XI.6 after a 2x2 rectangular convolution.	104

List of Figures (Continued)

Figure Number	Title	Page
XI.10	Shows Figure XI.4 after a 3x3 rectangular convolution.	104
XI.11	Shows Figure XI.5 after a 3x3 rectangular convolution.	105
XI.12	Shows Figure XI.6 after a 3x3 rectangular convolution.	105
XI.13	Number of reserved decisions as a function of probability threshold alpha for best 2 band pairs with texture for edit #9.	106
XI.14	Number of reserved decisions as a function of probability threshold alpha for best 3 band pairs spectral only for edit #9.	107
XI.15	The classification of the best 3 band pairs for alpha-beta thresholds of .3 and .021.	109
XI.16	The classified image of Figure XI.15 after 4-shrink and complete filling operations.	109
XI.17	The classified image of Figure XI.15 after 4-fill, 4-shrink, and complete filling operations.	111
XI.18	The classification of the best 3 band pairs for alpha-beta thresholds of .7 and .049 after 4-fill, 8-fill, 4-shrink, 8-shrink, and complete filling operations.	111
XI.19	The classification of the best 2 band pairs for alpha-beta thresholds of .3 and .021.	115
XI.20	The classified image of Figure XI.19 after 4-fill, 4-shrink, and complete filling operations.	115
XI.21	The classified image of Figure XI.19 after 4-shrink and complete filling operations.	117
XII.1	The .82 - .88 micrometer band used for the texture transform.	119
XII.2	The texture transform of Figure XII.1 with a 3x3 rectangular convolution before the texture transform and a 3x3 rectangular convolution after.	119

List of Figures (Continued)

Figure Number	Title	Page
XII.3	The texture transform of Figure XII.1 with no rectangular convolution before the texture transform and a 3x3 rectangular convolution after.	120
XIII.1	Number of reserved decisions as a function of probability threshold alpha for best 2 band pairs with texture for edit #3.	125
XIII.2	Number of reserved decisions as a function of probability threshold alpha for best 3 band pairs with texture for edit #3.	127
XIII.3	The classification of the three best band pairs for alpha-beta thresholds of .6 and .042.	129
XIII.4	The classified image of Figure XIII.3 after 4-fill and 8-fill operations.	129
XIII.5	The classified image of Figure XIII.3 after 4-fill, 8-fill and 4-shrink operations.	132
XIII.6	The classified image of Figure XIII.3 after 4-fill, 8-fill, 4-shrink, 8-shrink, and complete filling operations.	132

## List of Tables

Table Number	Title	Page
I.1	The type (classes) and condition classes (sub-classes of forest features of interest in Sam Houston National Forest of Texas.	2
I.2	Summarizes the error rates obtained from the spectral versus the spectral-textural classification using 3 band pairs and no spatial post processing.	5
I.3	Summarizes the error rates obtained from the spectral versus the spectral-textural classification using 3 band pairs and spatial post processing.	5
VI.1	The contingency table of the best 2 band pairs for alpha-beta thresholds of .3 and .021.	32
VI.2	The contingency table of the best 2 band pairs after a complete filling.	32
VI.3	The contingency table of the best 2 band pairs after complete filling, 4-shrink, and complete filling operations.	33
VI.4	The contingency table of the best 2 band pairs after 4-fill, 8-fill, 4-shrink, and complete filling operations.	33
VI.5	The contingency table of the best 2 band pairs after 4-fill, 8-fill, 4-shrink, 8-shrink, and complete filling operations.	35
VI.6	The contingency table of the best 2 band pairs after 4-fill, 8-fill, 4-shrink, 8-shrink, 4-shrink, 8-shrink and complete filling operations.	35
VI.7	The contingency table for the best 3 band pairs for alpha-beta thresholds of .6 and .042.	37
VI.8	The contingency table of the best 3 band pairs after a complete filling.	37
VI.9	The contingency table of the best 3 band pairs after complete filling, 4-shrink, and complete filling operations.	39
VI.10	The contingency table of the best 3 band pairs after 4-fill, 8-fill, 4-shrink, 8-shrink, and complete filling operations.	39

List of Tables (Continued)

Table Number	Title	Page
VI.11	The contingency table of the best 3 band pairs after 4-fill, 8-fill, 4-shrink, 8-shrink, 4-shrink, 8-shrink and complete filling operations.	40
VII.1	The contingency table of the best 2 band pairs for alpha-beta thresholds of .3 and .021.	44
VII.2	The contingency table of the best 2 band pairs after a complete filling.	44
VII.3	The contingency table of the best 2 band pairs after complete filling, 4-shrink, and complete filling operations.	46
VII.4	The contingency table of the best 2 band pairs after 4-shrink, and complete filling operations.	46
VII.5	The contingency table of the best 3 band pairs for alpha-beta thresholds of .6 and .042.	49
VII.6	The contingency table of the best 3 band pairs after a complete filling.	49
VII.7	The contingency table of the best 3 band pairs after 4-fill, 8-fill, 4-shrink, 8-shrink, and complete filling operations.	51
VIII.1	The contingency table of the best 2 band pairs for alpha-beta thresholds of .3 and .021.	56
VIII.2	The contingency table of the best 2 band pairs after 4-fill, 8-fill, 4-shrink, 8-shrink, and complete filling operations.	56
VIII.3	The contingency table of the best 3 band pairs for alpha-beta thresholds of .6 and .042.	57
VIII.4	The contingency table of the best 3 band pairs after a complete filling.	57
VIII.5	The contingency table of the best 3 band pairs after complete filling and 4-shrink operations.	59
VIII.6	The contingency table of the best 3 band pairs after complete filling, 4-shrink and complete filling operations.	59
VIII.7	The contingency table of the best 3 band pairs after a 4-fill operation.	61
VIII.8	The contingency table of the best 3 band pairs after 4-fill, and 8-fill operations.	61

List of Tables (Continued)

Table Number	Title	Page
VIII.9	The contingency table of the best 3 band pairs after 4-fill, 8-fill and 4-shrink operations.	63
VIII.10	The contingency table of the best 3 band pairs after 4-fill, 8-fill, 4-shrink, and 8-shrink operations.	63
VIII.11	The contingency table of the best 3 band pairs after 4-fill, 8-fill, 4-shrink, 8-shrink and complete filling operations.	65
IX.1	The contingency table of the best 2 band pairs for alpha-beta thresholds of .3 and .021.	61
IX.2	The contingency table of the best 2 band pairs for alpha-beta thresholds of .4 and .028.	71
IX.3	The contingency table of the best 2 band pairs for alpha-beta thresholds of .5 and .035.	72
IX.4	The contingency table of the best 2 band pairs for alpha-beta thresholds of .5 and .035 after a complete filling.	72
IX.5	The contingency table of the best 3 band pairs for alpha-beta thresholds of .5 and .035.	74
IX.6	The contingency table of the best 3 band pairs after 4-fill and 8-fill operations.	74
IX.7	The contingency table of the best 3 band pairs after 4-fill, 8-fill and 4-shrink operations.	76
IX.8	The contingency table of the best 3 band pairs after 4-fill, 8-fill, 4-shrink, 8-shrink, and complete filling operations.	76
IX.9	Contingency table created by combining subclass types of the same class.	78
X.1	The contingency table of the best 2 band pairs for alpha-beta thresholds of .3 and .021.	83
X.2	The contingency table of the best 2 band pairs for alpha-beta thresholds of .3 and .021 after a complete filling.	83

List of Tables (Continued)

Table Number	Title	Page
X.3	The contingency table of the best 2 band pairs for alpha-beta thresholds of .3 and .021 after complete filling, 4-shrink, and complete filling operations.	85
X.4	The contingency table of the best 2 band pairs for alpha-beta thresholds of .3 and .021 after 4-fill, 8-fill, 4-shrink, 8-shrink, and complete filling operations.	85
X.5	The contingency table of the best 2 band pairs for alpha-beta thresholds of .3 and .021 after 4-fill, 8-fill, 4-shrink, 8-shrink, 4-shrink, 8-shrink, and complete filling operations.	87
X.6	The contingency table of the best 2 band pairs for alpha-beta thresholds of .5 and .035.	87
X.7	The contingency table of the best 2 band pairs for alpha-beta thresholds of .5 and .035 after a complete filling.	89
X.8	The contingency table of the best 2 band pairs for alpha-beta thresholds of .5 and .035 after complete filling, 4-shrink, and complete filling operations.	89
X.9	The contingency table of the best 2 band pairs for alpha-beta thresholds of .5 and .035 after 4-fill, 8-fill, 4-shrink, 8-shrink, and complete filling operations.	91
X.10	The contingency table of the best 2 band pairs for alpha-beta thresholds of .5 and .035 after 4-fill, 8-fill, 4-shrink, and complete filling operations.	91
X.11	The contingency table of the best 3 band pairs for alpha-beta thresholds of .7 and .049.	93
X.12	The contingency table of the best 3 band pairs after a complete filling.	93
X.13	The contingency table of the best 3 band pairs after 4-fill, 8-fill, 4-shrink, 8-shrink and complete filling operations.	94
X.15	The contingency table of the best 3 band pairs after 4-fill, 8-fill, 4-shrink, 8-shrink, 4-shrink 8-shrink, and complete filling operations.	96

List of Tables (Continued)

Table Number	Title	Page
XI.1	The contingency table of the best 3 band pairs for alpha-beta thresholds of .3 and .021.	108
XI.2	The contingency table of the best 3 band pairs for alpha-beta thresholds of .3 and .021 after 4-shrink and complete filling operations.	108
XI.3	The contingency table of the best 3 band pairs for alpha-beta thresholds of .3 and .021 after 4-fill, 4-shrink and complete filling operations.	110
XI.4	The contingency table of the best 3 band pairs for alpha-beta thresholds of .6 and .042.	110
XI.5	The contingency table of the best 3 band pairs for alpha-beta thresholds of .7 and .049.	112
XI.6	The contingency table of the best 3 band pairs for alpha-beta thresholds of .8 and .063.	112
XI.7	The contingency table of the best 3 band pairs for alpha-beta thresholds of .7 and .049 after a complete filling.	113
XI.8	The contingency table of the best 3 band pairs for alpha-beta thresholds of .7 and .049 after 4-fill, 8-fill, 4-shrink, 8-shrink, and complete filling operations.	113
XI.9	The contingency table of the best 2 band pairs for alpha-beta thresholds of .3 and .021.	114
XI.10	The contingency table of the best 2 band pairs after 4-fill, 4-shrink, and complete filling operations.	114
XI.11	The contingency table of the best 2 band pairs after 4-shrink and complete filling operations.	116
XII.1	The contingency table of the best 2 band pairs for alpha-beta thresholds of .3 and .021.	121
XII.2	The contingency table of the best 2 band pairs after 4-fill, 8-fill, 4-shrink, and 8-shrink operations.	121
XII.3	The contingency table of the best 2 band pairs after 4-fill, 8-fill, 4-shrink, 8-shrink and complete filling operations.	122

List of Tables (Continued)

Table Number	Title	Page
XIII.1	The contingency table of the best 2 band pairs for alpha-beta thresholds of .5 and .035.	126
XIII.2	The contingency table of the best 2 band pairs after 4-fill, 8-fill, 4-shrink, 8-shrink and complete filling operations.	126
XIII.3	The contingency table of the best 3 band pairs for alpha-beta thresholds of .6 and .042.	128
XIII.4	The contingency table of the best 3 band pairs after 4-fill, and 8-fill operations.	128
XIII.5	The contingency table of the best 3 band pairs after 4-fill, 8-fill, and 4-shrink operations.	130
XIII.6	The contingency table of the best 3 band pairs after 4-fill, 8-fill, 4-shrink and 8-shrink operations.	130
XIII.7	The contingency table of the best 3 band pairs after 4-fill, 8-fill, 4-shrink, 8-shrink and complete filling operations.	131

## I Introduction

This research was undertaken in an effort to aid the Forestry Application Project on Timber Resources. Mission M230 of the C-130 aircraft was flown over the Sam Houston National Forest on March 21, 1973 at 10,000 feet altitude. The Bendix 24 channel multispectral scanner collected the data. Four forest scenes of this data set were selected for study. They were edits 3, 6, 9, and 14. The categories of timber classes and subclasses are shown in Table I.1.

The application oriented research was to apply and document the capability of existing textural and spatial automatic processing techniques at the University of Kansas to classify the MSS imagery into specified timber categories. The ground truth for the study was supplied by the Forestry Applications Project.

Over a hundred classification experiments were performed on this data using feature selected from the spectral bands and a textural transform band. The textural transform band is an image whose resolution cells have grey tone intensities which indicate one parameter of local neighborhood texture. The textural transform concept is discussed in Section III. The classification was done by equal interval quantizing the images to 32 levels and using a non-parametric table look-up rule discussed in Section II. The various spatial pre- and post-processing options are discussed in Sections IV and V. Sections VI through IX discuss the results using only spectral features. Sections X through XIII discuss the combined spectral textural results.

The results indicate that

- (1) spatial post-processing a classified image can cut the classification error to  $1/2$  or  $1/3$  of its initial value.
- (2) spatial post-processing the classified image using combined spectral and textural features produces a resulting image with less error than post-processing a classified image using only spectral features.
- (3) classification without spatial post processing using the combined spectral textural features tends to produce about the same error rate as a classification without spatial post processing using only spectral features.

TABLE I.1 THE TYPE (CLASSES) AND CONDITION CLASSES (SUBCLASSES)  
OF FOREST FEATURES OF INTEREST IN SAM HOUSTON NATIONAL FOREST OF TEXAS

Type No.	Type (Class)	Subclass No.	Condition Class (Subclass)
1	Shortleaf pine	1.1	Plantation - 3 years old
		1.2	Poletimber - immature
		1.3	Sawtimber - immature
		1.4	Sawtimber - mature
2	Loblolly pine	2.1	Plantation - 1 year old
		2.2	Plantation - 3 years old
		2.3	Seedling and Sapling - adequately stocked
		2.4	Poletimber - immature
		2.5	Sawtimber - immature
		2.6	Sawtimber - mature
3	Laurel oak - willow oak	3.1	Sawtimber - immature
4	Sweetgum - nuttal oak - willow oak	4.1	Sawtimber - low quality
		4.2	Sawtimber - immature
		4.3	Sawtimber - mature
5	Post oak - black oak	5.1	Sawtimber - immature
6	Loblolly pine - hardwoods	6.1	Sawtimber - immature
7	Cut-over land	7.1	Site prepared and windrowed
		7.2	Not site prepared

These results mean that regardless of how the image is classified, spatial post-processing should be used to reduce the error rate. Furthermore, the best post processing results can be obtained if textural features are used; but, if no spatial post-processing is going to be utilized, spectral bands only will give about the same results as the combined spectral textural bands.

These conclusions are based on classification into all timber subclasses using large training sets averaging more than 25,000 points per image. Because the training sets were orders of magnitude larger than the number of categories times the number of features, the statistics must be considered as large sample statistics and we used, justifiably, the training data as the test data.

Tables I.2 and I.3 summarize the basis of our conclusions. The results of each experiment can be summarized in three ways: by average error, by average misidentification error, and by average false identification error. The average error is defined as the total number of incorrect category assignments divided by the total number of assignments. The average misidentification error is defined as the equally weighted average over all categories of the number of times the category is incorrectly assigned divided by the total number of times the category occurs in the ground truth. The average false identification error is defined as the equally weighted average over all categories of the number of times an incorrect assignment is made to the category divided by the total number of times an assignment is made to the category.

When the ground truth has each category occurring with equal frequency, the average misidentification error will equal the average error. When the number of assignments to each category is the same, the average false identification error will equal the average error. If the prior probability for a category is high and the category has a high misidentification error, then all other things being equal, the average error will be higher than the average misidentification error. If the prior probability for a category is low, and the category has high misidentification error, then all other things being equal, the average error will be lower than the average misidentification error.

From Tables I.2 and I.3 it is readily apparent that both the use of textural features and spatial post processing tends to increase and equalize the average misidentification error and false identification error while cutting the average error to less than half its initial value.

## I.1 Contingency Tables of Classification Results

All results are reported with a complete contingency table. The contingency tables are all organized in the same manner. The title for the contingency table tells which images are being compared. The first nine character file name is the name of the ground truth image file. The number following it is the symbolic band number used from that multi-image file. The second nine character file name is the name of the classified image file. The number following it is the number of the symbolic band used from that multi-image file. The row label UNKWN means unknown true category identification. The column label R DEC means reserved decision.

The contingency tables have a column labeled ERR. This column designates the number of the resolution cells in each category misidentified. The next column is labeled % ERR and it designates the percent of misidentification error. The contingency tables have a row labeled ERR. This row designates the number of resolution cells in each category falsely identified. The next row is labeled % ERR and it designates the percent of false identification error. The label % SD stands for the percent standard deviation of the error estimates. The entry whose row is labeled TOTAL and whose column is weighted % ERR is the equally weighted average of the misidentification error percentages. The entry whose column is labeled total and whose row is weighted % ERR is the equally weighted average of the false identification error percentages.

	Average Error	Average Misidentification Error	Average False Identification Error	Average Error	Average Misidentification Error	Average False Identification Error
Edit 6	22%	30%	5%	22%	23%	6%
Edit 9	28%	9%	9%	28%	8%	11%
Edit 14	30%	13%	9%	texture band not selected by feature selector		
Edit 3	42%	14%	25%	40%	25%	29%

Table I.2 summarizes the error rates obtained from the spectral versus the spectral-textural classification using 3 band pairs and no spatial post processing.

	Spectral			Spectral-Texture		
	Average Error	Average Misidentification Error	Average False Identification Error	Average Error	Average Misidentification Error	Average False Identification Error
Edit 6	9.3%	34%	33%	6.8%	38%	37%
Edit 9	19%	25%	32%	15%	27%	33%
Edit 14	12%	32%	31%	texture band not selected by feature selector		
Edit 3	24%	35%	40%	12%	40%	44%

Table I.3 summarizes the error rates obtained from the spectral versus the spectral-textural classification using 3 band pairs and spatial post processing.

## II Table Look-Up Decision Rule

Brooner, Haralick and Dinstein (1971) used a table look-up approach on high altitude multiband photography flown over Imperial Valley, California to determine crop types. Their approach to the storage problem was to perform an equal probability quantizing from the original 64 digitized grey levels to ten quantized levels for each of the three bands: green, red, and near infrared. Then after the conditional probabilities were empirically estimated, they used a Bayes rule to assign a category to each of the  $10^3$  possible quantized vectors in the 3-dimensional measurement space. Those vectors which occurred too few times in the training set for any category were deferred assignment.

The rather direct approach employed by Brooner et al. has the disadvantage of requiring a rather small number of quantized levels. Furthermore, it cannot be used with measurement vectors of dimension greater than four; for if the number of quantized levels is about 10, then the curse of dimensionality forces the number of possible quantized vectors to an unreasonably large size. Recognizing the grey level precision restriction forced by the quantizing coarsening effect, Eppler, Helmke, and Evans (1971) suggest a way to maintain greater quantizing precision by defining a quantization rule for each category - measurement dimension as follows:

- (1) fix a category and a measurement dimension component;
- (2) determine the set of all measurement patterns which would be assigned by the decision rule to the fixed category;
- (3) examine all the measurement patterns in this set and determine the minimum and maximum grey levels for the fixed measurement component;
- (4) construct the quantizing rule for the fixed category and measurement dimension pair by dividing the range between the minimum and maximum grey levels for the category into equal spaced quantizing intervals.

This multiple quantizing rule in effect determines for each category a rectangular parallelepiped in measurement space which contains all the measurement patterns assigned to it. Then as shown in Figure II.1, the equal interval quantizing lays a grid over the rectangular parallelepiped. Notice how for a fixed number of quantizing levels, the use of multiple quantizing rules in each band allows greater

grey level quantizing precision compared to the single quantization rule for each band.

A binary table for each category can be constructed by associating each entry of the table with one corresponding cell in the gridded rectangular parallel-epiped. An entry is a binary 1 if the decision rule assigns a majority of the measurement patterns in the corresponding cell to the specified category; otherwise, the entry is assigned to be a binary 0.

The binary tables are used in the implementation of the multiple quantization rule table look-up in the following way. Order the categories in some meaningful manner such as by prior probability. Quantize the multispectral measurement pattern using the quantization rule for category  $c_1$ . Use the quantized pattern as an address to look up the entry in the binary table for category  $c_1$  to determine whether or not the pre-stored decision rule would assign the pattern to category  $c_1$ . If the decision rule makes the assignment to category  $c_1$  the entry would be a binary 1 and, all is finished. If the decision rule does not make the assignment to category  $c_1$ , the entry would be a binary 0 and the process would repeat in a similar manner with the quantization rule and table for the next category.

One advantage to this form of the table look-up decision rule is the flexibility to use different subsets of bands for each category look-up table and thereby take full advantage of the feature selecting capability to define an optimal subset of bands to discriminate one category from all the others. A disadvantage to this form of the table look-up decision rule is the large amount of computational work required to determine the rectangular parallelepipeds for each category and the still large amount of memory storage required (about 5,000 8 bit bytes per category).

Eppler (1974) discusses a modification of the table look-up rule which enables memory storage to be reduced by five times and decision rule assignment time to be decreased by 2 times. Instead of pre-storing in tables a quantized measurement space image of the decision rule, he suggests a systematic way of storing in tables the boundaries or end-points for each region in measurement space satisfying a regularity condition and having all its measurement patterns assigned to the same category.

Let  $D = D_1 \times D_2 \times \dots \times D_N$  be measurement space. A subset  $R \subseteq D_1 \times D_2 \times \dots \times D_N$  is a regular region if and only if there exists constants

$L_1$  and  $H_1$  and functions  $L_2, L_3, \dots, L_N, H_2, H_3, \dots, H_N$

$$((L_n: D_1 \times D_2 \times \dots \times D_{n-1} \rightarrow (-\infty, \infty); H_n: D_1 \times D_2 \times \dots \times D_{n-1} \rightarrow (-\infty, \infty))$$

such that

$$R = \left\{ (x_1, \dots, x_N) \in D \mid \begin{aligned} &L_1 \leq x_1 \leq H_1 \\ &L_2(x_1) \leq x_2 \leq H_2(x_1) \\ &\vdots \\ &L_N(x_1, x_2, \dots, x_{N-1}) \leq x_N \leq H_N(x_1, x_2, \dots, x_{N-1}) \end{aligned} \right\}$$

From the definition of a regular region, it is easy to see how the table look-up by boundaries decision rule can be implemented. Let  $d = (d_1, \dots, d_N)$  be the measurement pattern to be assigned a category. To determine if  $d$  lies within a regular region  $R$  associated with category  $c$  we look up the numbers  $L_1$  and  $H_1$  and test to see if  $d_1$  lies between  $L_1$  and  $H_1$ . If so, we look up the numbers  $L_2(d_1)$  and  $H_2(d_1)$  and so on. If all the tests are satisfied, the decision rule can assign measurement pattern  $d$  to category  $c$ . If one of the tests fails, tests for the regular region corresponding to the next category can be made.

The memory reduction in this kind of table look-up rule is achieved by only storing boundary or end-points of decision regions and the speed-up is achieved by having one-dimensional tables whose addresses are easier to compute than the three or four-dimensional tables required by the initial table look-up decision rule. However, the price paid for by these advantages is the regularity condition imposed on the decision regions for each category. This regularity condition is stronger than set connectedness but weaker than set convexity.

Another approach to the table look-up rule can be based on Ashby's (1964) technique of constraint analysis. Ashby suggests representing in an approximate way subsets of Cartesian product sets by their projections on various smaller dimensional spaces. Using this idea for two-dimensional spaces we can formulate the following kind of table look-up rule.

Let  $D = D_1 \times D_2 \times \dots \times D_N$  be measurement space,  $C$  be the set of categories, and  $J \subseteq \{1, 2, \dots, N\} \times \{1, 2, \dots, N\}$  be an index set for the selected two-dimensional

spaces. Let the probability threshold  $\alpha$  be given. Let  $(i, j) \in J$ ; for each  $(x_1, x_2) \in D_i \times D_j$ , define the set  $S_{ij}(x_1, x_2)$  of categories having the highest conditional probabilities given  $(x_1, x_2)$  by

$$S_{ij}(x_1, x_2) = \{c \in C \mid P_{x_1, x_2}(c) \geq \alpha_{ij}\}, \text{ where } \alpha_{ij} \text{ is the largest number}$$

which satisfies

$$\sum_{c \in S_{ij}(x_1, x_2)} P_{x_1, x_2}(c) \geq \alpha$$

$S_{ij}(x_1, x_2)$  is the set of likely categories given that components  $i$  and  $j$  of the measurement pattern take the values  $(x_1, x_2)$ .

The sets  $S_{ij}$ ,  $(i, j) \in J$ , can be represented in the computer by tables. In the  $(i, j)^{\text{th}}$  table  $S_{ij}$  the  $(x_1, x_2)^{\text{th}}$  entry contains the set of all categories of sufficiently high conditional probabilities given the marginal measurements  $(x_1, x_2)$  from measurement components  $i$  and  $j$ , respectively. This set of categories is easily represented by a one word table entry; a set containing categories  $c_1$ ,  $c_7$ ,  $c_9$ , and  $c_{12}$ , for example, would be represented by a word having bits 1, 7, 9, and 12 on and all other bits off.

The decision region  $R(c)$  containing the set of all measurement patterns to be assigned to category  $c$  can be defined from the  $S_{ij}$  sets by

$$R(c) = \left\{ (d_1, d_2, \dots, d_N) \in D_1 \times D_2 \times \dots \times D_N \mid \{c\} = \bigcap_{(i, j) \in J} S_{ij}(d_i, d_j) \right\}$$

This kind of a table look-up rule can be implemented by using successive pairs of components (defined by the index set  $J$ ) of the (quantized) measurement patterns as addresses in the just mentioned two-dimensional tables. The set intersection required by the definition of the decision region  $R(c)$  is implemented by taking the Boolean AND of the words obtained from the table look-ups for the measurement to be assigned a category. Note that this Boolean operation makes full use of the natural parallel compute capability the computer has on bits of a word. If the  $k^{\text{th}}$  bit is the only bit which remains on in the resulting word, then the measurement pattern is assigned to category  $c_k$ . If there is more than one bit on or no bits are on, then the measurement pattern is deferred its assignment (reserved decision).

Thus we see that this form of a table look-up rule utilizes a set of "loose" Bayes rules in the lower dimensional projection spaces and intersects the resulting multiple category assignment sets to obtain a category assignment for the measurement pattern in the full measurement space.

Because of the natural effect which the category prior probabilities have on the category assignments produced by a Bayes rule it is possible for a measurement pattern to be the most probable pattern for one category yet be assigned by the Bayes rule to another category having much higher prior probability. This effect will be pronounced in the table look-up rule just described because the elimination of such a category assignment from the set of possible categories by one table look-up will completely eliminate it from consideration because of the Boolean AND or set intersection operation. However, by using an appropriate combination of maximum likelihood and Bayes rules, something can be done about this.

For any pair  $(i, j)$  of measurement components, fixed category  $c$ ; and probability threshold  $\beta$ , we can construct the set of  $T_{ij}(c)$  having the most probable pairs of measurement values from component  $i$  and  $j$  arising from category  $c$ . The set  $T_{ij}(c)$  is defined by

$$T_{ij}(c) = \{(x_1, x_2) \in D_i \times D_j \mid P_c(x_1, x_2) \geq \beta_{ij}(c)\},$$

where  $\beta_{ij}(c)$  is the largest number satisfying

$$\sum_{(x_1, x_2) \in T_{ij}(c)} P_c(x_1, x_2) \geq \beta$$

Tables which can be addressed by (quantized) measurement components can be constructed by combining the  $S_{ij}$  and  $T_{ij}$  sets. Define  $Q_{ij}(x_1, x_2)$  by

$$Q_{ij}(x_1, x_2) = \{c \in C \mid (x_1, x_2) \in T_{ij}(c)\} \cup S_{ij}(x_1, x_2)$$

The set  $Q_{ij}(x_1, x_2)$  contains all the categories whose respective conditional probabilities given measurement values  $(x_1, x_2)$  of components  $i$  and  $j$  are sufficiently high (a Bayes rule criteria) as well as all those categories whose most probable measurement values for components  $i$  and  $j$  respectively are  $(x_1, x_2)$  (a maximum likelihood criteria). A decision region  $R(c)$  containing all the (quantized) measurement patterns can then be defined as before using the  $Q_{ij}$  sets:

$$R(c) = \left\{ (d_1, d_2, \dots, d_N) \in D_1 \times D_2 \times \dots \times D_N \mid \{c\} = \bigcap_{(i,j) \in J} Q_{ij}(d_i, d_j) \right\}$$

A majority vote version of this kind of table look-up rule can be defined by assigning a measurement to the category most frequently selected in the lower dimensional spaces.

$$R(c) = \left\{ (d_1, d_2, \dots, d_N) \in D_1 \times D_2 \times \dots \times D_N \mid \right. \\ \left. \# \left\{ (i,j) \in J \mid c \in Q_{ij}(d_i, d_j) \right\} \geq \# \left\{ (i,j) \in J \mid c \in Q_{ij}(d_i, d_j) \right\} \right. \\ \left. \text{for every } c \in C - \{c\} \right\}$$

Classification results were run with  $\beta = .07\alpha$  and  $\alpha$  chosen to minimize the number of reserved decisions. Figure II.2 illustrates a graph of the number of reserved decisions versus probability threshold  $\alpha$ .

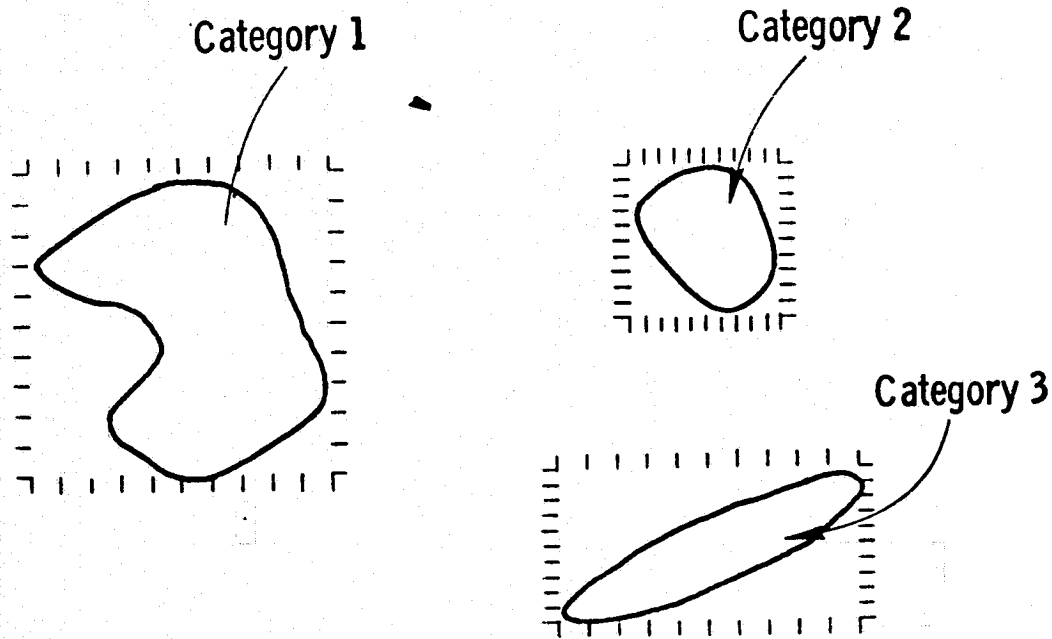


Figure II.1 illustrates how quantizing can be done differently for each category thereby enabling more accurate classification by the following table look-up rule: (1) quantize the measurement by the quantizing rule for category one (2) use the quantized measurement as an address in a table and test if the entry is a binary one or binary zero, (3) if it is a binary one assign the measurement to category one; if it is a binary zero, repeat the procedure for category two.

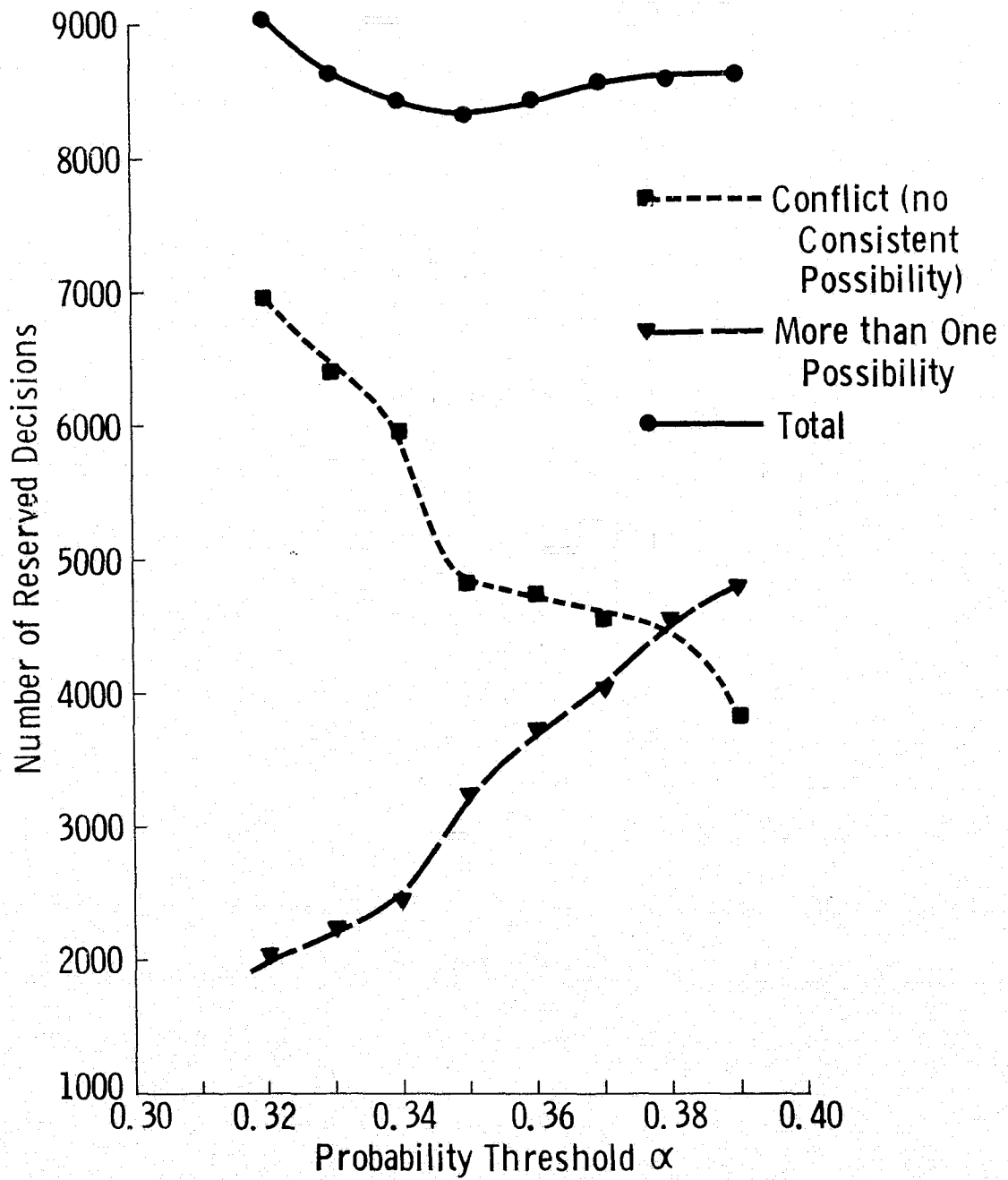


Figure 11.2 illustrates a graph of the number of reserved decisions versus probability threshold  $\alpha$ .

### III Texture

Spatial environments can be understood as being spatial distributions of various area-extensive objects having characteristic size and reflectance or emissive qualities. The spatial organization and relationships of the area-extensive objects appear as spatial distributions of grey tone on imagery taken of the environment. We call the pattern of spatial distributions of grey tone, texture.

Figure III.1, taken from Lewis (1971), illustrates how texture relates to geomorphology. There are some plains, low hills, high hills, and mountains in the Panama and Columbia area taken by the Westinghouse AN/APQ 97 K-band radar imager system. The plains have apparent relief of 0-50 meters, the hills have apparent relief of 50-350 meters, and the mountains have apparent relief of more than 350 meters. The low hills have little dissection and are generally smooth convex surfaces whereas the high hills are highly dissected and have prominent ridge crests.

The mountain texture is distinguishable from the hill texture on the basis of the extent of radar shadowing (black tonal areas). The mountains have shadowing over more than half the area and the hills have shadowing over less than half the area. The hills can be subdivided from low to high on the basis of the abruptness of tonal change from terrain front slope to terrain back slope.

There have been six basic approaches to the measurement and quantification of image texture: autocorrelation functions (Kaizer, 1955), optical transforms, (Lendaris and Stanley, 1970), digital transforms, (Gramenopoulos, 1973; Hornung and Smith, 1973; Kirvida and Johnson, 1973), edgeness (Rosenfeld and Thurston, 1971), structural elements, (Matheron, 1967; Serra, 1973), and spatial grey tone co-occurrence probabilities, (Haralick et al., 1973). The first three of these approaches are related in that they all measure spatial frequency directly or indirectly. Spatial frequency is related to texture because fine textures are rich in high spatial frequencies while coarse textures are rich in low spatial frequencies.

An alternative to viewing texture as spatial frequency distribution is to view texture as amount of edge per unit area. Coarse textures have a small number of edges per unit area. Fine textures have a high number of edges per unit area.

The structural element approach uses a matching procedure to detect the spatial regularity of shapes called structural elements in a binary image. When

the structural elements themselves are single resolution cells, the information provided by this approach is the autocorrelation function of the binary image. By using larger and more complex shapes, a more generalized autocorrelation can be computed.

The grey tone co-occurrence approach characterizes texture by the spatial distribution of its grey tones. Coarse textures are those for which the distribution changes only slightly with distance and fine textures are those for which the distribution changes rapidly with distance.

### III.1 Optical Processing Methods and Texture

Edward O'Neill's (1956) article on spatial filtering introduced the engineering community to the fact that optical systems can perform filtering of the kind used in communication systems. In the case of the optical systems, however, the filtering is two-dimensional. The basis for the filtering capability of optical systems lies in the fact that the light amplitude distributions at the front and back focal planes of lens are Fourier Transforms of one another. The light distribution produced by the lens is more commonly known as the Fraunhofer diffraction pattern. Thus, optical methods facilitate two-dimensional frequency analysis of images.

The paper by Cutrona et al. (1960) provides a good review of optical processing methods for the interested reader. More recent books by Goodman (1968), Preston (1972), Shulman (1970) comprehensively survey the area.

In this section, we describe the experiments done by Lendaris and Stanley, Egbert et al., and Swanlund using optical processing methods in aerial or satellite imagery. Lendaris and Stanley (1970) illuminated small circular sections of low altitude aerial photography and used the Fraunhofer diffraction pattern as features for identifying the sections. The circular sections represented a circular area on the ground of 750 feet. The major category distinction they were interested in making was man-made versus non man-made. They further subdivided the man-made category into roads, road intersections, buildings, and orchards.

The pattern vectors they used from the diffraction pattern consisted of 40 components. Twenty components were averages of the energy in  $9^\circ$  wedges of the diffraction pattern. They obtained over 90 percent identification accuracy.

Ulaby and McNaughton used an optical processing system to examine the texture of ERTS imagery over Kansas. They used circular areas corresponding to a ground diameter of about 37 km and looked at the diffraction patterns for four different physiographic regions in Kansas. They used a diffraction pattern sampling unit having 32 sector wedges and 32 annular rings to sample and measure the diffraction patterns. (See Jensen (1973) for a description of the sampling unit and its use in coarse diffraction pattern analysis.) They were able to interpret the resulting angular orientation graphs in terms of dominant drainage patterns, roads and fields but interpreted the spatial frequency graphs in terms of stress patterns, rough terrain and field patterns. Their results indicated that the spatial frequency information was highly correlated with physiography.

Swanlund (1969) has done work using optical processing on aerial images to identify species of trees. Using imagery obtained from Itasca State Park in northern Minnesota, photo interpreters identified five (mixture) species of trees on the basis of the texture: Upland Hardwoods, Jack pine overstory/Aspen understory/Upland Hardwoods understory, Red pine overstory/Aspen understory, and Aspen. They achieved classification accuracy of over 90 percent.

### III.2 Texture and Edges

The autocorrelation function, the optical transforms, and the fast digital transforms (FFT and FHT) basically all reference texture to spatial frequency. Rosenfeld and Thurston (1971) conceive of texture not in terms of spatial frequency but in terms of edgeness per unit area. An edge passing through a resolution cell is detected by comparing the values for local properties obtained in pairs of non-overlapping neighborhoods boarding the resolution cell. To detect microedges, small neighborhoods must be used. To detect macroedges, large neighborhoods must be used.

The local property which Rosenfeld and Thurston suggested was the quick Roberts gradient (the sum of the absolute value of the differences between diagonally opposite neighboring pixels). Thus, a measure of texture for any subimage is obtained by computing the Roberts gradient image for the subimage and from it determining the average value of the gradient in the subimage. Triendl (1972) uses the Laplacian instead of the Roberts gradient.

Sutton and Hall (1972) extended Rosenfeld and Thurston's idea by making the gradient a function of the distance between the pixels. Thus, for every distance  $d$  and subimage  $I$  defined over a neighborhood  $N$  of resolution cells, they compute

$$g(d) = \sum_{(i,j) \in N} \{ |I(i,j) - I(i+d,j)| + |I(i,j) - I(i-d,j)| \\ + |I(i,j) - I(i,j+d)| + |I(i,j) - I(i,j-d)| \}.$$

The graph of  $g(d)$  is like the graph of the minus autocorrelation function translated vertically.

Sutton and Hall applied this textural measure in a pulmonary disease identification experiment using radiographic imagery and obtained identification accuracy in the 80 percentile range for discriminating between normal and abnormal lungs when using a  $128 \times 128$  subimage.

### III.3 Digital Transform Methods and Texture

In the digital transform method of texture analysis, the digital image is typically divided into a set of non-overlapping small square subimages. Suppose the size of the subimage is  $n \times n$  resolution cells, then the  $n^2$  grey tones in the subimage can be thought of as the  $n^2$  components of an  $n^2$ -dimensional vector. In the transform technique, each of these vectors is re-expressed in a new coordinate system. The Fourier Transform uses the sine-cosine basis set. The Hadamard Transform uses the Walsh function basis set, etc. The point to the transformation is that the basis vectors of the new coordinate system have an interpretation that relates to spatial frequency (sequency) and since frequency (sequency) is a close relative of texture, we see that such transformation can be useful.

Gramenopoulos (1973) used a transform technique using the sine-cosine basis vectors (and implemented it with the FFT algorithm) on ERTS imagery to investigate the power of texture and spatial pattern to do terrain type recognition. He used subimages of  $32 \times 32$  resolution cells and found that on Phoenix, Arizona ERTS image 1940-17324-5 spatial frequencies larger than 3.5 cycles/km and smaller than 5.9 cycles/km contain most of the information needed to discriminate between terrain types. The terrain classes were: clouds, water, desert, farms, mountains, urban, riverbed, and cloud shadows. He achieved an overall identification accuracy of 87 percent.

Hornung and Smith (1973) have done work similar to Gramenopoulos but with aerial multispectral scanner imagery instead of ERTS imagery. Maurer (1974)

used Fourier series analysis on some color aerial film to obtain textural features to help determine crop types.

Kirvida and Johnson (1973) compared the fast Fourier, Hadamard, and Slant Transforms for textural features on ERTS imagery over Minnesota. They used 8 x 8 subimages and five categories: Hardwoods, Conifers, Open, Water, City. Using only spectral information, they obtained 74 percent correct identification accuracy. When they added textural information, they increased the identification accuracy to 99 percent. They found little difference between the different transform methods.

### III.4 Spatial Grey Tone Dependence: Co-occurrence

One aspect of texture is concerned with the spatial distribution and spatial dependence among the grey tones in a local area. Darling (1968) used statistics obtained from the nearest neighbor grey tone transition matrix to measure this dependence for satellite images of clouds and was able to identify cloud types on the basis of their texture. Read and Jayaramamurthy (1972) divided an image into all possible (overlapping) subimages of reasonably small and fixed size and counted the frequency for all the distinct grey tone patterns. This is one step more general than Darling but one that requires too much memory if the grey tones can take on very many values. Haralick (1971) and Haralick et al. (1972, 1973) suggested an approach which is a compromise between the two. He measures the spatial dependence of grey tones in a co-occurrence matrix for each fixed distance and/or angular spatial relationship and uses statistics of the matrix as measures of image texture.

The co-occurrence matrix  $P = (p_{ij})$  has its  $(i, j)^{th}$  entry  $P_{ij}$  defined as the number of times grey tone  $i$  and grey tone  $j$  occur in resolution cells of a subimage having a specified spatial relation, such as distance 1 neighbors. The textural features for the subimage are obtainable from the co-occurrence matrix by measures such as

$$\sum_i \sum_j P_{ij}^2, \sum_i \sum_j P_{ij} \log p_{ij},$$

and

$$\sum_i \sum_j \frac{P_{ij}}{1 + |i-j|}$$

Haralick et al. (1973) list 14 different kinds of measures.

Using statistics of the co-occurrence matrix, Haralick performed a number of identification experiments. On a set of aerial imagery and eight terrain classes (old residential, new residential, lake, swamp, marsh, urban, railroad yard, scrub or wooded), he obtained 82 percent correct identification with 64 x 64 subimages. On an ERTS Monterey Bay, California, image, he obtained 84 percent correct identification using 64 x 64 subimages and both spectral and textural features on seven terrain classes: coastal forest, woodlands, annual grasslands, urban areas, large irrigated fields, small irrigated fields, and water. On a set of sandstone photomicrographs, he obtained 89 percent correct identification on five sandstone classes: Dexter-L, Dexter-H, St. Peter, Upper Muddy, Gaskel.

The wide class of images on which they found that grey tone co-occurrence carries much of the texture information is probably indicative of the power and generality of this approach.

### III.5 A Textural Transform

Each of the approaches described for the quantification of textural features had the common property that the textural features were computed for subimages of typical sizes such as 8 x 8, 16 x 16, 32 x 32, or 64 x 64 resolution cells. To determine the textural features for one pixel we would naturally center a subimage on the specified resolution cell and compute the textural features for the subimage. If we had to determine the textural features for each pixel in an image we would be in for a lot of computation work and would significantly increase the size of our data set. Thus, the usual approach has been to divide the image into mutually exclusive subimages and compute the textural features on the selected subimages. Unfortunately, this procedure produces textural features at a coarser resolution than the original image.

In this section we generalize the grey tone co-occurrence textural feature extractor to the textural transform mode and show how by only doubling or tripling the computation time required to determine the grey tone co-occurrence matrix it is possible to produce a resolution preserving textural transform in which each pixel in the transformed image has textural information about its own neighborhood derived from both local and global grey tone co-occurrence in the image. This kind of textural transform is in the class of image dependent non-linear spatial filters.

Let  $Z_r \times Z_c$  be the set of resolution cells of an image I (by row-column coordinates). Let  $G$  be the set of grey tones possible to appear on image I. Then  $I: Z_r \times Z_c \rightarrow G$ . Let  $R$  be a binary relation on  $Z_r \times Z_c$  pairing together all those resolution cells in the desired spatial relation. The co-occurrence matrix  $P, P: G \times G \rightarrow [0, 1]$ , for image I and binary relation R is defined by

$$P(i, j) = \frac{\# \{((a, b), (c, d)) \in R \mid I(a, b) = i \text{ and } I(c, d) = j\}}{\#R}$$

The textural transform  $J, J: Z_r \times Z_c (-\infty, \infty)$ , of image I relative to function  $f$ , is defined by

$$J(y, x) = \frac{1}{\#R(y, x)} \sum_{(a, b) \in R(y, x)} f[P(I(y, x), I(a, b))]$$

Assuming  $f$  to be the identity function, the meaning of  $J(y, x)$  is as follows. The set  $R(y, x)$  is the set of all those resolution cells in  $Z_r \times Z_c$  in the desired spatial relation to resolution cell  $(y, x)$ . For any resolution cell  $(a, b) \in R(y, x)$ ,  $P(I(y, x), I(a, b))$  is the relative frequency by which the grey tone  $I(y, x)$ , appearing at resolution cell  $(y, x)$ , and the grey tone  $I(a, b)$ , appearing at resolution cell  $(a, b)$ , co-occur together in the desired spatial relation on the entire image. The sum

$$\sum_{(a, b) \in R(y, x)} P(I(y, x), I(a, b))$$

is just the sum of the relative frequencies of grey tone co-occurrence over all resolution cells in the specified relation to resolution cell  $(y, x)$ . The factor  $\frac{1}{\#R(y, x)}$ , the reciprocal of the number of resolution cells in the desired spatial relation to  $(y, x)$  is just a normalizing factor.

#### IV Spatial Pre-Processing

Spatial enhancement processes can be implemented before or after the classification of the original images. One spatial averaging process which can be used before classification of the original image is rectangular convolution. A  $2 \times 2$  rectangular convolution, for example, is the process that replaces the left upper resolution cell of each  $2 \times 2$  window by the average of the grey tones in the  $2 \times 2$  window. A  $3 \times 3$  rectangular convolution replaces each grey tone with the average of the grey tones in a  $3 \times 3$  window centered around it. The process of rectangular convolution can be implemented before or after texture transform. The window size for the rectangular convolution process can be as big as required.

Figure IV illustrates how the rectangular convolution can enhance the textural transform processed images. Notice that the rectangular region on the left lower corner is not easy to distinguish on the image with no rectangular convolution before or after texture transform, Figure IV a, but it is distinguishable on Figure IV d, the image with  $2 \times 2$  rectangular convolution before texture transform and no rectangular convolution after texture transform, as it is on Figures IV e to IV i. The two strips on the middle of the image are not easily distinguished on Figures IV a to IV f, but they are easily distinguished on Figure IV g, the image with  $3 \times 3$  rectangular convolution before texture transform and no rectangular convolution after texture transform. They are also distinguishable on images IV h and IV i which have been processed with a  $3 \times 3$  convolution after the textural transform. For distinguishing rectangular region and the two strips on the image, Figure IV i, the image with  $3 \times 3$  rectangular convolution before and after texture transform seems best.

## V Spatial Post-Processing

Spatial post processing the classified image can be used to reduce image complexity and achieve some degree of spatial simplification and generalization. Two post processing techniques are region filling and shrinking. A region filling operation assigns an unassigned resolution cell to the category assignment of one of its neighboring resolution cells.

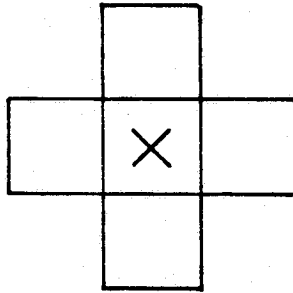
A resolution cell can be defined to have the four resolution cells above, below, to the left, and to the right of it as neighbors or to have those plus the resolution cells diagonally neighboring it as its neighbors. The first set of resolution cells is called its 4-neighbors and the second set of resolution cells is called its 8-neighbors. The concepts of 4-neighboring and 8-neighboring is illustrated in Figure V.1.

A region filling operation which assigns an unlabeled resolution cell to the category assignment of one of its four nearest neighbors is called a 4-fill operation. A region filling operation which assigns an unlabeled resolution cell to the category assignment of one of its eight nearest neighbors is called an 8-fill operation. A region filling operation which iterates first filling using 4 neighbors and then 8 neighbors then 4 then 8 etc., until all resolution cells are labeled, we shall for simplicity call region filling.

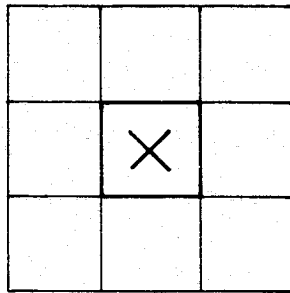
Figure V.2 illustrates the advantage of region filling alternating between 4-neighbors or 8-neighbors. A labeled resolution cell in an area of unlabeled resolution cells would grow as a diamond region under repetitive 4-fill operations. It would grow as a square region under repetitive 8-fill operations. And it would grow almost as a circle under repetitive 8-fill and 4-fill operations.

Region shrinking is the opposite kind of operation from region filling. A region shrinking operation assigns a labeled resolution to "unassigned" if its neighbors have different labels from it.

A region shrinking operation which assigns a labeled resolution cell to "unassigned" if  $k$  of its four nearest neighbors have labels which are different than its own label is called a 4- $k$  shrink operation. A region shrinking operation which assigns a labeled resolution cell to "unassigned" if  $k$  of its eight nearest neighbors have labels which are different from its own label is called an 8- $k$  shrink operation.



a



b

Figure V.1 a illustrates the 4-neighborhood of a resolution cell and  
Figure V.1 b illustrates the 8-neighborhood of a resolution cell.

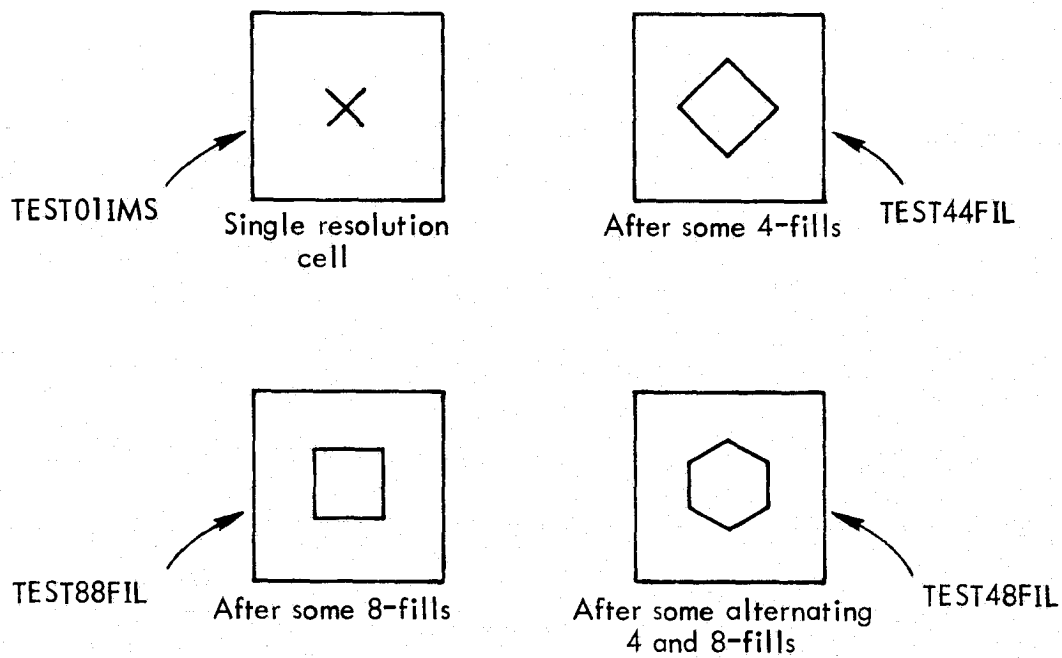


Figure V.2 illustrates the effect of 4 and 8-filling or a single resolution cell.

In Figure V.3 we illustrate the effect of the filling and shrinking operations on a classified image. Figure V.3a is a classified image. The black areas represent unassigned resolution cells. (The decision rule leaves unassigned those resolution cells having multispectral signatures which do not provide enough information to make a reliable assignment.) Figure V.3b shows the classified image of Figure V.3a after a complete region filling. Notice that after a complete region filling, all resolution cells have a label. Figure V.3c shows the classified image of Figure V.3a after a 4-0 shrink. Notice that it has more black area than the image in Figure V.3a due to the effect of its relabeling labeled resolution cells to "unassigned".

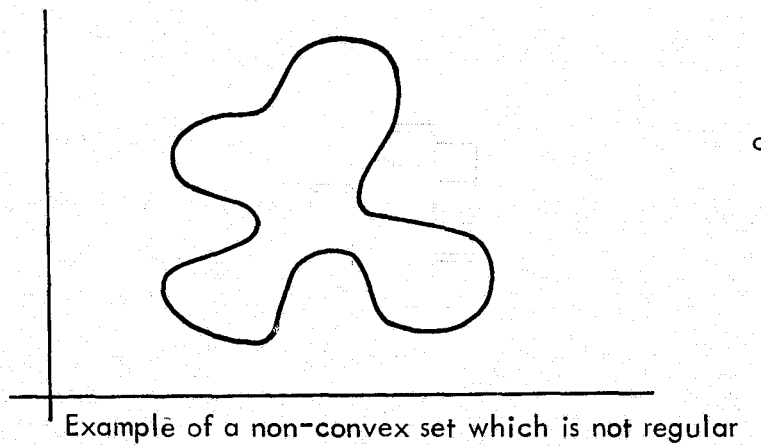
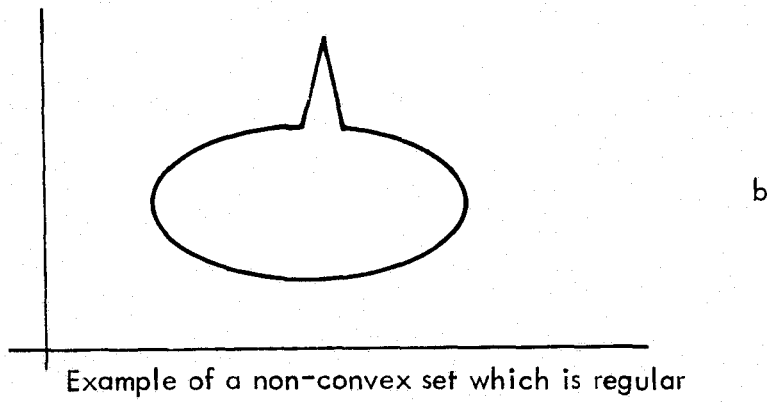
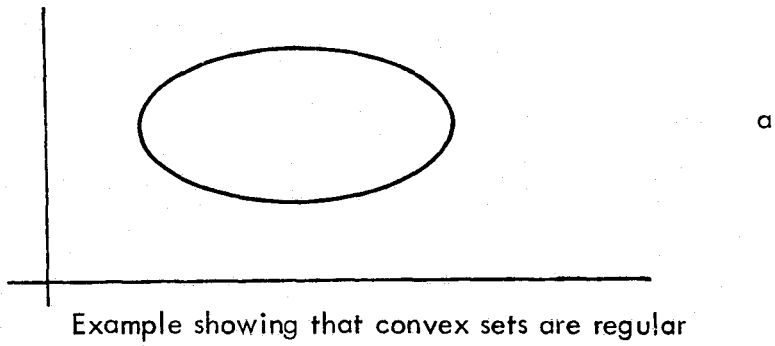


Figure 3 illustrates the relationship between set convexity and regularity

## VI Spectral Analysis: Edit 6

Of the 6 best spectral bands on edit #6, .40 - .44, .588 - .643, .65 - .69, .72 - .76, .981 - 1.045, and 2.10 - 2.36 micrometers, the feature selection procedure selected band pairs .40 - .44 and .65 - .60 with .40 - .44 and 2.10 - 2.36 micrometers as the best 2 band pairs for the table look-up rule. Figure VI.1 shows the .72 - .76 micrometer band and Figure VI.2 shows the ground truth training data overlay on this band. The alpha-beta thresholds were set at .3 and .021. This threshold selection was too low for of the 159,500 points to be classified, 67,323 were reserved assignments because of incompatible assignments between the first and second band pairs and 6,928 were reserved assignment because there was more than one possible assignment common to the two band pairs. Figure VI.3 shows the resulting classification. The contingency table, Table VI.1 shows an equally weighted misidentification error rate of 36% and equally weighted false identification error rate of 34%. The largest cause of the misidentification error was category 2.4, immature poletimber loblolly pine, being assigned to category 1.3, immature sawtimber shortleaf pine, and category 2.6, mature sawtimber loblolly pine being assigned to category 2.5, immature sawtimber loblolly pine and being assigned to category 2.3, seedling and sapling loblolly pine.

If the classified image is filled so that all resolution cells whose category assignment was reserved is assigned to the category of its spatially nearest resolution cell neighbor which is assigned, the error rate remains substantially the same, about a 36% misidentification and false identification error rate (Figure VI.4 and Table VI.2). This implies that for those resolution cells whose assignment was reserved because of the low probability of correct assignment, category assignments, almost as good as those originally assigned, can be made using the spatial information carried by the initially classified image with the reserved decisions.

Perhaps what is even more surprising about the amount of spatial information the classified image has is that by performing spatial operations on it, the classification accuracy can increase. For example, if the completely filled image is shrunk for one iteration with a simple 4-shrink operator and then filled up again, Table VI.3 shows an accuracy increase: 33% misidentification error rate and 35% false identification error rate. Comparable results are also obtained by using the initially classified image with reserved decisions and performing a 4-fill iteration followed

by an 8-fill iteration followed by a 4-shrink iteration and then completely filled (Figure VI.5 and Table VI.4).

The best (percentage wise) 2 band pair results came from starting with the initially classified image with reserved decisions and doing a 4-fill, an 8-fill, a 4-shrink, an 8-shrink, and then a complete filling up. This yields a 31% misidentification error rate and 7% false identification error rate (Table VI.5 and Figure VI.6). Notice, however, that all the points in category 2.4, poletimber immature loblolly, have been misidentified as category 1.3, sawtimber immature shortleaf pine, and all the points in category 2.6, mature sawtimber loblolly pine, have been misidentified as categories 1.3, 2.3 and 2.5. Furthermore, no points were assigned to categories 2.4 and 2.6. This suggests that the tree stands in those areas of immature loblolly and mature sawtimber loblolly pine had a substantial number of trees spectrally similar to those in categories 1.3, 2.3, and 2.5. Areas predominately in categories 2.4 and 2.6 would have some resolution cells initially assigned to categories 2.4 and 2.6 plus wrong assignments to categories 1.3, 2.3, or 2.5. Hence, a context sensitive shrinking operation on the 4-fill and 8-fill image which would leave alone any resolution cell assigned to category 2.4 if it neighbors a resolution cell of category 1.3 and which would leave alone any resolution cell assigned to category 2.6 if it neighbors a resolution cell of category 1.3, 2.3 or 2.5 has the possibility of permitting a higher probability of correct identification.

If instead of doing only one 4-shrink then 8-shrink iterations, two such iterations are made before a complete filling, then the results are not quite as good: 34% misidentification error rate and 6% false identification error rate. (Table VI.6).

The use of additional spectral bands can sometimes increase identification accuracy. In the case of the edit #6 data, this did not seem to be the case. The three best band pairs were:

- (1) .40 - .44 and .65 - .69 micrometers
- (2) .40 - .44 and 2.10 - 2.36 micrometers
- (3) .72 - .76 and .981 - 1.045 micrometers

The alpha-beta thresholds were set at .6 and .042, respectively. The resulting number of reserved decisions due to no common category assignment was 51,794

and the number of reserved decisions due to more than one possible category assignment was 19,706 (Figure VI.7 and Table VI.7). Higher thresholds would have been better.

After a complete filling, there was a 34% misidentification and 33% false identification error rate (Figure VI.8 and Table VI.8). If the completely filled image had a 4-shrink operation and then another complete filling, the misidentification error rate improved to 31% and false identification error rate improved to 16% (Figure VI.9 and Table VI.9). If before the complete filling is done an iteration of a 4-fill followed by an 8-fill and a 4-shrink followed by an 8-shrink is done, the misidentification error rate improves to 30% and the false identification error rate improves to 5%, the best 3-band pair result (Figure VI.10 and Table VI.10). As in the two band pair case, doing two iterations of the 4-shrink followed by the 8-shrink instead of one iteration, does not provide as much improvement: a 36% misidentification error rate and a 6% false identification error rate (Table VI.11). The best 3 band pair result confused the same categories as the best 2 band pair result. Category 2.4, poletimber immature loblolly was assigned as category 1.3, immature shortleaf pine. Category 2.6, mature sawtimber loblolly pine was assigned to categories 2.3 and 2.5, seedling and sapling loblolly and sawtimber immature loblolly pine.

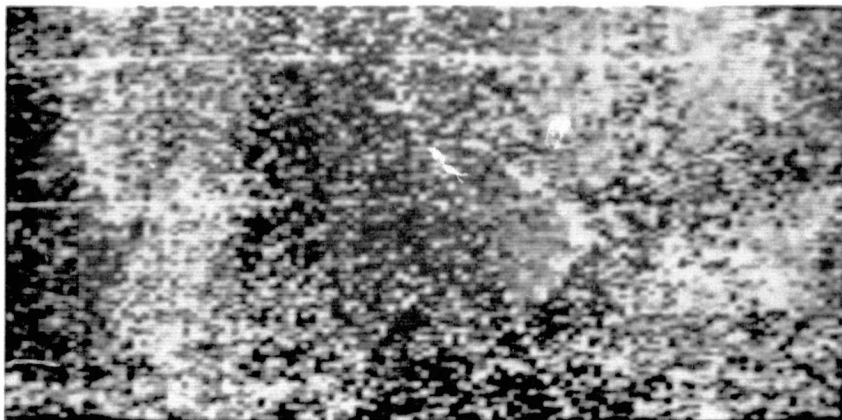


Figure VI.1 The .72 - .76 micrometer band

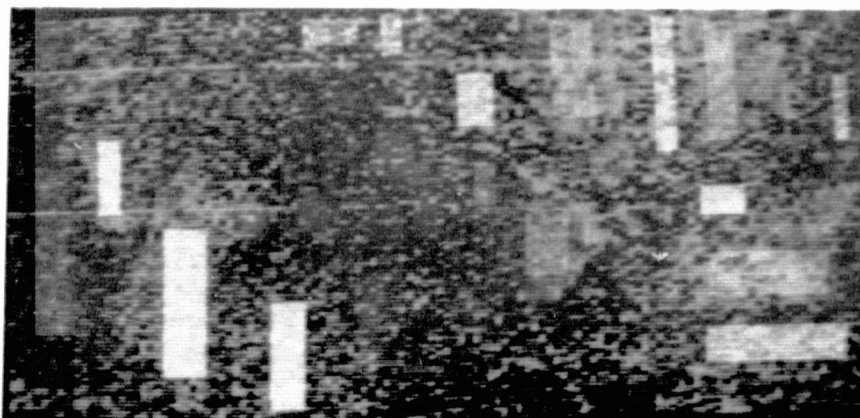


Figure VI.2 The ground truth training data overlaid on the .72 - .76 micrometer band.



Figure VI.3 The classification of the best two band pairs for alpha-beta thresholds of .3 and .021.

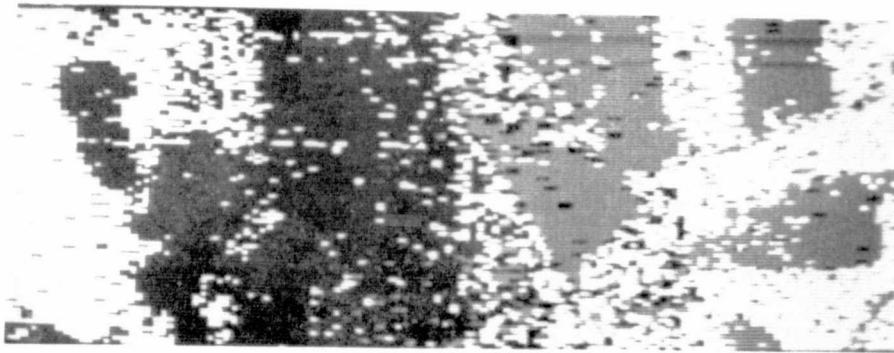


Figure VI.4 The classified image of Figure VI.3 after a complete filling.

CONTINGENCY TABLE FOR SAMH21GDT - 1 SAMH28B01 - 1 SCALE FACTOR 10\*\* 0

COL. = ASSIGN CAT      ROW = TRUE CAT

R DEC	1.3	1.4	2.3	2.4	2.5	2.6	7.2	TOTAL	ERR	ERR	
UNKWN	63106	12483	12809	19901	1002	3473	1024	10627	130425	0	0
1.3	3475	2696	274	243	75	86	24	83	6956	785	23
1.4	561	8	2000	41	0	27	7	26	2670	109	5
2.3	2013	62	18	5336	31	212	37	18	7727	378	7
2.4	311	244	14	16	42	0	0	2	629	276	87
2.5	2387	140	52	235	16	1140	61	3	4034	507	31
2.6	793	94	26	198	0	276	45	2	1434	596	93
7.2	1615	95	76	29	70	0	7	3738	5625	272	7
TOTAL	74261	15822	15269	25999	1236	11214	1200	14499	159500	2923	36
ERR	0	643	460	762	192	601	131	134	2923	*****	*****
ERR	0	19	19	12	82	35	74	3	34	*****	*****

Table VI.1 The contingency table of the best 2 band pairs for alpha-beta thresholds of .3 and .021.

CONTINGENCY TABLE FOR SAMH2 GDT - 1 SMH2F7B01 - 1 SCALE FACTOR 10\*\* 0

COL. = ASSIGN CAT      ROW = TRUE CAT

R DEC	1.3	1.4	2.3	2.4	2.5	2.6	7.2	TOTAL	ERR	ERR	
UNKWN	0	26653	22904	33017	1737	25591	2596	17928	130425	0	0
1.3	0	5337	612	466	143	175	53	170	6956	1619	23
1.4	0	16	2455	76	0	60	19	44	2670	215	8
2.3	0	88	30	7119	41	361	61	27	7727	608	8
2.4	0	482	32	36	76	0	0	3	629	553	88
2.5	0	329	128	511	30	2891	140	5	4034	1143	28
2.6	0	214	68	433	0	615	100	4	1434	1334	93
7.2	0	197	164	43	91	0	5	5125	5625	400	9
TOTAL	0	33316	26393	41701	2118	29693	2973	23306	159500	5972	36
ERR	0	1326	1034	1565	305	1211	278	253	5972	*****	*****
ERR	0	20	30	18	80	30	74	5	36	*****	*****

Table VI.2 The contingency table of the best 2 band pairs after a complete filling.

CONTINGENCY TABLE FOR SAMH2 GDT - 1 SMH2F8901 - 1 SCALE FACTOR 10\*\* 0

		COL. = ASSIGN CAT							ROW = TRUE CAT		
R DEC	1.3	1.4	2.3	2.4	2.5	2.6	7.2	TOTAL	ERR	ERR	
UNKNOWN	0	26835	22575	34649	837	27555	525	17449	130425	0	0
1.3	0	6065	680	49	109	0	0	53	6956	891	13
1.4	0	2	2499	97	0	72	0	0	2670	171	6
2.3	0	0	0	7571	6	150	0	0	7727	156	2
2.4	0	555	6	11	57	0	0	0	629	572	91
2.5	0	324	20	323	45	3314	0	0	4034	720	18
2.6	0	166	0	586	0	682	0	0	1434	1434	100
7.2	0	55	100	0	0	0	0	5470	5625	155	3
TOTAL	0	34002	25880	43286	1054	31773	533	22972	159500	4099	33
ERR	0	1102	806	166	160	904	0	53	4099	*****	*****
ERR	0	15	24	12	74	21	100	1	35	*****	*****

Table VI.3 The contingency table of the best 2 band pairs after complete filling, 4-shrink, and complete filling operations.

CONTINGENCY TABLE FOR SAMH2 GDT - 1 SMH2F0B01 - 1 SCALE FACTOR 10\*\* 0

		COL. = ASSIGN CAT							ROW = TRUE CAT		
R DEC	1.3	1.4	2.3	2.4	2.5	2.6	7.2	TOTAL	ERR	ERR	
UNKNOWN	0	26835	22574	34653	837	27552	525	17449	130425	0	0
1.3	0	6065	680	49	109	0	0	53	6956	891	13
1.4	0	2	2499	97	0	72	0	0	2670	171	6
2.3	0	0	0	7571	6	150	0	0	7727	156	2
2.4	0	555	6	11	57	0	0	0	629	572	91
2.5	0	324	20	323	45	3314	0	0	4034	720	18
2.6	0	166	0	586	0	682	0	0	1434	1434	100
7.2	0	55	100	0	0	0	0	5470	5625	155	3
TOTAL	0	34002	25879	43290	1054	31770	533	22972	159500	4099	33
ERR	0	1102	806	1066	160	904	0	53	4099	*****	*****
ERR	0	15	24	12	74	21	100	1	35	*****	*****

Table VI.4 The contingency table of the best 2 band pairs after 4-fill, 8-fill, 4-shrink, and complete filling operations.

ORIGINAL PAGE IS  
OF POOR QUALITY

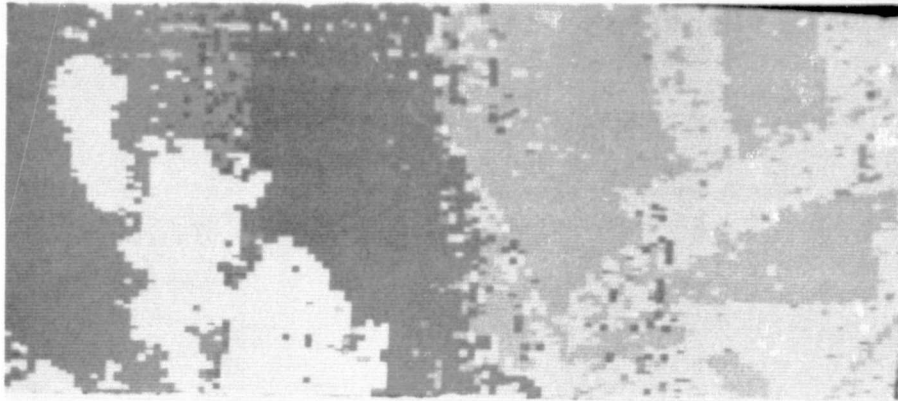


Figure VI.5 The classified image of Figure VI.3 after 4-fill, 8-fill, 4-shrink, and then complete filling operations.

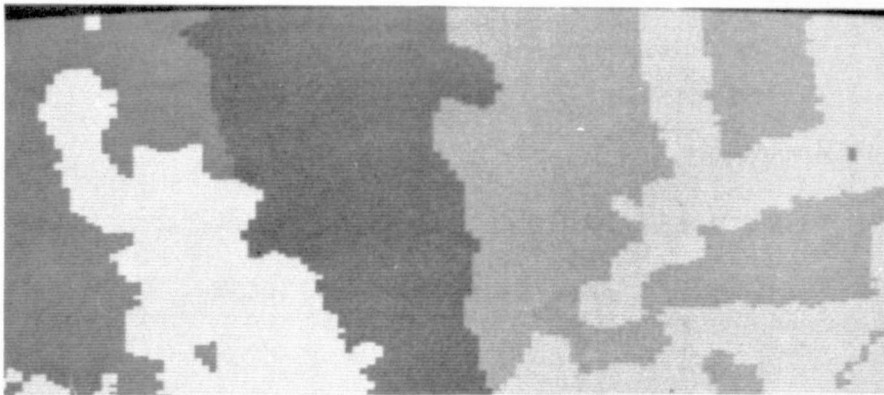


Figure VI.6 The classified image of Figure VI.3 after 4-fill, 8-fill, 4-shrink, 8-shrink, and then complete filling operations.

CONTINGENCY TABLE FOR SAMH2 GDT - 1 SMH2F9B01 - 1 SCALE FACTOR 10\*\* 0

COL. = ASSIGN CAT      ROW = TRUE CAT

R DEC	1.3	1.4	2.3	2.4	2.5	2.6	7.2	TOTAL	FRR	ERR
UNKNW	0 2725	21595	35342		0 27636		n 18607	130425	0	0
1.3	0 6551	4.6	0		0 0		n 0	6956	406	6
1.4	0 0	2499	70		0 101		n 0	2670	171	6
2.3	0 0	0	7727		0 0		n 0	7727	0	0
2.4	0 629	0	0		0 0		n 0	629	629	100
2.5	0 351	0	72		0 3611		n 0	4034	423	10
2.6	0 523	0	303		0 608		n 0	1434	1434	100
7.2	0 0	12	0		0 0		n 5613	5625	12	0
TOTAL	0 35303	24512	43514		0 31956		n 24215	159500	3075	31
FRR	0 1503	418	445		0 709		n 0	3075	*****	*****
FRR	0 19	14	5		0 16		n 0	7	*****	*****

Table VI.5 The contingency table of the best 2 band pairs after 4-fill, 8-fill, 4-shrink, 8-shrink, and complete filling operations.

CONTINGENCY TABLE FOR SAMH2 GDT - 1 SMH2F4B01 - 1 SCALE FACTOR 10\*\* 0

COL. = ASSIGN CAT      ROW = TRUE CAT

R DEC	1.3	1.4	2.3	2.4	2.5	2.6	7.2	TOTAL	ERR	ERR
UNKNW	0 26667	19271	50182		0 15793		n 18512	130425	0	0
1.3	0 6911	0	45		0 0		n 0	6956	45	1
1.4	0 0	2499	171		0 0		n 0	2670	171	6
2.3	0 0	0	7727		0 0		n 0	7727	0	0
2.4	0 629	0	0		0 0		n 0	629	629	100
2.5	0 351	0	1157		0 2526		n 0	4034	1508	37
2.6	0 0	0	1228		0 206		n 0	1434	1434	100
7.2	0 0	0	0		0 0		n 5625	5625	0	0
TOTAL	0 34558	21770	60510		0 18525		n 24137	159500	3787	34
ERR	0 980	0	2601		0 206		n 0	3787	*****	*****
FRR	0 12	0	25		0 8		n 0	6	*****	*****

Table VI.6 The contingency table of the best 2 band pairs after 4-fill, 8-fill, 4-shrink, 8-shrink, 4-shrink, 8-shrink and complete filling operations.

ORIGINAL PAGE IS  
OF POOR QUALITY

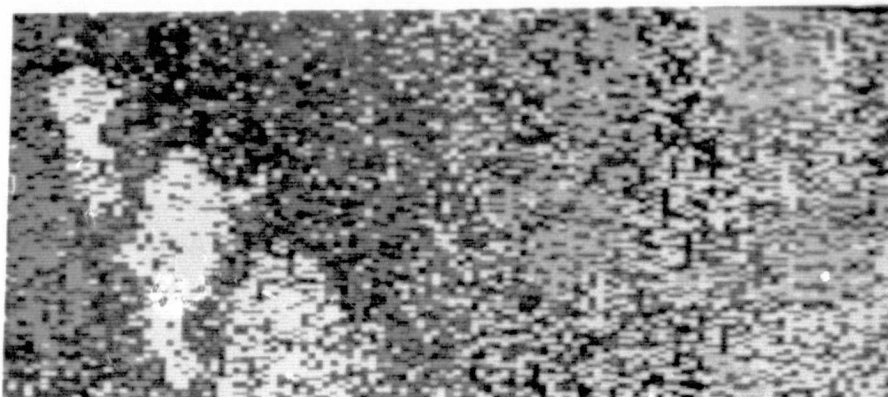


Figure VI.7 The classification of the three best band pairs for alpha - beta thresholds of .6 and .042.

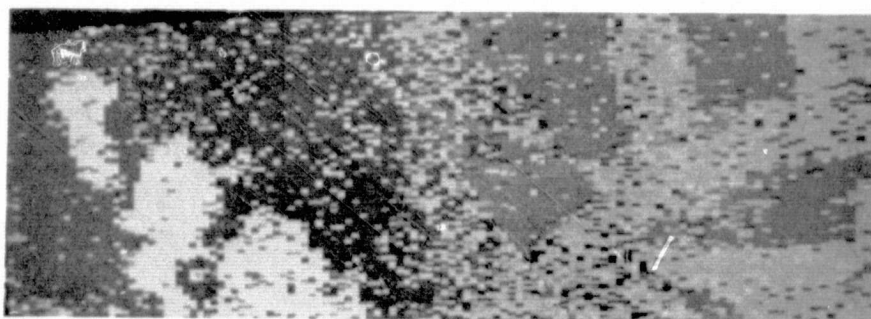


Figure VI.8 The classified image of Figure VI.7 after a complete filling.

CONTINGENCY TABLE FOR SAMH21GDT - 1 SAMH2BB02 - 1 SCALE FACTOR 10\*\* 0

COL. = ASSIGN CAT      ROW = TRUE CAT

R DEC	1.3	1.4	2.3	2.4	2.5	2.6	7.2	TOTAL	ERR	ERR	
UNKWN	60679	15894	9302	14353	390	15106	4988	9713	130425	0	0
1.3	2903	3387	113	74	66	157	117	139	6956	666	16
1.4	750	34	1807	7	0	43	22	7	2670	113	6
2.3	2541	139	7	4521	2	339	137	41	7727	665	13
2.4	311	217	13	4	23	31	21	9	629	295	93
2.5	1879	260	20	84	3	1535	246	7	4034	620	29
2.6	754	137	6	83	2	290	152	10	1434	528	78
7.2	1683	115	119	47	2	1	5	3653	5625	289	7
TOTAL	71500	20183	11387	19173	488	17502	5688	13579	159500	3176	34
ERR	0	902	278	299	75	861	548	213	3176	*****	*****
ERR	0	21	13	6	77	36	78	6	33	*****	*****

Table VI.7 The contingency table of the best 3 band pairs for alpha - beta thresholds of .6 and .042.

CONTINGENCY TABLE FOR SAMH2 GDT - 1 SMH2F7B02 - 1 SCALE FACTOR 10\*\* 0

COL. = ASSIGN CAT      ROW = TRUE CAT

R DEC	1.3	1.4	2.3	2.4	2.5	2.6	7.2	TOTAL	ERR	ERR	
UNKWN	0	30672	20097	23471	819	29310	9972	16134	130425	0	0
1.3	0	5716	260	132	117	279	194	258	6956	1240	18
1.4	0	63	2433	16	0	100	46	12	2670	237	9
2.3	0	287	13	6444	3	554	264	62	7727	1283	17
2.4	0	414	24	10	53	66	42	20	629	576	92
2.5	0	472	41	195	4	2799	511	12	4034	1235	31
2.6	0	273	9	184	3	618	330	17	1434	1104	77
7.2	0	253	294	77	5	5	6	4985	5625	640	11
TOTAL	0	38100	23171	30529	1004	33831	11365	21500	159500	6315	36
ERR	0	1762	641	614	132	1722	1063	381	6315	*****	*****
ERR	0	24	21	9	71	38	76	7	35	*****	*****

Table VI.8 The contingency table of the best 3 band pairs after a complete filling.

ORIGINAL PAGE IS  
OF POOR QUALITY

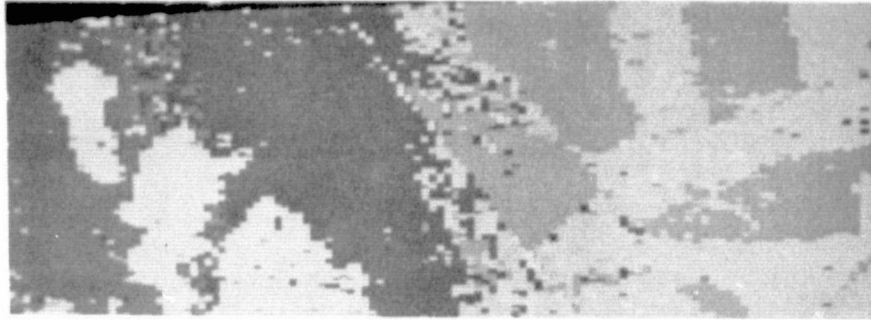


Figure VI.9 The classified image of Figure VI.8 after a 4-shrink operation and then a complete filling.

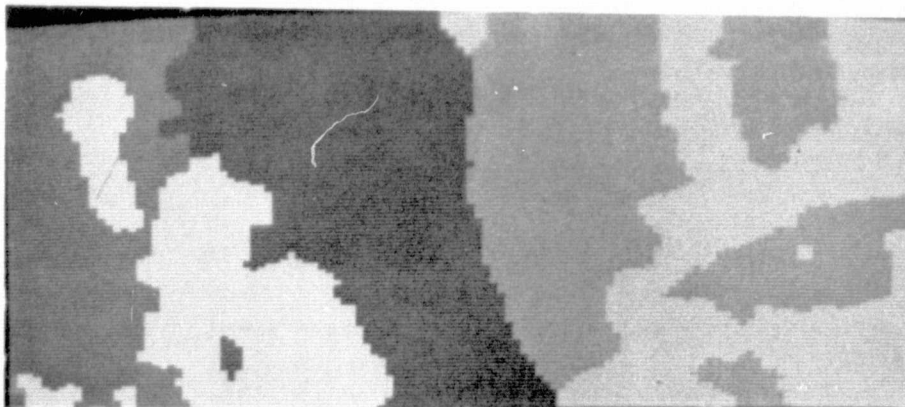


Figure VI.10 The classified image of Figure VI.7 after 4-fill, 8-fill, 4-shrink, 8-shrink and complete filling operations.

CONTINGENCY TABLE FOR SAMH2 GDT - 1 SMH2F8B02 - 1 SCALE FACTOR 10\*\* 0

COL. = ASSIGN CAT      ROW = TRUE CAT

	R DEC	1.3	1.4	2.3	2.4	2.5	2.6	7.2	TOTAL	FRR	ERR
UNKN	0	31497	20434	24952	73	33093	4516	15859	130425	0	0
1.3	0	6745	122	19	0	9	15	46	6956	211	3
1.4	0	30	2490	16	0	111	10	4	2670	180	7
2.3	0	53	0	7141	0	525	9	0	7727	586	8
2.4	0	590	0	0	34	0	5	0	629	555	95
2.5	0	374	0	108	0	3417	134	1	4034	617	15
2.6	0	283	0	211	0	774	166	0	1434	1268	88
7.2	0	118	180	0	0	0	0	5327	5625	258	5
TOTAL	0	39690	23226	32448	107	37929	4863	21237	159500	3755	31
ERR	0	1448	302	354	0	1419	181	51	3755	*****	*****
FRR	0	18	11	5	0	29	57	1	16	*****	*****

Table VI.9 The contingency table of the best 3 band pairs after complete filling, 4-shrink, and complete filling operations.

CONTINGENCY TABLE FOR SAMH2 GDT - 1 SMH2F0B02 - 1 SCALE FACTOR 10\*\* 0

COL. = ASSIGN CAT      ROW = TRUE CAT

	R DEC	1.3	1.4	2.3	2.4	2.5	2.6	7.2	TOTAL	FRR	ERR
UNKN	0	31595	19955	32859	0	29219	0	16797	130425	0	0
1.3	0	6956	0	0	0	0	0	0	6956	0	0
1.4	0	0	2499	171	0	0	0	0	2670	171	6
2.3	0	0	0	7644	0	83	0	0	7727	83	1
2.4	0	629	0	0	0	0	0	0	629	629	100
2.5	0	351	0	27	0	3656	0	0	4034	378	9
2.6	0	0	0	825	0	609	0	0	1434	1434	100
7.2	0	0	15	0	0	0	0	5610	5625	15	0
TOTAL	0	34531	22469	41526	0	33567	0	22407	159500	2710	30
FRR	0	980	15	1023	0	692	0	0	2710	*****	*****
FRR	0	17	1	12	0	16	0	0	5	*****	*****

Table VI.10 The contingency table of the best 3 band pairs after 4-fill, 8-fill, 4-shrink, 8-shrink, and complete filling operations.

ORIGINAL PAGE IS  
OF POOR QUALITY

CONTINGENCY TABLE FOR SAMH2 GDT - 1 SMH2F6B02 - 1 SCALE FACTOR 10\*\* 0

COL. = ASSIGN CAT ROW = TRUE CAT

	R DEC	1.3	1.4	2.3	2.4	2.5	2.6	7.2	TOTAL	ERR	ERR	
UNKNOWN	0	23561	18825	55311		0	11429	0	21299	130425	0	0
1.3	0	6948	8	0		0	0	0	0	6956	8	0
1.4	0	0	2499	171		0	0	0	0	2670	171	6
2.3	0	0	0	7727		0	0	0	0	7727	0	0
2.4	0	629	0	0		0	0	0	0	629	629	100
2.5	0	31	0	1905		0	2098	0	0	4034	1936	48
2.6	0	0	0	1408		0	26	0	0	1434	1434	100
7.2	0	0	14	0		0	0	0	5611	5625	14	0
TOTAL	0	31169	21346	66522		0	13553	0	26910	159500	4192	36
FRR	0	660	22	3484		0	26	0	0	4192	*****	*****
FRR	0	9	1	31		0	1	0	0	6	*****	*****

Table VI.11 The contingency table of the best 3 band pairs after 4-fill, 8-fill, 4-shrink, 8-shrink, 4-shrink, 8-shrink and complete filling operations.

ORIGINAL PAGE IS  
OF POOR QUALITY

## VII Spectral Analysis: Edit 9

Using the same initial six spectral bands to select features from, the feature selector chose band pairs .40 - .44 and .65 - .69 with .72 - .76 and .981 - 1.045 micrometers as the best 2 band pairs for the table look-up rule. Figure VII.1 shows the .72 - .76 micrometer band and Figure VII.2 shows the ground truth training data overlaid on this band. The alpha-beta thresholds were set at .3 and .021.

The contingency table (Table VII.1) for the best 2 band pairs classification with an alpha threshold of .3 and a beta threshold of .021 gave a misidentification error rate of 22% and a false identification error rate of 32%. There were 79,670 reserved assignments because of incompatible assignments between the first and second band pairs and 2,357 were reserved assignments because there was more than one possible assignment common to the two band pairs. The raw classified image is shown in Figure VII.3. The main cause of error is the confusion between category 1.3, shortleaf pine, and category 2.5, loblolly pine. This error is due to assigning category 1.3 when the true category is 2.5. A look at the timber stand map for edit #9 shows a patch of category 2.5, which is surrounded by category 1.3, in the lower right-hand corner. It is this area that gets misassigned the most.

If the classified image is filled so that all resolution cells whose category assignment was reserved is assigned to the category of its spatially nearest resolution cell neighbor which is assigned, the error rate remains substantially the same, about a 25% misidentification error rate and 32% false identification error rate (Figure VII.4 and Table VII.2) If we do 6 iterations of 4-fills and then do a 4-shrink and fill up, the resulting contingency table is Table VII.3. The misidentification and false identification error rates of 21% and 26% are lower than before, but the misidentification error rate category 2.5 went from 43% to 44% with category 1.3 still the problem.

The best 2 band pair results were obtained from doing a 4-shrink following the original classification and then filling (Figure VII.5). Table VII.4 shows a misidentification error rate of 14% and a false identification error rate of 17%, but still the misidentification of category 2.5 is the main cause of error. The

shrinking first does eliminate a significant amount of error between category 3.1, laurel oak, and category 4.2, low quality sweetgum. Neither procedure has trouble classifying category 2.5 on the left-side of the timber stand. Only on the right side where category 2.5 resembles category 1.3 spectrally is there confusion. This confusion could be ultimately due to sun angle.

The three best band pairs were:

- (1) .40 - .44 and .65 - .69 micrometers
- (2) .72 - .76 and .981 - 1.045 micrometers
- (3) .40 - .44 and 2.10 - 2.36 micrometers

Figure VII.6 shows a plot of the alpha threshold versus the number of reserved decisions. For the three best band pairs, the alpha and beta thresholds that minimized the number of reserved decisions was .6 and .042, respectively. The raw classified image is shown in Figure VII.7. The contingency table indicates a misidentification error of 24% and a false identification error of 30% (Table VII.5).

After a complete filling, there was a 25% misidentification and 32% false identification error rate (Figure VII.8 and Table VII.6). If instead, our post processing consisted of a 4-fill, 8-fill, 4-shrink, 8-shrink and then a complete filling the misidentification error rate was 9% and the false identification error rate was 9% (Table VII.7 and Figure VII.9).

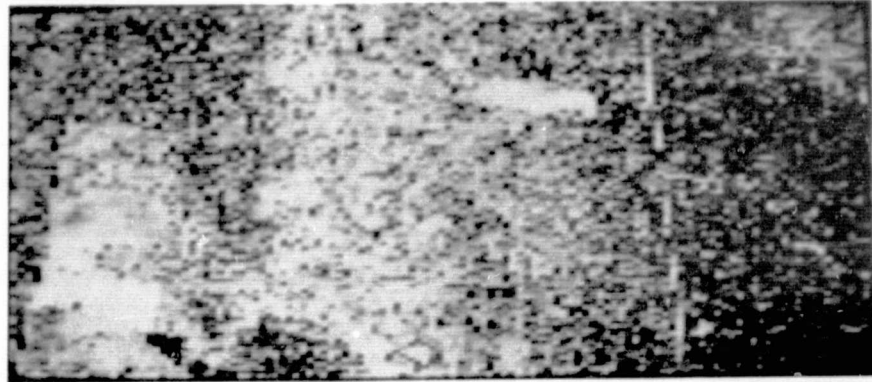


Figure VII.1 The .72 - .76 micrometer band.

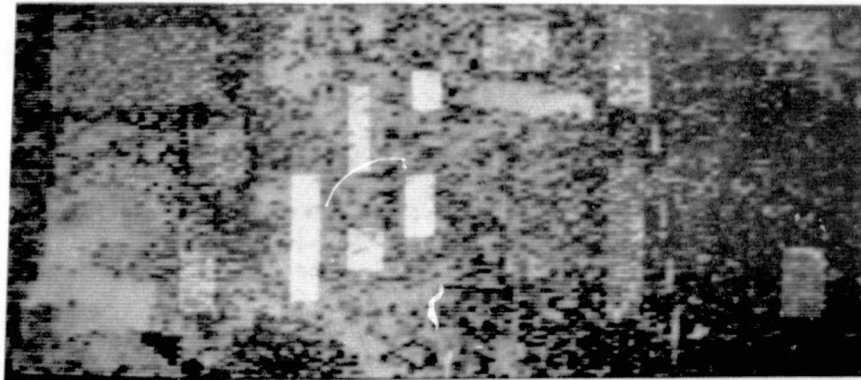


Figure VII.2 The ground truth training data overlaid on the .72 - .76 micrometer band.

CONTINGENCY TABLE FOR SAMH34GID - 1 --- SAH3BC71 - 1

COL. = ASSIGN CAT      ROW = TRUE    CAT

	R DEC	1.3	2.3	2.5	2.6	3.1	4.2	7.2	TOTAL	ERR	ERR
UNKN	0	13754	1414	9975	7423	3256	4815	5798	116183	0	0
1.3	2992	5476	129	86	35	0	0	7	8685	257	4
2.3	584	15	272	2	6	0	1	25	925	49	14
2.5	5327	1705	200	2614	715	13	80	16	11679	2738	43
2.6	1625	12	25	211	586	27	70	19	2645	364	33
3.1	816	0	0	2	27	599	66	18	1527	112	16
4.2	966	0	0	29	41	184	472	12	1791	262	36
7.2	627	0	3	0	12	6	20	526	1205	50	9
TOTAL	8227	21162	2463	13719	8845	4181	5542	6411	144550	3832	22
ERR	0	1732	357	340	836	226	254	97	3832	*****	*****
ERR	0	24	55	8	59	27	35	16	32	*****	*****

50

Table VII.1 The contingency table of the best 2 band pairs for alpha - beta thresholds of .3 and .021.

CONTINGENCY TABLE FOR SAMH3 GDT - 1 SMH3F1C71 - 1 SCALE FACTOR 10\*\* 0

COL. = ASSIGN CAT      ROW = TRUE    CAT

	R DEC	1.3	2.3	2.5	2.6	3.1	4.2	7.2	TOTAL	#ERR	% ERR
UNKN	0	26128	5502	21805	20888	8814	13025	20021	116183	0	0
1.3	0	8197	236	164	69	0	0	19	8685	488	6
2.3	0	50	789	6	19	0	6	55	925	136	15
2.5	0	3657	471	6072	1257	21	167	34	11679	5607	48
2.6	0	44	83	511	1621	96	215	75	2645	1024	39
3.1	0	0	0	6	97	1185	174	65	1527	342	22
4.2	0	0	0	61	99	393	1121	27	1701	580	34
7.2	0	0	6	0	42	16	87	1054	1205	151	13
TOTAL	0	38076	7087	28625	24092	10525	14795	21350	144550	8328	25
#ERR	0	3751	796	748	1583	526	649	275	8328	*****	*****
% ERR	0	31	50	11	49	31	37	21	32	*****	*****

Table VII.2 The contingency table of the best 2 band pairs after a complete filling.

ORIGINAL PAGE IS OF POOR QUALITY

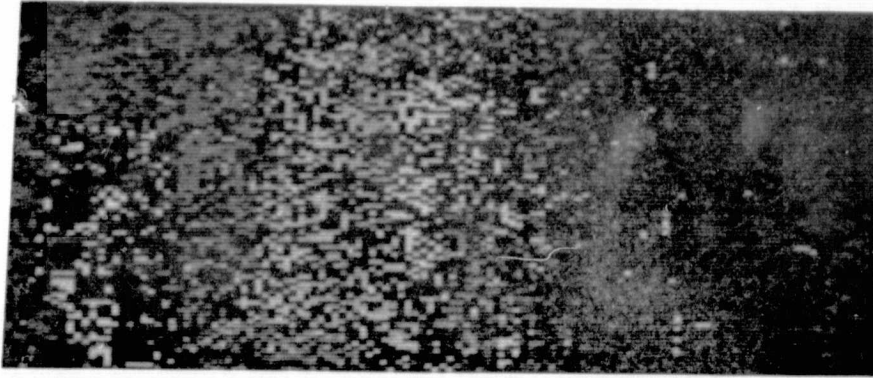


Figure VII.3 The classification of the best two band pairs for alpha - beta thresholds of .3 and .021.

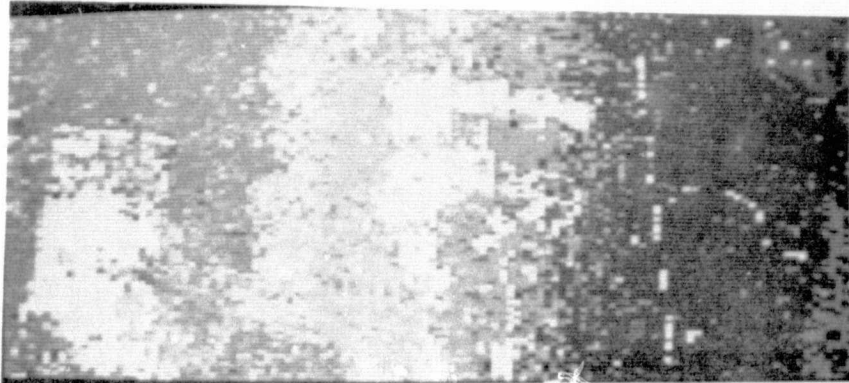


Figure VII.4 The classified image of Figure VII.3 after a complete filling.

CONTINGENCY TABLE FOR SAMH34GTD - 1 --- SMH3E7C71 - 1

		COL. = ASSIGN CAT							ROW = TRUE CAT		
	R DEC	1.3	2.3	2.5	2.6	3.1	4.2	7.2	TOTAL	ERR.	ERR
UNKNWN	0	27122	4879	22124	20345	8679	12850	20165	116183	0	0
1.3	0	8463	121	61	22	0	0	0	8685	222	3
2.3	0	44	827	3	10	0	7	34	925	93	11
2.5	0	3940	381	6486	793	2	50	18	11679	5193	44
2.6	0	27	81	492	1723	88	171	63	2645	922	35
3.1	0	0	0	2	86	1243	144	52	1527	284	19
4.2	0	0	0	29	74	332	1251	15	1701	457	26
7.2	0	0	5	0	37	6	70	1078	1205	127	11
TOTAL	0	39596	6303	29207	23090	10350	14570	21424	144550	7205	21
ERR	0	4011	597	587	1022	428	460	191	7296	*****	*****
ERR	0	32	42	8	37	26	27	15	26	*****	*****

Table VII.3 The contingency table of the best 2 band pairs after complete filling, 4-shrink, and complete filling operations.

CONTINGENCY TABLE FOR SAMH34GTD - 1 --- SMH3E9C71 - 1

		COL. = ASSIGN CAT							ROW = TRUE CAT		
	R DEC	1.3	2.3	2.5	2.6	3.1	4.2	7.2	TOTAL	ERR	ERR
UNKNWN	0	28958	3222	22459	19124	8025	11277	23118	116183	0	0
1.3	0	8629	41	15	0	0	0	0	8685	56	1
2.3	0	29	882	0	0	0	0	13	925	42	5
2.5	0	4353	227	6781	309	0	0	9	11679	4893	42
2.6	0	0	89	476	1959	42	77	2	2645	683	26
3.1	0	0	0	0	0	1360	105	62	1527	167	11
4.2	0	0	0	31	22	196	1452	0	1701	242	15
7.2	0	0	0	0	6	0	35	1164	1205	41	3
TOTAL	0	41269	4462	29762	21420	9623	12946	24368	144550	6132	14
ERR	0	4382	357	522	337	238	217	86	6139	*****	*****
ERR	0	34	29	7	15	15	13	7	17	*****	*****

Table VII.4 The contingency table of the best 2 band pairs after 4-shrink, and complete filling operations.

FINAL PAGE IS  
POOR QUALITY

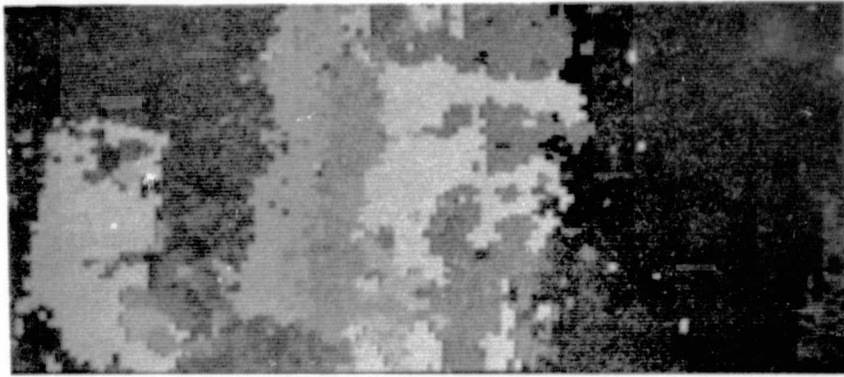


Figure VII.5 The classified image of Figure VII.3 after 4-shrink and complete filling operations.

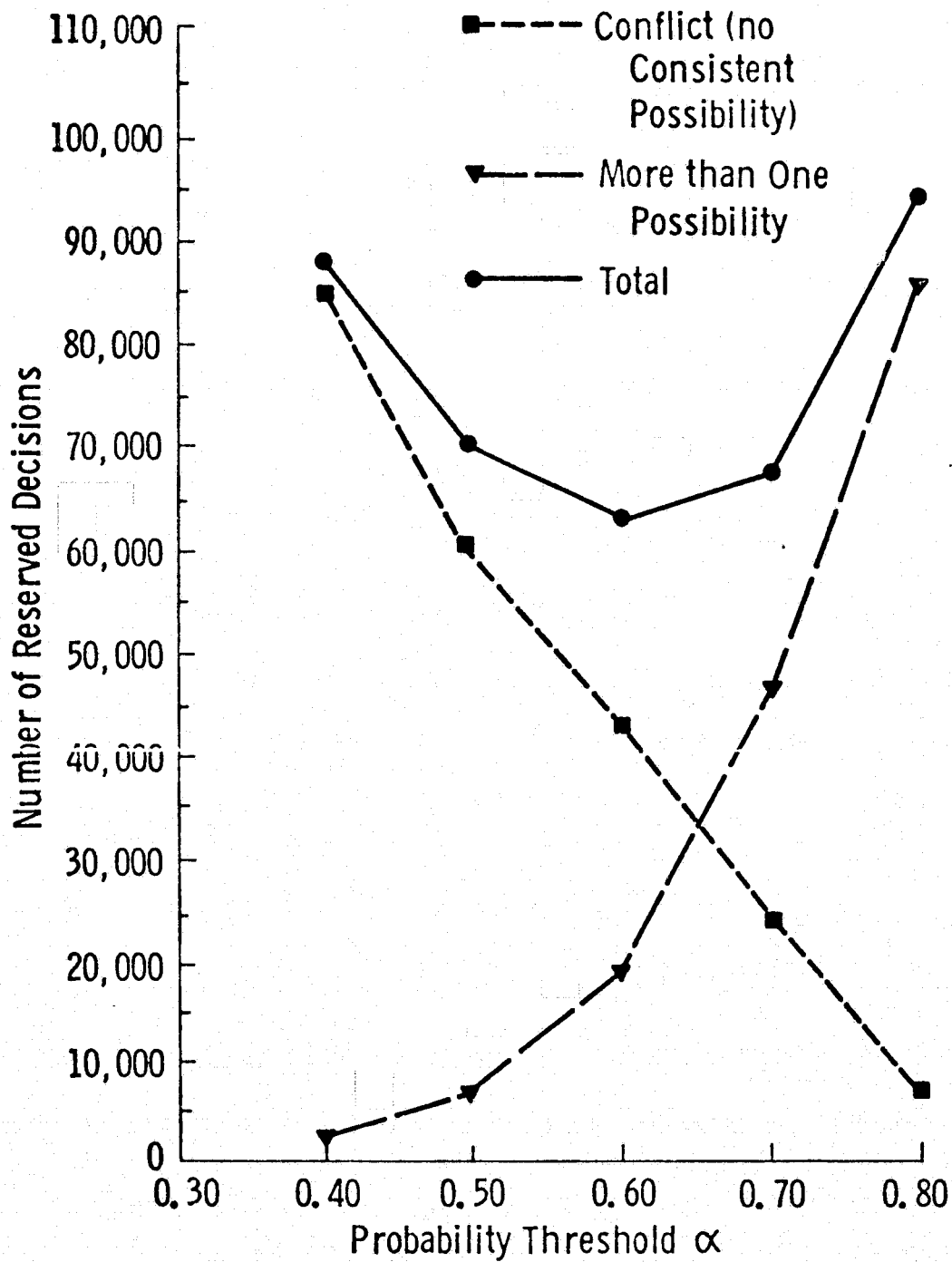


Figure VII.6 A plot of the alpha thresholds versus number of reserved decisions

CONTINGENCY TABLE FOR SAMH34GTD - 1 --- SAMH3BB04 - 1

---

COL. = ASSIGN CAT      ROW = TRUE CAT

---

	R DEC	1.3	2.3	2.5	2.6	3.1	4.2	7.2	TOTAL	ERR	ERR
UNKWN	52820	17881	2536	12053	10805	5216	6084	8789	116183	0	0
1.3	1755	6450	119	253	98	0	1	9	8685	480	7
2.3	402	16	425	12	17	4	0	49	925	98	19
2.5	4894	2219	198	3700	507	11	127	23	11679	3085	45
2.6	1348	9	41	265	789	50	114	24	2645	508	39
3.1	591	0	0	13	41	722	134	26	1527	214	23
4.2	723	0	2	37	45	154	727	18	1701	256	26
7.2	436	0	8	0	13	32	18	698	1205	71	9
TOTAL	62969	26575	3329	16333	12315	6189	7204	9636	144550	4712	24
ERR	0	2244	368	580	721	251	399	149	4712	*****	*****
ERR	0	26	46	14	48	26	36	18	30	*****	*****

Table VII.5 The contingency table of the best 3 band pairs for alpha - beta thresholds of .6 and .042.

CONTINGENCY TABLE FOR SAMH3 GDT - 1 SMH3F1B04 - 1 SCALE FACTOR 10\*\* 0

---

COL. = ASSIGN CAT      ROW = TRUE CAT

---

	R DEC	1.3	2.3	2.5	2.6	3.1	4.2	7.2	TOTAL	#ERR	% ERR
UNKWN	0	24910	4982	23392	22411	10315	11921	18252	116183	0	0
1.3	0	7945	195	389	139	0	1	16	8685	740	9
2.3	0	27	748	31	32	8	0	79	925	177	19
2.5	0	3293	332	6730	1001	16	267	40	11679	4949	42
2.6	0	16	79	566	1532	130	268	54	2645	1113	42
3.1	0	0	0	29	78	1137	229	54	1527	390	26
4.2	0	0	6	59	86	278	1226	46	1701	475	28
7.2	0	0	12	0	29	60	33	1071	1205	134	11
TOTAL	0	36191	6354	31196	25308	11944	13945	19612	144550	7978	25
#ERR	0	3336	624	1074	1365	492	798	289	7978	*****	*****
% ERR	0	30	45	14	47	30	39	21	32	*****	*****

Table VII.6 The contingency table of the best 3 band pairs after a complete filling.

ORIGINAL PAGE IS  
OF POOR QUALITY

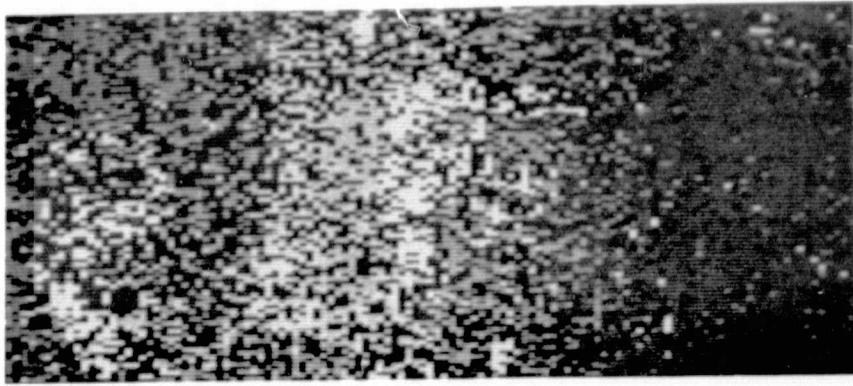


Figure VII.7 The classification of the three best band pairs for alpha - beta thresholds of .6 and .042.

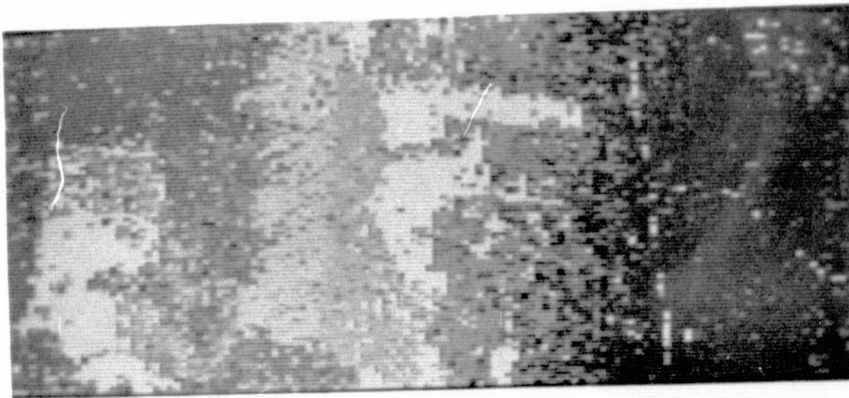


Figure VII.8 The classified image of Figure VII.7 after a complete filling.

COL. = ASSIGN CAT      ROW = TRUE    CAT

	R DEC	1. 3	2. 3	2. 5	2. 6	3. 1	4. 2	7. 2	TOTAL	#ERR	% ERR
UNKWN	0	30218	2169	21299	17317	8203	10275	26702	116183	0	0
1. 3	0	8685	0	0	0	0	0	0	8685	0	0
2. 3	0	0	925	0	0	0	0	0	925	0	0
2. 5	0	4489	0	6906	0	0	0	284	11679	4773	41
2. 6	0	0	0	531	2039	0	7	68	2645	606	23
3. 1	0	0	0	0	0	1521	0	6	1527	6	0
4. 2	0	0	0	0	0	0	1701	0	1701	0	0
7. 2	0	0	0	0	0	0	0	1205	1205	0	0
TOTAL	0	43392	3094	28736	19356	9724	11983	28265	144550	5385	9
#ERR	0	4489	0	531	0	0	7	358	5385	*****	*****
% ERR	0	34	0	7	0	0	0	23	9	*****	*****

Table VII.7      The contingency table of the best 3 band pairs after 4-fill, 8-fill, 4-shrink, 8-shrink, and complete filling operations.

ORIGINAL PAGE IS  
OF POOR QUALITY

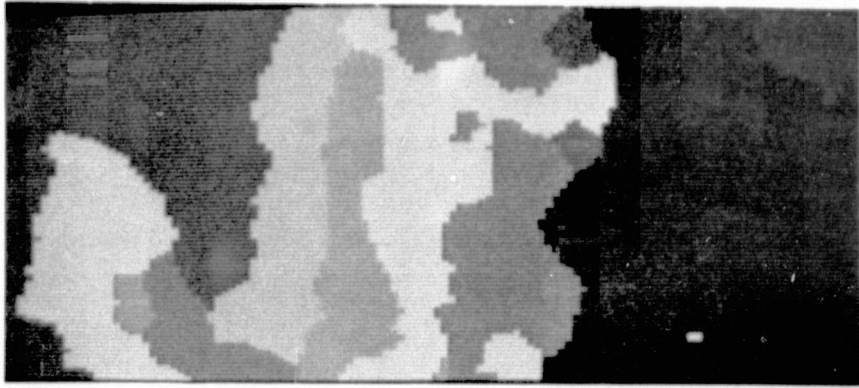


Figure VII.9 The classified image of Figure VII.7 after 4-fill, 8-fill, 4-shrink, 8-shrink, and complete filling operations.

### VIII Spectral Analysis: Edit 14

The same six spectral bands were chosen from edit #14 as were taken from edit #6 and edit #9. Figure VIII.1 shows the .72 - .76 micrometer band for edit 14 and Figure VIII.2 shows the selected ground truth training data. The selection procedure chose .40 - .44 and 2.10 - 2.36 with .588 - .643 and 2.10 - 2.36 micrometers as the best 2 band pairs for the table look-up rule. The alpha and beta thresholds were set at .3 and .021 respectively. The thresholds were too low and resulted in 56,320 reserved decisions in the contingency table for classification (Table VIII.1). The resulting misidentification error rate was 28% and false identification error rate was 29%. The result on the best 2 band pairs with 4-fill, 8-fill, 4-shrink, 8-shrink, and complete filling operations (Table VIII.2), was a misidentification error rate of 15% and a false identification error rate of 17%.

The feature selection procedure chose band pairs .40 - .44 and .65 - .69 micrometers, along with the best 2 band pairs for the best 3 band pairs. Using alpha and beta thresholds of .6 and .042, respectively, the number of reserved decisions was 43,236, with 25,794 points reserved because no assignment was possible and 17,442 reserved due to possible multiple assignments.

The largest cause of error for best 3 band pairs (Table VIII.3) was the confusion between categories 2.3 and 2.5, different ages of loblolly pine, and the confusion of each of these with category 4.1, low quality sweetgum. The misidentification and false identification error rates (46% and 48%) for category 4.1 are high but the number of points whose true category is 4.1 is small. Figure VIII.3 shows the resulting classification. There was such a small area of sweetgum, category 4.1, on the timber stand map that the ground truth may not be adequate to allow good spectral estimation.

The first post processing procedure we used was a complete filling (Table VIII.4 and Figure VIII.4). The errors were increased by the procedure, so one 4-shrink operation was performed on the image and this reduced the misidentification error to 9% and false identification error to 4% (Table VIII.5 and Figure VIII.5), but the low error rates were helped by the fact that there were 84,828 reserved decisions. Table VIII.5 does show that the confusion with category 4.1, was almost eliminated, though the misidentification error rate caused by assigning

2.3 to 2.5, 21% was still high. Completely filling the image resulted in a misidentification error rate of 17% and false identification error rate of 13% (Table VIII.6 and Figure VIII.6).

If on the raw classified image we do one 4-fill (Table VIII.7 and Figure VIII.7) and then one 8-fill, the resulting contingency table (Table VIII.8 and Figure VIII.8) is almost identical to Table VIII.3. The error rates on each are exactly the same. Then doing a 4-shrink (Table VIII.9 and Figure VIII.9) we find a contingency table almost identical to Table VIII.4. But if instead of filling we do an 8-shrink, we almost totally eliminate error (Table VIII.10 and Figure VIII.10). Only 2 points are incorrectly identified. Now if we completely fill the image we get our best results (Table VIII.11 and Figure VIII.11): 13% misidentification and 9% false identification error rates. Visual comparisons show the closeness of the two operations. Following the fills with a 4-shrink produces Figure VIII.5. Figure VIII.6 is the final classified image after complete filling, a 4-shrink and then a complete filling, while Figure VIII.11 is the final result of a 4-fill, 8-fill, 4-shrink, 8-shrink, and complete filling. From the figures, we can see that the extra shrink allowed the categories to be more dense. The contingency table of the image should show better results since the categories on the timber stand map tend to be dense, which is the case.

The results of the shrinking operations indicate that the errors that did occur were sparse enough to be wiped out with the shrinking. The reason that a shrink operation is not performed first on the image is that it tends to eliminate small area categories, even though correctly assigned, on the image.

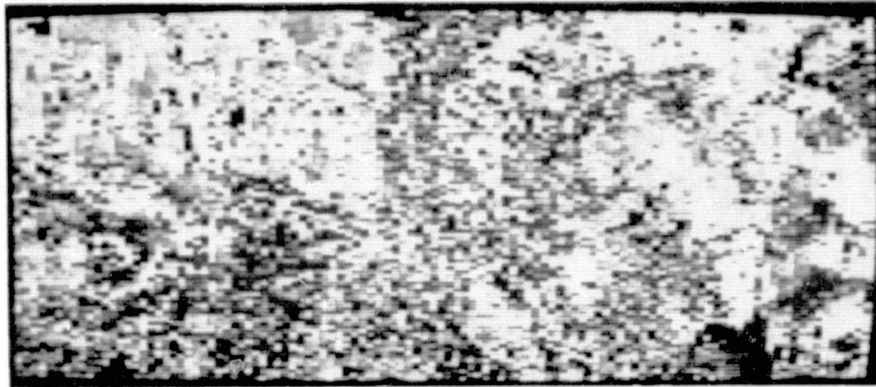


Figure VIII.1 The .72 - .76 micrometer band.

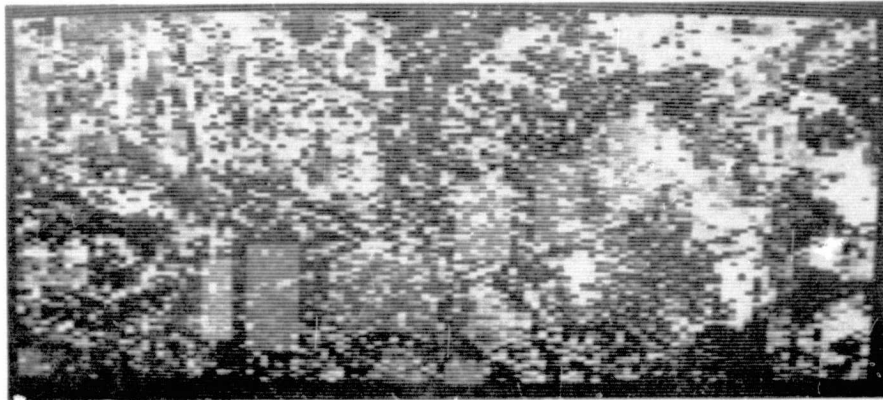


Figure VIII.2 The ground truth training data overlaid on the .72 - .76 micrometer band.

CONTINGENCY TABLE FOR SAMH4 GDT - 1 SAMH4 R05 - 1 SCALE FACTOR 10\*\* 0

		COL. = ASSIGN CAT				ROW = TRUE CAT			
R DEC	2.3	2.5	4.1	7.2	TOTAL	FRR	FRR	SD	
UNKWN	1893	8418	19856	13565	29402	123134	0	0	
2.3	1959	1553	739	515	209	4975	1462	49	
2.5	958	196	3567	193	64	4978	452	11	
4.1	765	233	147	594	10	1749	390	40	
7.2	745	81	158	75	1855	2914	314	14	
TOTAL	56320	10481	24467	14942	31540	137750	2620	28	
FRR	0	510	1044	783	283	2620	*****	*****	
FRR	0	25	23	57	13	29	*****	*****	

Table VIII.1 The contingency table of the best 2 band pairs for alpha - beta thresholds of .3 and .021.

CONTINGENCY TABLE FOR SAMH4 GDT - 1 SMH4F5B05 - 1 SCALE FACTOR 10\*\* 0

		COL. = ASSIGN CAT				ROW = TRUE CAT			
R DEC	2.3	2.5	4.1	7.2	TOTAL	FRR	ERR	SD	
UNKWN	0	6857	41525	18750	56002	123134	0	0	
2.3	0	2680	1234	1061	0	4975	2295	46	
2.5	0	130	4848	0	0	4978	130	3	
4.1	0	0	128	1621	0	1749	128	7	
7.2	0	0	195	0	2719	2914	195	7	
TOTAL	0	9667	47930	21432	58721	137750	2748	15	
ERR	0	130	1557	1061	0	2748	*****	*****	
ERR	0	5	24	40	0	17	*****	*****	

Table VIII.2 The contingency table of the best 2 band pairs after 4-fill, 8-fill, 4-shrink, 8-shrink, and complete filling operations.

CONTINGENCY TABLE FOR SAMH4 GDT - 1 SAMH4 B06 - 1 SCALE FACTOR 10\*\* 0

	COL. = ASSIGN CAT					ROW =	TRUE	CAT	
R DEC	2.3	2.5	4.1	7.2	TOTAL	ERR	ERR	SD	
UNKWN	39754	14646	23477	10471	34786	123134	0	0	0
2.3	1568	1931	782	391	303	4975	1476	43	0
2.5	717	364	3725	109	63	4978	536	13	0
4.1	664	323	151	590	21	1749	495	46	1
7.2	533	249	218	36	1878	2914	502	21	0
TOTAL	43236	17513	28353	11597	37051	137750	2010	30	0
FRR	0	936	1151	536	387	3010	*****	*****	*****
ERR	0	33	24	48	17	30	*****	*****	*****

Table VIII.3 The contingency table of the best 3 band pairs for alpha - beta thresholds of .6 and .042.

CONTINGENCY TABLE FOR SAMH4 GDT - 1 SMH4F1806 - 1 SCALE FACTOR 10\*\* 0

	COL. = ASSIGN CAT					ROW =	TRUE	CAT	
R DEC	2.3	2.5	4.1	7.2	TOTAL	ERR	ERR	SD	
UNKWN	0	23690	31739	17232	50473	123134	0	0	0
2.3	0	2832	1115	576	452	4975	2142	43	0
2.5	0	497	4227	157	97	4978	751	15	0
4.1	0	507	260	951	31	1749	792	46	1
7.2	0	364	289	56	2205	2914	700	24	0
TOTAL	0	27890	37630	18972	53258	137750	4401	32	0
FRR	0	1368	1664	789	580	4401	*****	*****	*****
ERR	0	33	28	45	21	31	*****	*****	*****

Table VIII.4 The contingency table of the best 3 band pairs after a complete filling.

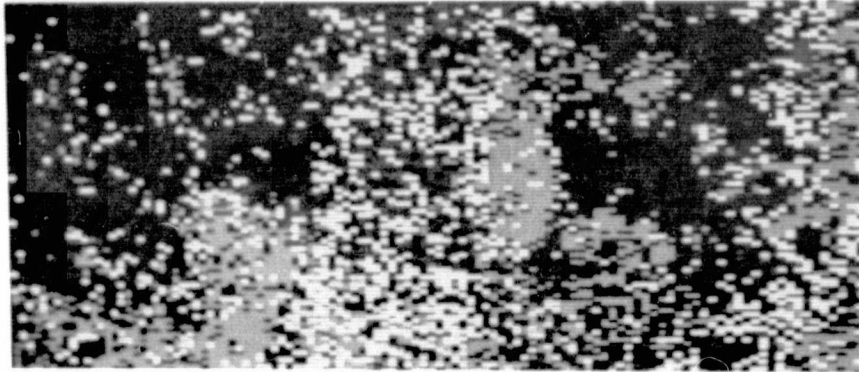


Figure VIII.3 The classification of the three best band pairs for alpha-beta thresholds of .6 and .042.

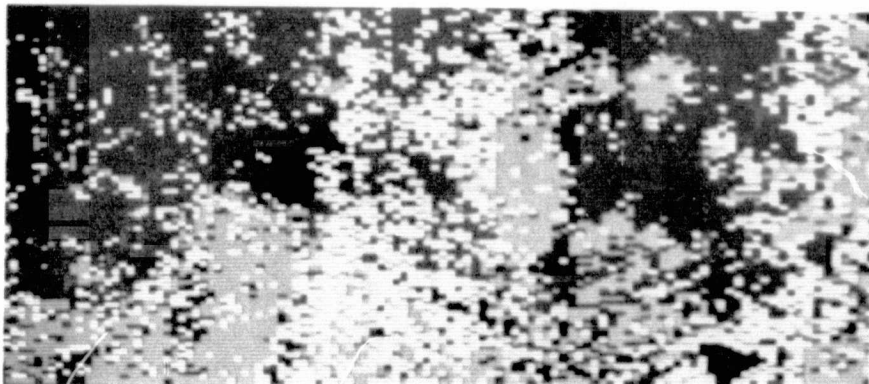


Figure VIII.4 The classified image of Figure VIII.3 after a complete filling.

CONTINGENCY TABLE FOR SAMH4 GDT - 1 SMH4S1B06 - 1 SCALE FACTOR 10\*\* 0

		COL. = ASSIGN CAT				ROW = TRUE CAT		
R DEC	2.3	2.5	4.1	7.2	TOTAL	FRP	ERR	SD
UNKWN	75944	2744	12650	3200	28497	123134	0	0
2.3	4095	697	119	6	58	4975	182	21
2.5	1977	10	2984	4	3	4978	17	1
4.1	1421	29	10	289	0	1749	30	12
7.2	1391	10	35	0	1478	2914	45	3
TOTAL	84828	3490	15708	3598	30036	137750	284	9
ERR	0	49	164	10	61	284	*****	*****
FRR	0	7	5	2	4	4	*****	*****

Table VIII.5 The contingency table of the best 3 band pairs after complete filling and 4-shrink operations.

CONTINGENCY TABLE FOR SAMH4 GDT - 1 SMH4F2B06 - 1 SCALE FACTOR 10\*\* 0

		COL. = ASSIGN CAT				ROW = TRUE CAT		
R DEC	2.3	2.5	4.1	7.2	TOTAL	ERP	ERR	SD
UNKWN	0	18379	36805	12408	55542	123134	0	0
2.3	0	3728	849	75	323	4975	1247	25
2.5	0	130	4810	19	19	4978	168	3
4.1	0	338	162	1249	0	1749	500	29
7.2	0	90	320	0	2504	2914	410	14
TOTAL	0	22665	42946	13751	58388	137750	2325	17
ERR	0	558	1331	94	342	2325	*****	*****
FRR	0	13	22	7	12	13	*****	*****

Table VIII.6 The contingency table of the best 3 band pairs after complete filling, 4-shrink, and complete filling operations.

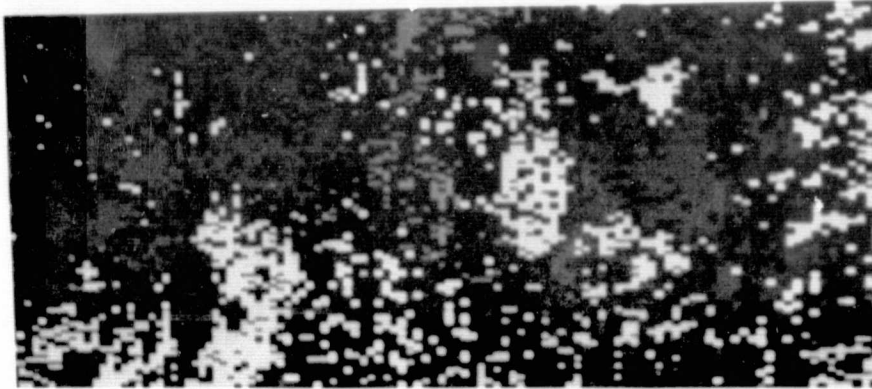


Figure VIII.5 The classified image of Figure VIII.4 after a 4-shrink operation.

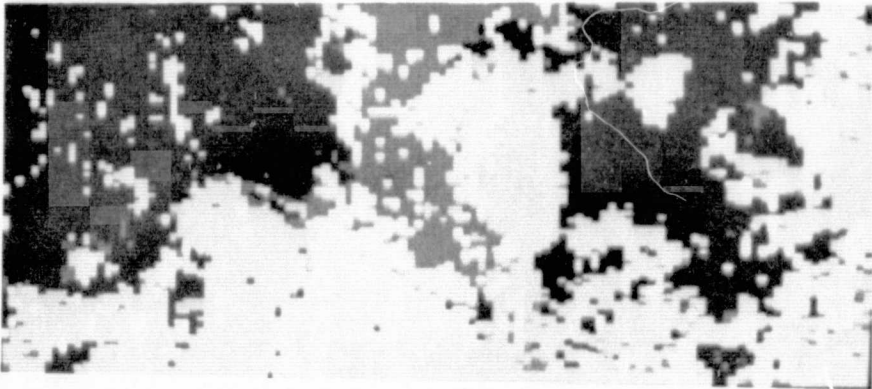


Figure VIII.6 The classified image of Figure VIII.5 after a complete filling.

CONTINGENCY TABLE FOR SAMH4 GDT - 1 SMH4F3B06 - 1 SCALE FACTOR 10\*\* 0

	COL. = ASSIGN CAT					ROW = TRUE	CAT		
	R DEC	2.3	2.5	4.1	7.2	TOTAL	ERR	ERR	SD
UNKWN	2375	2332	31470	16785	49202	123134	0	0	0
2.3	23	2821	1111	573	447	4975	2131	43	0
2.5	19	495	4216	154	94	4978	742	15	0
4.1	16	52	258	242	31	1749	791	46	1
7.2	6	363	289	55	2201	2914	707	24	0
TOTAL	2439	27483	37344	18509	51975	137750	4375	32	0
FRR	0	1360	1658	782	572	4372	*****	*****	*****
FRR	0	33	28	45	21	31	*****	*****	*****

Table VIII.7 The contingency table of the best 3 band pairs after a 4-fill operation.

CONTINGENCY TABLE FOR SAMH4 GDT - 1 SMH4F4B06 - 1 SCALE FACTOR 10\*\* 0

	COL. = ASSIGN CAT					ROW = TRUE	CAT		
	R DEC	2.3	2.5	4.1	7.2	TOTAL	ERR	ERR	SD
UNKWN	116	23687	31735	17192	50404	123134	0	0	0
2.3	0	2832	1115	576	452	4975	2142	43	0
2.5	0	497	4227	157	97	4978	751	15	0
4.1	0	507	260	951	31	1749	798	46	1
7.2	0	364	289	56	2205	2914	700	24	0
TOTAL	116	27887	37626	18922	53189	137750	4401	32	0
FRR	0	1368	1664	789	580	4401	*****	*****	*****
FRR	0	33	28	45	21	31	*****	*****	*****

Table VIII.8 The contingency table of the best 3 band pairs after 4-fill, and 8-fill operations.

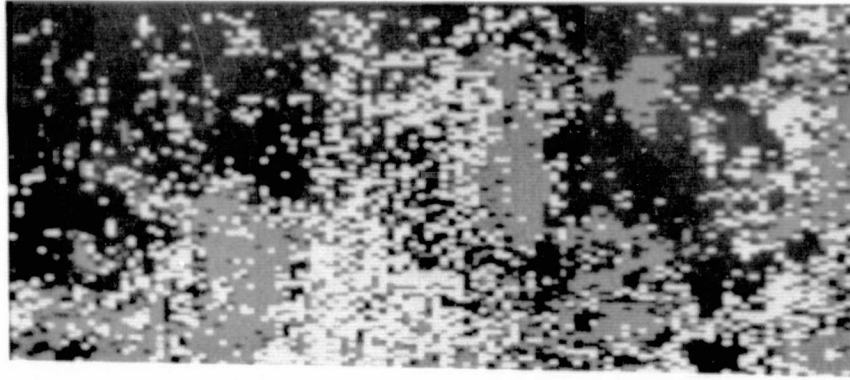


Figure VIII.7 The classified image of Figure VIII.3 after a 4-fill operation.

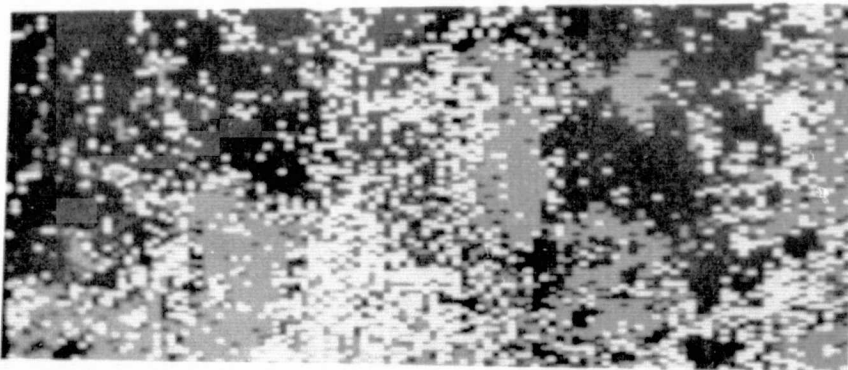


Figure VIII.8 The classified image of Figure VIII.3 after 4-fill and 8-fill operations.

CONTINGENCY TABLE FOR SAMH4 GDT - 1 SMH4S3R06 - 1 SCALE FACTOR 10\*\* 0

	COL. = ASSIGN CAT				ROW = TRUE	CAT		
R DFC	2.3	2.5	4.1	7.2	TOTAL	ERP	ERR	SD
UNKNOWN	76121	2744	12647	3259	28363	123134	0	0
2.3	4095	697	119	6	58	4975	183	21
2.5	1977	10	2984	4	3	4978	17	1
4.1	1421	29	10	289	0	1749	30	12
7.2	1391	10	35	0	1478	2914	45	3
TOTAL	85005	3490	15795	3558	29902	137750	284	9
FRR	0	49	164	10	61	284	*****	*****
FRR	0	7	5	3	4	4	*****	*****

Table VIII.9 The contingency table of the best 3 band pairs after 4-fill, 8-fill and 4-shrink operations.

CONTINGENCY TABLE FOR SAMH4 GDT - 1 SMH4S4R06 - 1 SCALE FACTOR 10\*\* 0

	COL. = ASSIGN CAT				ROW = TRUE	CAT		
R DFC	2.3	2.5	4.1	7.2	TOTAL	ERP	ERR	SD
UNKNOWN	*****	65	3448	567	13030	123134	0	0
2.3	4967	8	0	0	0	4975	0	0
2.5	3708	0	1270	0	0	4978	0	0
4.1	1737	0	0	12	0	1749	0	0
7.2	2270	0	2	0	642	2914	2	0
TOTAL	*****	73	4720	574	13672	137750	2	0
FRR	0	0	2	0	0	2	*****	*****
FRR	0	0	0	0	0	0	*****	*****

Table VIII.10 The contingency table of the best 3 band pairs after 4-fill, 8-fill, 4-shrink, and 8-shrink operations.

ORIGINAL PAGE IS  
OF POOR QUALITY

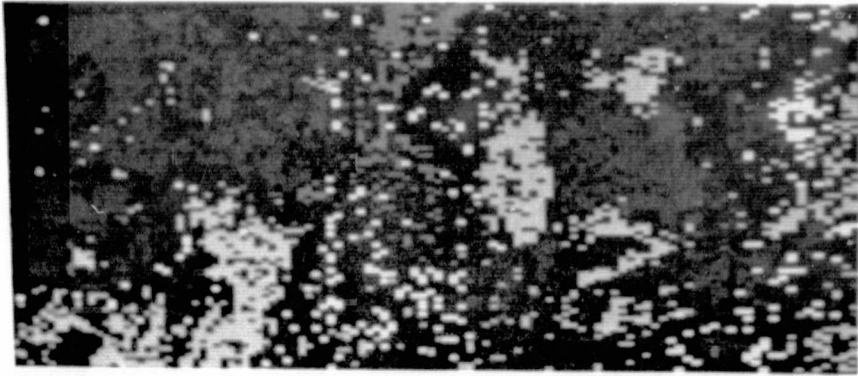


Figure VIII.9 The classified image of Figure VIII.3 after 4-fill, 8-fill, and 4-shrink operations.

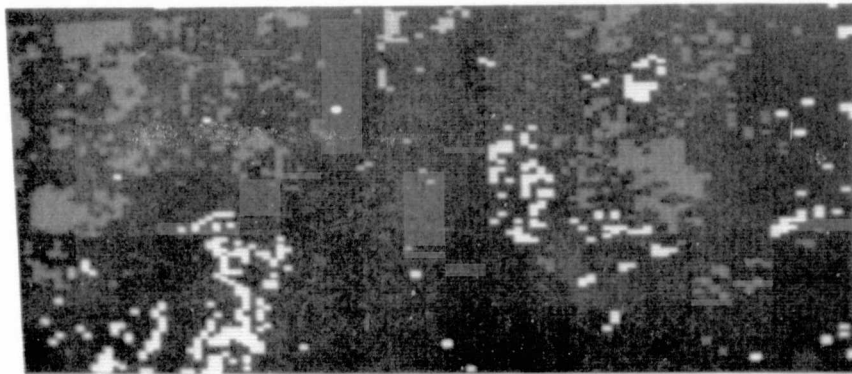


Figure VIII.10 The classified image of Figure VIII.3 after 4-fill, 8-fill, 4-shrink and 8-shrink operations.

CONTINGENCY TABLE FOR SAMH4 GDT - 1 SMH4F5B06 - 1 SCALE FACTOR 10\*\* 0

		COL. = ASSIGN CAT				ROW = TRUE		CAT	
	R DEC	2.3	2.5	4.1	7.2	TOTAL	ERR	ERR	SD
UNKNW	J	9922	39868	11186	62158	123134	0	0	0
2.3	0	4488	314	173	0	4975	487	10	0
2.5	0	306	4672	0	0	4978	306	6	0
4.1	0	0	379	1370	0	1749	370	22	0
7.2	0	0	499	0	2415	2914	499	17	0
TOTAL	0	14716	45732	12729	64573	137750	1671	13	0
ERR	0	306	1192	173	0	1671	*****	*****	*****
ERR	0	6	20	11	0	9	*****	*****	*****

Table VIII.11 The contingency table of the best 3 band pairs after 4-fill, 8-fill, 4-shrink, 8-shrink and complete filling operations.

ORIGINAL PAGE IS  
OF POOR QUALITY

## IX Spectral Analysis: Edit 3

As with the other edits, the same 6 spectral bands were chosen, .40 - .44, .588 - .643, .65 - .69, .72 - .76, .981 - 1.045, and 2.10 - 2.36 micrometers. Figure IX.1 shows the .72 - .76 micrometer band of edit 3 and Figure IX.2 shows the selected ground truth training data.

The feature extractor chose bands .40 - .44 and .588 - .643 with .588 - .643 and .65 - .69 micrometers as the best 2 band pairs. To minimize the total number of reserved decisions and to try and equalize the number of reserved decisions due to more than one assignment and no assignment, classification for the two best band pairs was done using a variety of alpha and beta thresholds. Figure IX.3 is a graph of the thresholds versus the number of reserved decisions.

Table IX.1 is the contingency table for best 2 band pairs with .3 and .021 alpha and beta thresholds, respectively. The resulting error rates of 36% misidentification and 38% false identification are better than the corresponding error rates of 37% and 41% for the classification with alpha, beta thresholds of .4, .028 (Table IX.2) and the corresponding error rates of 37% and 40% for the classification with alpha, beta thresholds of .5, .035 (Table IX.3). But the total number of reserved decisions for the .3 and .021 thresholds is 47,749. This is the highest number of reserved decisions and the lower error rates could be caused by lack of assignments. In this case, the fill operations would tend to propagate the error. Therefore, we chose .5 and .035 thresholds to work with. The raw classified image was post processed with 4-fill, 8-fill, 4-shrink, 8-shrink and complete filling operations. The resulting contingency table (Table IX.4) indicates an 18% misidentification error and 27% false identification error. The major confusion was poletimber immature shortleaf pine being classified as sawtimber immature shortleaf pine or poletimber immature loblolly pine.

The three best band pairs consisted of the two best band pairs plus band pair .40 - .44 and .65 - .69 micrometers. To minimize the total number of reserved decisions and to try to equalize the two causes for reserved decisions, classification was done for the three best band pairs using a variety of alpha beta thresholds. The resulting graph (Figure IX.4) indicates good alpha beta thresholds

are .5 and .035. Contingency table (Table IX.5) shows a 34% misidentification rate and 38% false identification rate with 48,475 reserved decisions. Figure IX.5 shows the resulting classification. Category 1.2 was the largest cause of error. It was confused with category 1.3, sawtimber immature shortleaf pine and categories 2.4 and 2.6, two kinds of loblolly pine.

A 4-fill and an 8-fill operation reduces the misidentification error rate but propagates the false identification error rate (Table IX.6 and Figure IX.6). Doing a 4-shrink reduces the error rates to 18% and 23% for misidentification and false identification. This is as expected since fewer assignments are made to spatially uncertain categories but the misidentification error rate for category 2.1 was not reduced (Table IX.7 and Figure IX.7). The final 8-shrink and then fill all the way up results in a misidentification error rate of 14% and a false identification error rate of 25% (Table IX.8 and Figure IX.8). Most of the error is due to category 1.2 being confused with categories 1.3, 2.4, and 2.6. Thus, category 1.2 has a misidentification error rate of 60% compared to 6% for the next most highly confused category. Most of the confusion is between subclasses in the same class rather than between classes. Contingency table IX.9 shows the resulting classification when categories 1.2 and 1.3 are combined and categories 2.4 and 2.6 are combined. The misidentification error rate is 10% and the false identification error rate is 14%.

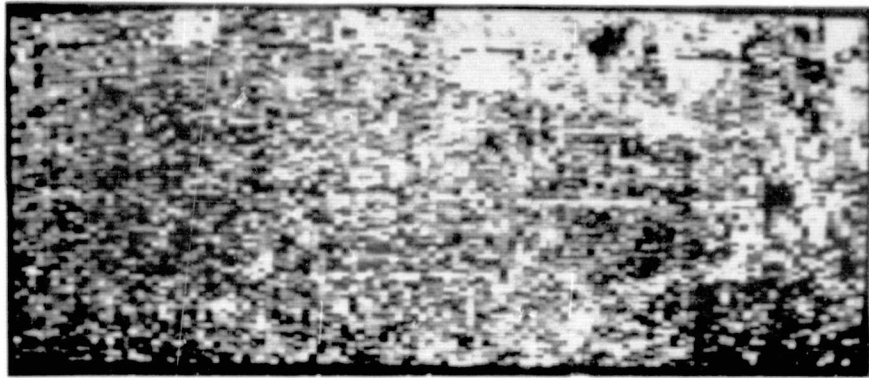


Figure IX.1 The .72 - .76 micrometer band.

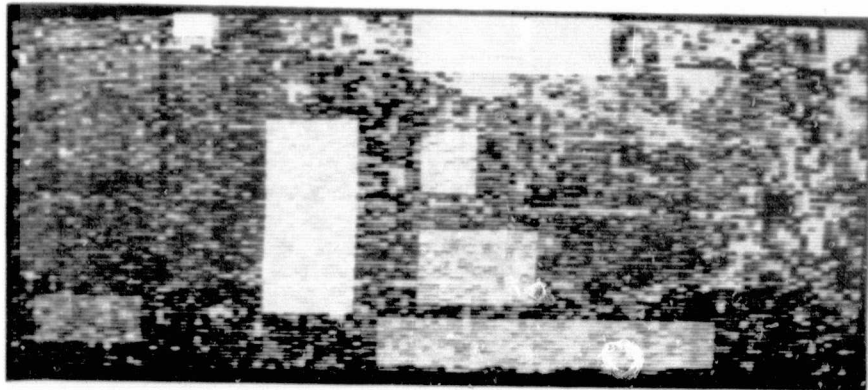


Figure IX.2 The ground truth training data overlaid on the .72 - .76 micrometer band.

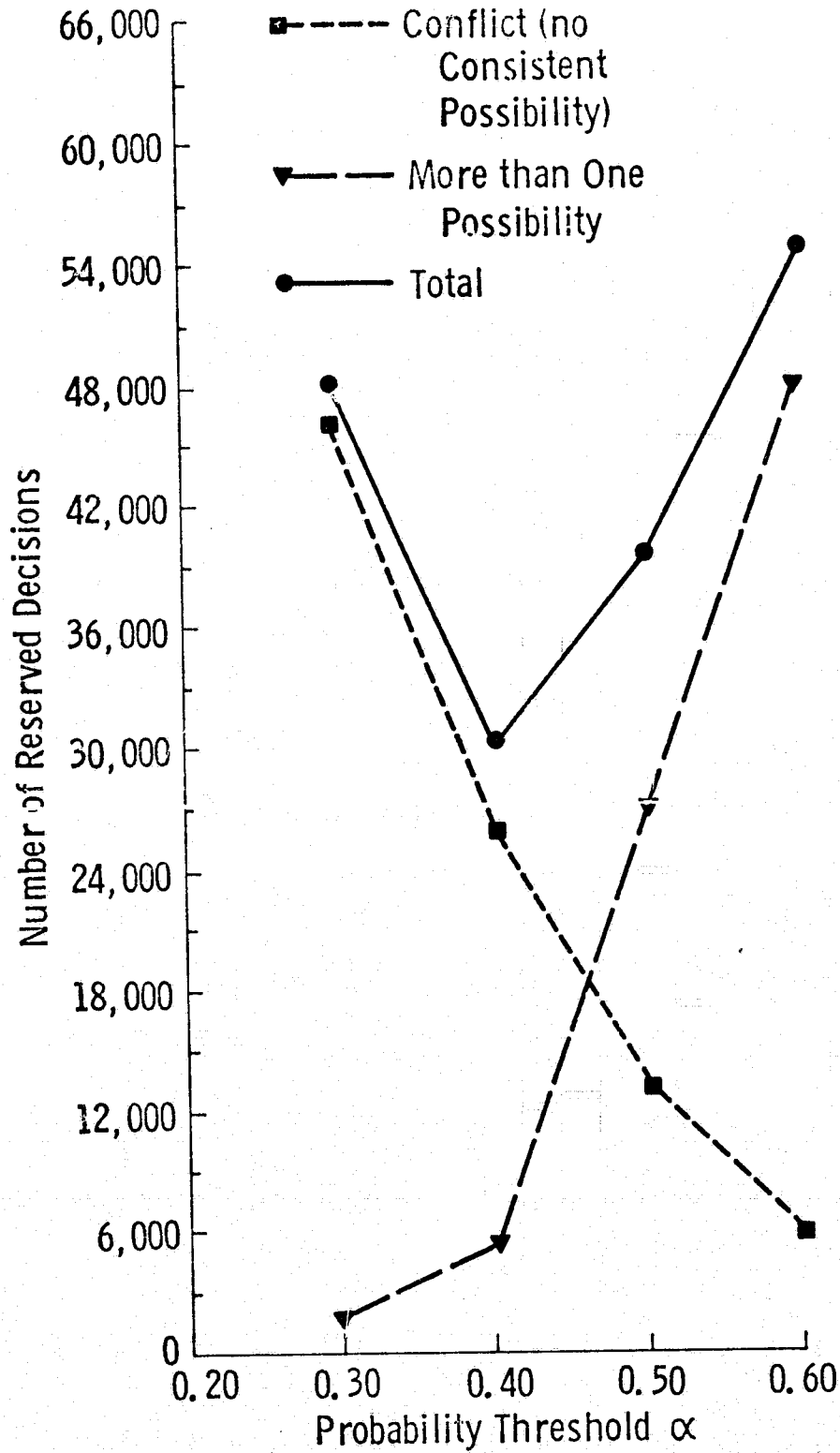


Figure IX.3 Number of reserved decisions as a function of probability threshold alpha for best 2 band pairs, spectral only for edit #3

CONTINGENCY TABLE FOR SAMH1 GDT - 1 SAMH1 B01 - 1 SCALE FACTOR 10\*\* 0

	COL. = ASSIGN CAT					ROW = TRUE CAT				
R DEC	1.2	1.3	2.4	2.6	7.1	TOTAL	FRR	FRR	SD	
UNKN	27548	427	5026	14649	6198	7911	70356	0	0	0
1.2	5825	2465	1244	1527	596	399	12069	3778	61	0
1.3	912	284	537	97	37	0	1862	414	44	0
2.4	4985	52	371	472	473	244	9972	1149	19	0
2.6	2997	249	61	1695	1626	57	6495	1772	52	0
7.1	372		23	191	36	3547	4160	250	7	0
TOTAL	47749	2277	7266	22612	7976	12154	104832	7354	36	0
FRR		585	1699	2228	1142	709	7254	*****	*****	*****
ERR		19	76	41	41	16	30	*****	*****	*****

Table IX.1 The contingency table of the best 2 band pairs for alpha - beta thresholds of .3 and .021.

CONTINGENCY TABLE FOR SAMH1 GDT - 1 SAMH1 B11 - 1 SCALE FACTOR 10\*\* 0

	COL. = ASSIGN CAT					ROW = TRUE CAT				
R DEC	1.2	1.3	2.4	2.6	7.1	TOTAL	ERR	FRR	SD	
UNKN	21722	5852	6794	17404	9128	9454	70356	0	0	0
1.2	3675	2917	1732	1711	1252	486	12069	5281	64	0
1.3	578	371	744	89	81	0	1862	541	42	1
2.4	2798	116	537	514	1164	343	9972	2160	30	0
2.6	1499	290	78	1639	2773	136	6405	2133	43	0
7.1	172	0	27	251	66	2653	4160	344	9	0
TOTAL	3649	9536	9912	26103	14564	14072	104832	10450	37	0
FRR		767	2274	360	2662	965	10450	*****	*****	*****
ERR		21	76	42	49	21	41	*****	*****	*****

Table IX.2 The contingency table of the best 2 band pairs for alpha - beta thresholds of .4 and .028.

ORIGINAL PAGE IS  
OF POOR QUALITY

CONTINGENCY TABLE FOR SAMH1 GDT - 1 SAMH1 B21 - 1 SCALE FACTOR 10\*\* 0

COL. = ASSIGN CAT      ROW = TRUE    CAT

R DEC	1.2	1.3	2.4	2.6	7.1	TOTAL	FRR	FRR	SD	
UNKN	274	4	242	5114	17552	6586	8157	70355	0	0
1.2	5796	2	5	1243	1748	835	441	12760	4267	68
1.3	962	164	532	102	96	0	1862	362	40	0
2.4	3776	151	373	5553	521	298	6979	1342	19	0
2.6	2152	265	87	1708	2549	107	6405	2167	51	0
7.1	247	0	41	272	32	3577	4160	345	9	0
TOTAL	29674	7827	7297	27235	10119	12580	104832	8484	37	0
FRR		58	1744	382	1484	846	8484	*****	*****	*****
SD		22	76	41	42	19	40	*****	*****	*****

Table IX.3 The contingency table of the best 2 band pairs for alpha - beta thresholds of .5 and .035.

CONTINGENCY TABLE FOR SAMH1 GDT - 1 SMH1F3B01 - 1 SCALE FACTOR 10\*\* 0

COL. = ASSIGN CAT      ROW = TRUE    CAT

R DEC	1.2	1.3	2.4	2.6	7.1	TOTAL	#ERR	% ERR	% SD
UNKN	0	11586	8018	25376	3425	21950	70355	0	0
1.2	0	6041	2853	1727	612	835	12068	6027	50
1.3	0	44	1760	59	0	0	1863	103	6
2.4	0	0	0	9476	0	496	9972	496	5
2.6	0	968	0	269	4632	536	6405	1773	28
7.1	0	0	0	124	0	4045	4169	124	3
TOTAL	0	18639	12631	37031	8669	27862	104832	8523	18
#ERR	0	1012	2853	2179	612	1867	8523	*****	*****
% ERR	0	14	62	19	12	32	27	*****	*****

Table IX.4 The contingency table of the best 2 band pairs for alpha - beta thresholds of .5 and .035 after a complete filling.

ORIGINAL PAGE IS  
OF POOR QUALITY

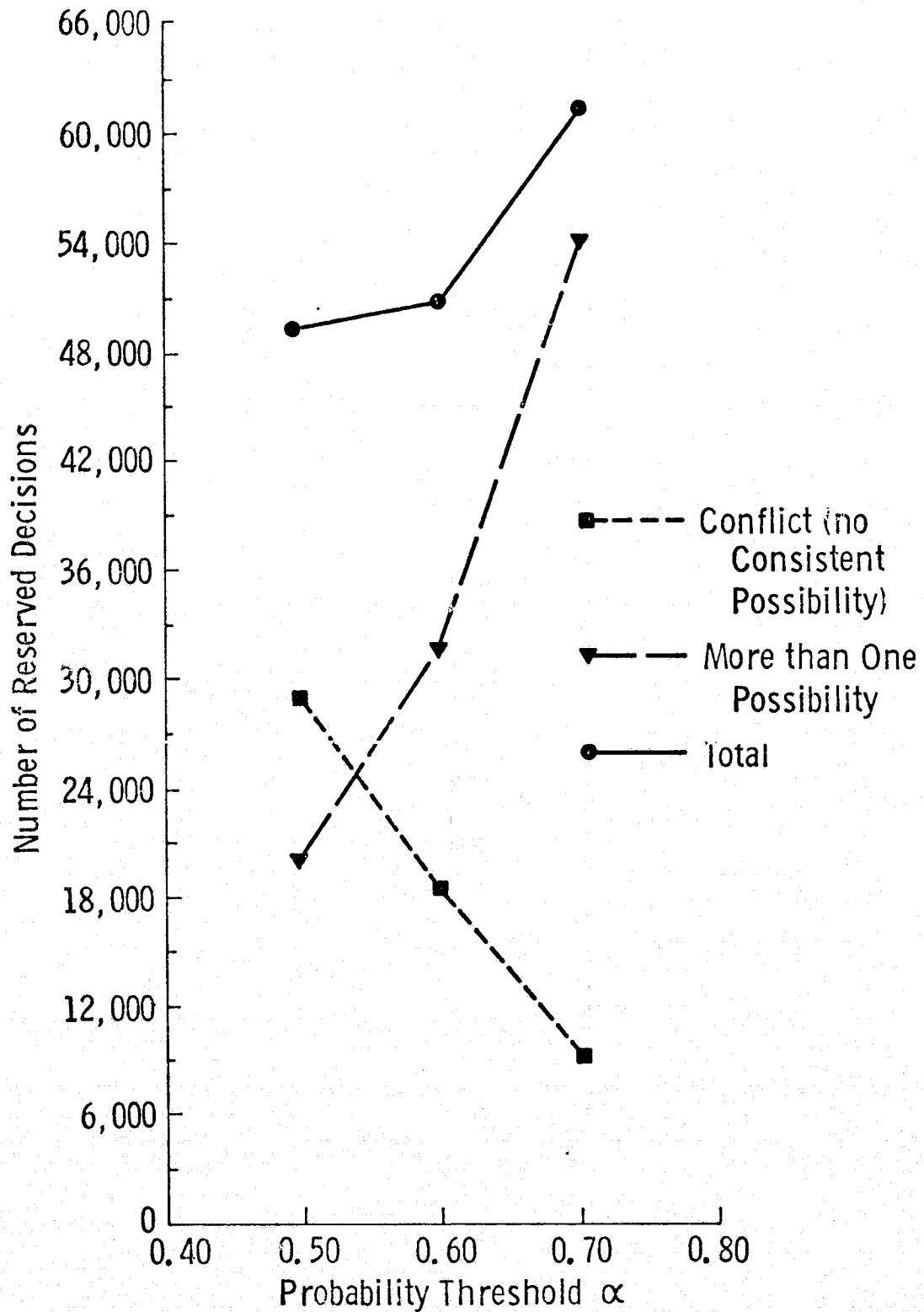


Figure IX.4 Number of reserved decisions as a function of probability threshold alpha for best 3 band pairs, spectral only for edit #3

CONTINGENCY TABLE FOR SAMH1 GDT - 1 SAMH1 P02 - 1 SCALE FACTOR 10\*\* 0

COL. = ASSIGN CAT      ROW = TRUE CAT

R DEC	1.2	1.3	2.4	2.6	7.1	TOTAL	FRR	FRR	SD	
UNKN	33313	2221	5264	12218	7465	8664	70355	0	0	0
1.2	672	1367	1322	1202	870	424	12068	4001	75	0
1.3	892	111	71	22	79	1	1863	270	28	0
2.4	4134	53	564	4244	672	302	9972	1592	27	0
2.6	3074	141	69	977	2068	76	6405	1263	38	0
7.1	342		21	145	72	3592	4160	238	6	0
TOTAL	48475	3022	8119	19482	11215	13056	104832	7364	34	0
FRR		3.5	2.53	25.1	16.5	803	7364	*****	*****	*****
% FRR		1.8	.75	.37	.45	.18	.38	*****	*****	*****

Table IX.5 The contingency table of the best 3 band pairs for alpha - beta thresholds of .5 and .035.

CONTINGENCY TABLE FOR SAMH1 GDT - 1 SMH1F2B02 - 1 SCALE FACTOR 10\*\* 0

COL. = ASSIGN CAT      ROW = TRUE CAT

R DEC	1.2	1.3	2.4	2.6	7.1	TOTAL	#ERR	% ERR	% SD	
UNKN	400	6172	11323	25736	15022	11702	70355	0	0	0
1.2	36	3689	3295	2503	1943	602	12068	8343	69	0
1.3	0	265	1267	169	160	2	1863	596	32	1
2.4	0	90	1032	7227	1166	457	9972	2745	28	0
2.6	0	259	147	1921	3916	162	6405	2489	39	0
7.1	0	0	36	247	132	3754	4169	415	10	0
TOTAL	436	10475	17100	37803	22339	16679	104832	14588	35	0
#ERR	0	614	4510	4840	3401	1223	14588	*****	*****	*****
% ERR	0	14	78	40	46	25	40	*****	*****	*****

Table IX.6 The contingency table of the best 3 band pairs after 4-fill and 8-fill operations.

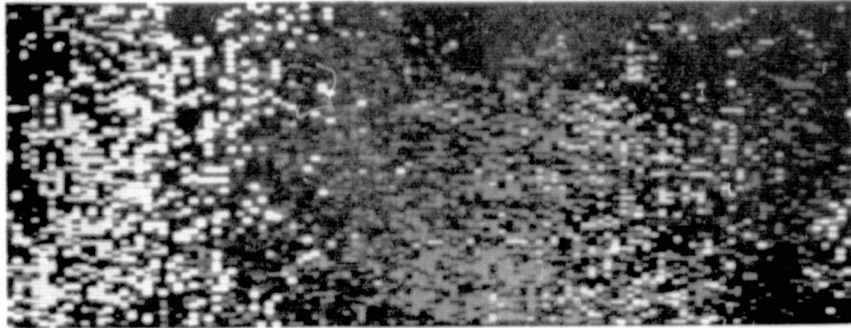


Figure IX.5 The classification of the three best band pairs for alpha - beta thresholds of .5 and .035.

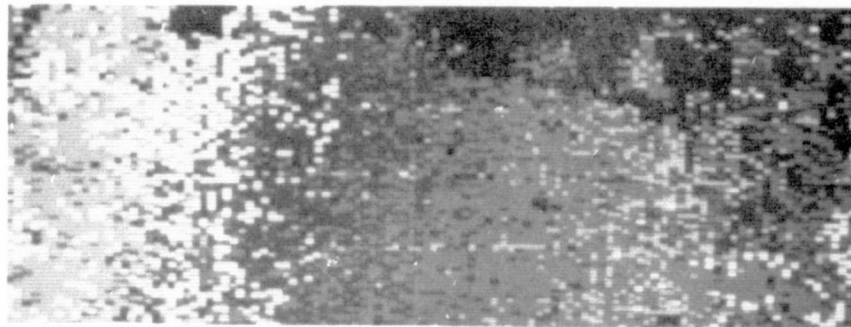


Figure IX.6 The classified image of Figure IX.5 after 4-fill and 8-fill operations.

CONTINGENCY TABLE FOR SAMH1 GDT - 1 SMH1S1B02 - 1 SCALE FACTOR 10\*\* 0

COL. = ASSIGN CAT      ROW = TRUE    CAT

R DEC	1. 2	1. 3	2. 4	2. 6	7.1	TOTAL	#ERR	% ERR	% SD	
UNKWN	50182	1053	3338	7257	2358	6167	70355	0	0	0
1. 2	8421	1073	1468	683	210	213	12068	2574	71	0
1. 3	1189	13	659	0	2	0	1863	15	2	0
2. 4	6350	0	56	3455	29	82	9972	167	5	0
2. 6	5080	4	1	157	1161	2	6405	164	12	0
7.1	714	0	0	52	10	3393	4169	62	2	0
TOTAL	71936	2143	5522	11604	3770	9857	104832	2982	18	0
#ERR	0	17	1525	892	251	297	2982	*****	*****	*****
% ERR	0	2	70	21	18	8	23	*****	*****	*****

Table IX.7      The contingency table of the best 3 band pairs after 4-fill, 8-fill and 4-shrink operations.

CONTINGENCY TABLE FOR SAMH1 GDT - 1 SMH1F3B02 - 1 SCALE FACTOR 10\*\* 0

COL. = ASSIGN CAT      ROW = TRUE    CAT

R DEC	1. 2	1. 3	2. 4	2. 6	7.1	TOTAL	#ERR	% ERR	% SD	
UNKWN	0	5027	11407	23738	12077	18106	70355	0	0	0
1. 2	0	4785	3780	1427	1241	835	12068	7283	60	0
1. 3	0	0	1863	0	0	0	1863	0	0	0
2. 4	0	0	192	9346	4	430	9972	626	6	0
2. 6	0	0	0	397	6008	0	6405	397	6	0
7.1	0	0	0	84	0	4035	4169	84	2	0
TOTAL	0	9812	17242	34992	19330	23456	104832	8390	14	0
#ERR	0	0	3972	1908	1245	1265	8390	*****	*****	*****
% ERR	0	0	68	17	17	24	25	*****	*****	*****

Table IX.8      The contingency table of the best 3 band pairs after 4-fill, 8-fill, 4-shrink, 8-shrink, and complete filling operations.

ORIGINAL PAGE IS  
OF POOR QUALITY

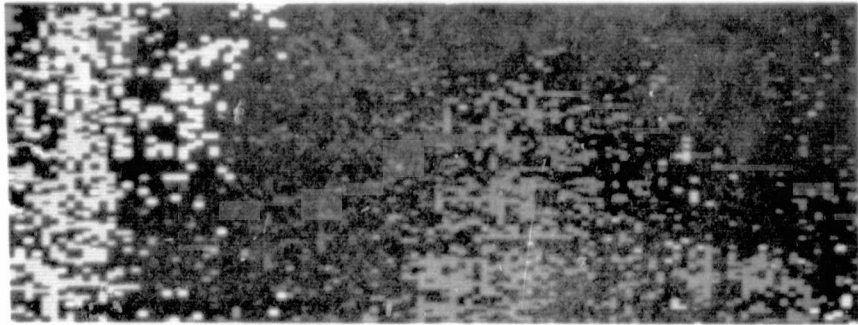


Figure IX.7 The classified image of Figure IX.5 after 4-fill, 8-fill and 4-shrink operations.

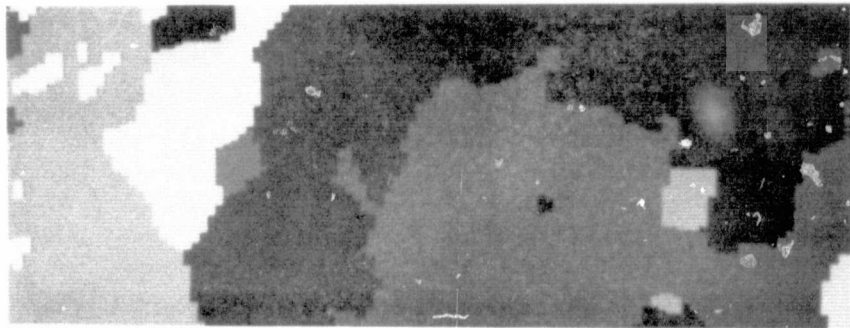


Figure IX.8 The classified image of Figure IX.5 after 4-fill, 8-fill, 4-shrink, 8-shrink and complete filling operations.

Col. = Assign Cat.

Row = True Cat.

	1	2	7	Total	#Err	% Err
Unknown	16434	35815	18106	70355	0	0
1	10428	2668	835	13931	3503	25
2	192	15755	430	16377	622	4
7	0	84	4085	4169	84	2
Total	27054	54322	23456	104832	4209	10
#Err	192	2752	1265	4209		
% Err	2	15	24	14		

Contingency Table Created by Combining  
Subclass Types of the Same Class

Table IX.9

X Spectral-Textural Analysis: Edit 6

We began the spectral-textural analysis of the edit #6 data by using five spectral bands and two texture bands and letting the feature selection procedure pick the best two and best three band pairs for the table look-up decision rule.

The five spectral bands were:

- .40 - .44 micrometers
- .65 - .69 micrometers
- .72 - .76 micrometers
- .981 - 1.045 micrometers
- 2.10 - 2.36 micrometers

The textural transform was done on a 3x3 convolution of the .82 - .88 micrometer band. A second textural information band was created by doing a 3x3 convolution of the initial textural transform image.

The feature selection procedure selected the two best band pairs consisting of:

- (1) .40 - .44 micrometer band with the 3x3 convolution before and after the textural transform of the .82 - .88 micrometer band
- (2) .65 - .69 and .981 - 1.045 micrometer bands.

The alpha-beta thresholds were set at .3 and .021, respectively. This threshold selection was too low for of the 159,500 points to be classified, 74,326 were reserved assignments because of incompatible category assignments between the first and second band pairs and 1,904 were reserved assignment because there was more than one possible assignment common to the two band pairs. The resulting contingency table, (Table X.1 and Figure X.1) shows a misidentification error rate of 36% and a false identification error rate of 37%. After filling the classified image to remove all reserved assignments, the misidentification error rate was 38% and false identification error rate was 39%, Table X.2 and Figure X.2. This is worse than the best two band pair spectral results indicating that either the alpha-beta thresholds used created such a high number of reserved decisions that the classification accuracy was lowered or that a feature selection procedure which minimizes a lower bound on the error rate does not necessarily produce the features of the best classification.

Spatial processing can improve the identification accuracy of the initially classified image. For example, if the completely filled image is shrunk for one iteration with a 4-shrink operator and then filled again, the misidentification and false identification error rates improve to 33%, Table X.3 and Figure X.3. The biggest cause of errors was category 2.4 being assigned to category 1.3 and category 2.6 being assigned to categories 1.3, 2.3 and 2.5. A still greater increase in identification accuracy results if the initially classified image with reserved decisions is operated on with a 4-fill, then 8-fill, then 4-shrink, then 8-shrink operations and then filled up completely (Figure X.4). The resulting contingency table, Table X.4, shows a 32% misidentification error rate and 7% false identification error rate. This is about the same as the best two-band spectral results.

Doing two iterations of a 4-shrink followed by an 8-shrink (Figure X.5) instead of just one iteration as described for the previous classification produces not as good results. Table X.5 shows a 34% misidentification error rate and 7% false identification error rate.

Repeating the 2 band experiment with an alpha threshold of .5 and a beta threshold of .035 reduces the number of reserved decisions to 42,226 with 25,173 reserved decisions due to no assignment and 17,053 reserved decisions due to multiple assignments. The resulting classification (Table X.6 and Figure X.6) gives a misidentification error rate of 37% and a false identification error rate of 38%.

A complete filling of the image (Table X.7 and Figure X.7) gives a misidentification error rate of 38% and 39%. The main cause of error is assigning category 1.3 when the true category is 2.4 and assigning 2.5 when the true category is 2.6. If we do a 4-shrink on the filled image and then completely fill it again (Table X.8 and Figure X.8) we get a misidentification error rate of 32% and a false identification error rate of 36%, but now categories 2.4 and 2.6 are completely misidentified. If instead we do a 4-fill, 8-fill, 4-shrink, 8-shrink and then completely fill up the raw classification (Table X.9 and Figure X.9) we get a misidentification error rate of 30% and a false identification error rate of only 5%. This improvement over the (.3 and .021) result is due to better thresholding. So, even though the raw classification using an alpha threshold of .3 was a few percentage points better than the raw classification using an alpha threshold of .5, the large number of reserved decisions hindered classification accuracy with the fill and shrink operations.

We also did a 4-fill, 8-fill, 4-shrink and complete filling (Table X.10 and Figure X.10) on the raw classification using alpha threshold of .5 to see if we were doing too much shrinking. The resulting misidentification error rate of 32% and false identification error rate of 36% indicates that we were not.

The best 3 band pairs results did significantly increase the accuracy over the two best spectral band pair accuracy and the two best spectral-textural band pair results. The band pairs selected by the feature selection procedure were:

- (1) .40 - .44 micrometer band with the 3x3 convolution before and after the textural transform of the .82 - .88 micrometer band
- (2) .65 - .69 and 2.10 - 2.36 micrometer bands
- (3) .72 - .76 and .981 - 1.045 micrometer bands.

The alpha-beta thresholds were set at .7 and .049, respectively. This resulted in 25,590 reserved decisions due to no common category assignment and 43,889 reserved decisions because of more than one possible category assignment. The thresholds were set just a little too high.

The contingency table of the initially classified image with reserved decisions is shown in Table X.11. It indicates a 35% misidentification error rate and 37% false identification error rate. Completely filling the initially classified image with reserved decisions yields a misidentification error rate of 38% and false identification error rate of 37%. This identification accuracy (Table X.12) is just below the best 3 band pair spectral results.

If the completely filled image is operated on with one iteration of a 4-shrink operation and then completely filled, the misidentification error rate improves to 29% and false identification error rate improves to 30% (Table X.13 and Figure X.11). The results indicate that almost all resolution cells originally assigned to category 2.4 were neighboring resolution cells of a different category. Hence, the 4-shrink operation eliminated most of the assignments to category 2.4.

The basically scattered assignments to category 2.4 was manifest in the next experiment in which we did a 4-fill, then an 8-fill, then a 4-shrink, then an 8-shrink and a complete filling of the initially classified image with reserved decisions. The contingency table (Table X.14 and Figure X.12) shows a 23% misidentification error rate and a 6% false identification error rate. These results

are definitely better than the corresponding three best spectral band pair results. The main reason for the identification accuracy increase is that most of category 2.6 was assigned to category 2.6; only some of category 2.6 was assigned to category 2.5 and hardly any at all to category 1.3. All of category 2.4, however, was misidentified as category 1.3.

Following the pattern of the previous results, if a double 4-shrink and then 8-shrink operation is applied instead of a single 4-shrink and then 8-shrink, the classification results are not quite as good: a 39% misidentification error rate and 12% false identification error rate. As shown in Table X.15, category 2.4 is misidentified as category 1.3 and category 2.6 is misidentified as category 2.3 and category 2.5.

CONTINGENCY TABLE FOR SAMH22GDT - 1 SAMH2BB03 - 1 SCALE FACTOR 10\*\* 0

		COL. = ASSIGN CAT							ROW = TRUE CAT		
R DEC	1.3	1.4	2.3	2.4	2.5	2.6	7.2	TOTAL	ERR	ERR	
UNKN	63115	12915	10822	12152	1057	14605	1888	10467	127021	0	0
1.3	3721	2409	166	199	79	215	85	82	6956	826	26
1.4	981	14	1605	22	14	19	6	9	2670	84	5
2.3	4333	59	14	3000	23	157	113	28	7727	394	12
2.4	305	222	9	15	42	25	8	3	629	282	87
2.5	1647	273	49	171	16	1798	69	11	4034	589	25
2.6	666	88	16	145	0	441	68	10	1434	700	91
7.2	1372	60	181	15	77	1	2	3917	5625	336	8
TOTAL	76140	16040	12862	15719	1308	17261	2239	14527	156096	3211	36
ERR	0	716	435	567	209	858	283	143	3211	*****	*****
ERR	0	23	21	16	83	32	81	4	37	*****	*****

Table X.1 The contingency table of the best 2 band pairs for alpha - beta thresholds of .3 and .021.

CONTINGENCY TABLE FOR SAMH22GDT - 1 SMH2F7B03 - 1 SCALE FACTOR 10\*\* 0

		COL. = ASSIGN CAT							ROW = TRUE CAT		
R DEC	1.3	1.4	2.3	2.4	2.5	2.6	7.2	TOTAL	ERR	ERR	
UNKN	0	29140	22028	28010	2397	24513	4524	16400	127021	0	0
1.3	0	5053	432	502	144	476	170	170	6956	1903	27
1.4	0	38	2463	56	20	50	26	17	2670	207	8
2.3	0	128	37	6720	115	322	297	108	7727	1007	13
2.4	0	417	16	27	89	53	10	8	629	540	86
2.5	0	539	133	409	37	2712	166	38	4034	1322	33
2.6	0	206	31	319	0	711	144	23	1434	1290	90
7.2	0	137	416	28	107	3	2	4931	5625	694	12
TOTAL	0	35667	25556	36071	2909	28840	5350	21695	156096	6963	38
ERR	0	1465	1065	1341	423	1615	690	364	6963	*****	*****
ERR	0	22	30	17	83	37	83	7	39	*****	*****

Table X.2 The contingency table of the best 2 band pairs for alpha - beta thresholds of .3 and .021 after a complete filling.

ORIGINAL PAGE IS  
OF POOR QUALITY

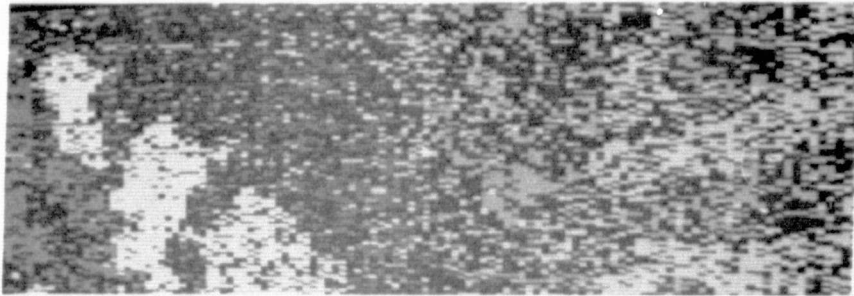


Figure X.1 The classification of the best 2 band pairs for alpha - beta thresholds of .3 and .021.

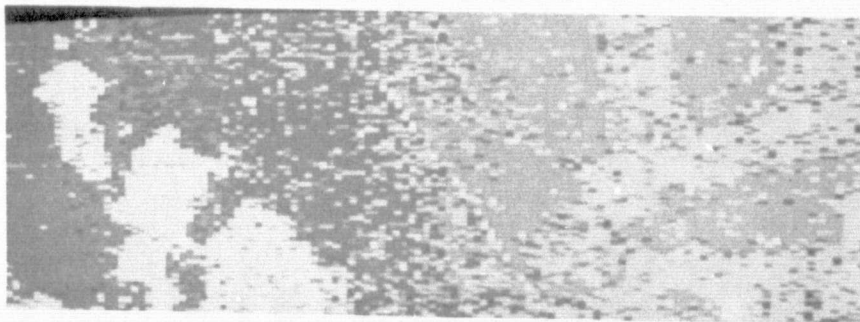


Figure X.2 The classified image of Figure X.1 after a complete filling.

CONTINGENCY TABLE FOR SAMH22GDT - 1 SMH2F8B03 - 1 SCALE FACTOR 10\*\* 0

COL. = ASSIGN CAT      ROW = TRUE CAT

	R DEC	1.3	1.4	2.3	2.4	2.5	2.6	7.2	TOTAL	ERR	ERR
UNKNOWN	0	29668	20824	30615	995	27276	990	16714	127021	0	0
1.3	0	6291	183	231	0	160	0	91	6956	665	10
1.4	0	30	2499	48	0	84	0	0	2670	171	6
2.3	0	9	0	7342	93	201	45	37	7727	385	5
2.4	0	550	0	0	70	1	8	0	629	559	89
2.5	0	424	79	290	32	3145	47	17	4034	889	22
2.6	0	188	1	507	0	727	8	3	1434	1426	99
7.2	0	24	307	0	0	0	0	5294	5625	331	6
TOTAL	0	37184	23873	39033	1190	31544	1116	22156	156096	4426	33
FRR	0	1225	570	1076	125	1173	109	148	4426	*****	*****
FRR	0	16	19	13	64	27	93	3	33	*****	*****

Table X.3 The contingency table of the best 2 band pairs for alpha - beta thresholds of .3 and .021 after complete filling, 4-shrink, and complete filling operations.

CONTINGENCY TABLE FOR SAMH22GDT - 1 SMH2F9B03 - 1 SCALE FACTOR 10\*\* 0

COL. = ASSIGN CAT      ROW = TRUE CAT

	R DEC	1.3	1.4	2.3	2.4	2.5	2.6	7.2	TOTAL	ERR	ERR
UNKNOWN	0	31960	18187	33949	0	26251	37	16637	127021	0	0
1.3	0	6709	0	0	0	247	0	0	6956	247	4
1.4	0	8	2499	163	0	0	0	0	2670	171	6
2.3	0	0	0	7727	0	0	0	0	7727	0	0
2.4	0	629	0	0	0	0	0	0	629	629	100
2.5	0	351	0	48	0	3635	0	0	4034	399	10
2.6	0	1	0	824	0	609	0	0	1434	1434	100
7.2	0	17	230	0	0	0	0	5378	5625	247	4
TOTAL	0	39675	20916	42711	0	30742	37	22015	156096	3127	32
FRR	0	1006	230	1035	0	856	0	0	3127	*****	*****
FRR	0	13	8	12	0	19	0	0	7	*****	*****

Table X.4 The contingency table of the best 2 band pairs for alpha - beta thresholds of .3 and .021 after 4-fill, 8-fill, 4-shrink, 8-shrink, and complete filling operations.

ORIGINAL PAGE IS  
OF POOR QUALITY

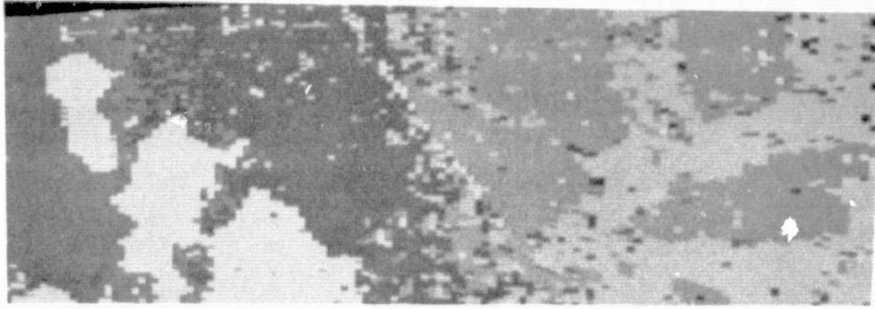


Figure X.3 The classified image of Figure X.1 after complete filling, 4-shrink, and complete filling operations.

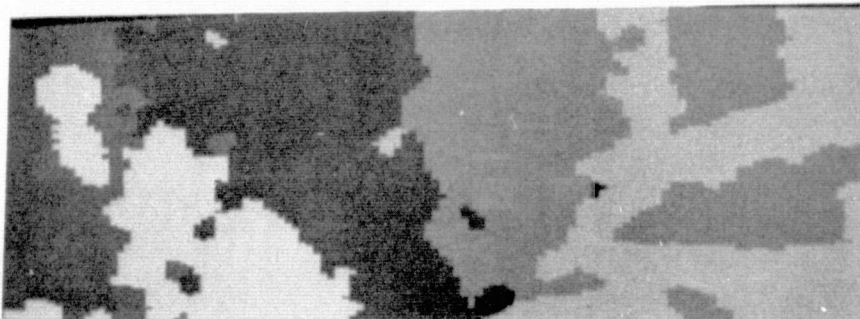


Figure X.4 The classified image of Figure X.1 after 4-fill, 8-fill, 4-shrink, 8-shrink and complete filling operations.

CONTINGENCY TABLE FOR SAMH226DT - 1 SMH2E3P03 - 1 SCALE FACTOR 10\*\* 0

COL = ASSIGN CAT      ROW = TRUE CAT

	R DEC	1.3	1.4	2.3	2.4	2.5	2.6	7.2	TOTAL	ERR	ERR	
UNKN	0	28283	15512	42380		0	20077	0	20769	127021	0	0
1.3	0	6956	0	0		0	0	0	6956	0	0	0
1.4	0	2	2492	169		0	0	0	2670	171	6	6
2.3	0	0	0	7727		0	0	0	7727	0	0	0
2.4	0	629	0	0		0	0	0	629	629	100	
2.5	0	28	0	1410		0	2596	0	4034	1438	36	
2.6	0	0	0	825		0	609	0	1434	1434	100	
7.2	0	0	19	0		0	0	0	5606	5625	19	0
TOTAL	0	35898	18030	52511		0	23282	0	26375	156096	3691	34
ERR	0	659	19	2404		0	609	0	3691	*****	*****	
ERR	0	9	1	24		0	19	0	7	*****	*****	

Table X.5 The contingency table of the best 2 band pairs for alpha - beta thresholds of .3 and .021 after 4-fill, 8-fill, 4-shrink, 8-shrink, 4-shrink, 8-shrink, and complete filling operations.

CONTINGENCY TABLE FOR SAMH226DT - 1 SAMH2 B15 - 1 SCALE FACTOR 10\*\* 0

COL = ASSIGN CAT      ROW = TRUE CAT

	R DEC	1.3	1.4	2.3	2.4	2.5	2.6	7.2	TOTAL	ERR	% ERR
UNKN	35503	24414	13567	18099	1339	19459	2868	11772	127021	0	0
1.3	1706	4328	273	140	59	276	64	110	6956	922	18
1.4	621	19	1894	25	23	56	10	22	2670	155	8
2.3	1875	110	12	5165	29	296	187	53	7727	687	12
2.4	177	359	20	6	24	29	11	3	629	428	95
2.5	1064	465	44	190	26	2106	131	8	4034	864	29
2.6	502	157	11	155	5	534	60	10	1434	872	94
7.2	778	180	201	29	43	1	5	4388	5625	459	9
TOTAL	42226	30032	16022	23809	1548	22757	3336	163661	156096	4387	37
ERR	0	1290	561	545	185	1192	408	206	4387	*****	*****
% ERR	0	23	23	10	89	36	87	4	38	*****	*****

Table X.6 The contingency table of the best 2 band pairs for alpha - beta thresholds of .5 and .035.

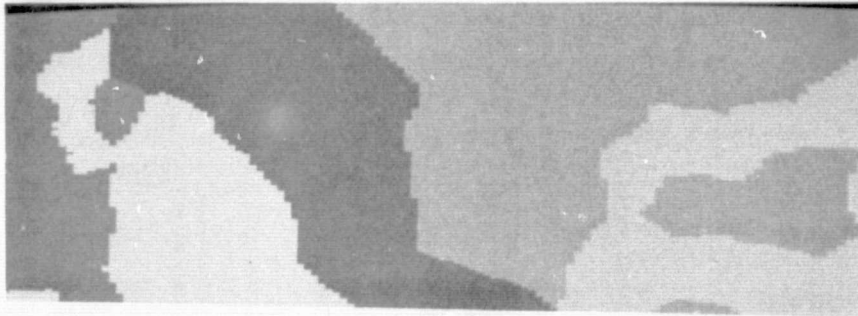


Figure X.5 The classified image of Figure X.1 after 4-fill, 8-fill, 4-shrink, 8-shrink, 4-shrink, 8-shrink and complete filling operations.

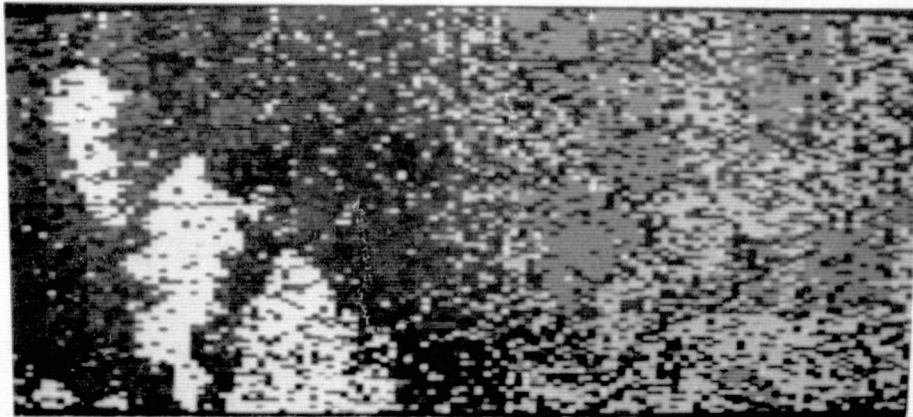


Figure X.6 The classification of the best 2 band pairs for alpha - beta thresholds of .5 and .035.

CONTINGENCY TABLE FOR SAMH22GDT - 1 SMH2F1B05 - 1 SCALE FACTOR 10\*\* 0

COL = ASSIGN CAT ROW = TRUE CAT

R DEC	1.3	1.4	2.3	2.4	2.5	2.6	7.2	TOTAL	#ERR	% ERR	
UNKN	0	33786	19822	24926	1979	27212	4298	14938	127021	0	0
1.3	0	5639	390	220	77	365	95	170	6956	1317	19
1.4	0	31	2436	45	30	79	17	32	2670	234	9
2.3	0	169	19	6683	48	443	295	70	7727	1044	14
2.4	0	496	24	9	35	41	19	5	629	594	94
2.5	0	625	70	285	39	2816	186	13	4034	1218	30
2.6	0	256	21	250	7	784	99	17	1434	1335	93
7.2	0	265	284	37	62	1	7	4969	5625	156	12
TOTAL	0	41267	23066	32515	2277	31741	5016	20214	56096	6398	38
#ERR	0	1842	808	846	263	1713	619	307	6398	****	****
% ERR	0	25	25	11	88	38	86	6	39	****	****

Table X.7 The contingency table of the best 2 band pairs for alpha - beta thresholds of .5 and .035 after a complete filling.

CONTINGENCY TABLE FOR SAMH22GDT - 1 SMH2F2B05 - 1 SCALE FACTOR 10\*\* 0

COL = ASSIGN CAT ROW = TRUE CAT

R DEC	1.3	1.4	2.3	2.4	2.5	2.6	7.2	TOTAL	#ERR	% ERR	
UNKN	0	33077	18716	27493	227	32230	246	15032	127021	0	0
1.3	0	6849	53	24	0	15	0	15	6956	107	2
1.4	0	12	2498	47	0	112	0	1	2670	172	6
2.3	0	20	0	7431	3	260	13	0	7727	296	4
2.4	0	629	0	0	0	0	0	0	629	629	100
2.5	0	387	10	154	0	3483	0	0	4034	551	14
2.6	0	130	0	330	0	974	0	0	1434	1434	100
7.2	0	112	133	0	8	0	0	5372	5625	253	4
TOTAL	0	41216	21410	35479	238	37074	259	20420	56096	3442	32
#ERR	0	1290	196	555	11	1361	13	16	3442	****	****
% ERR	0	16	7	7	100	28	100	0	36	****	****

Table X.8 The contingency table of the best 2 band pairs for alpha - beta thresholds of .5 and .035 after complete filling, 4-shrink, and complete filling operations.

ORIGINAL PAGE IS  
OF POOR QUALITY

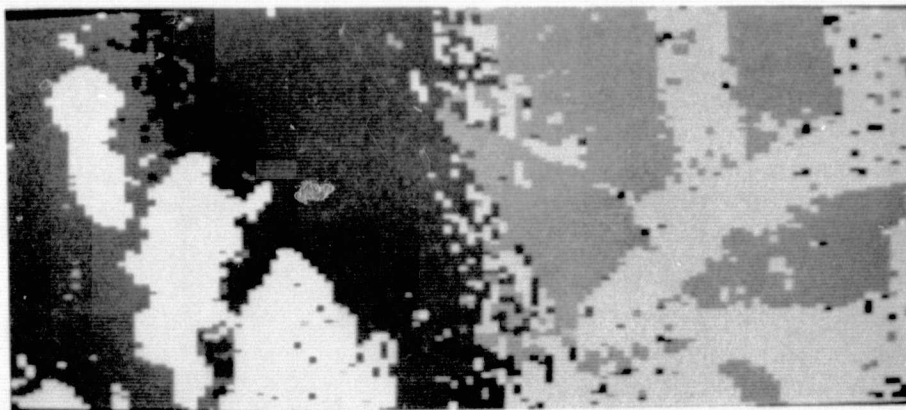


Figure X.7 The classified image of Figure X.6 after a complete filling.

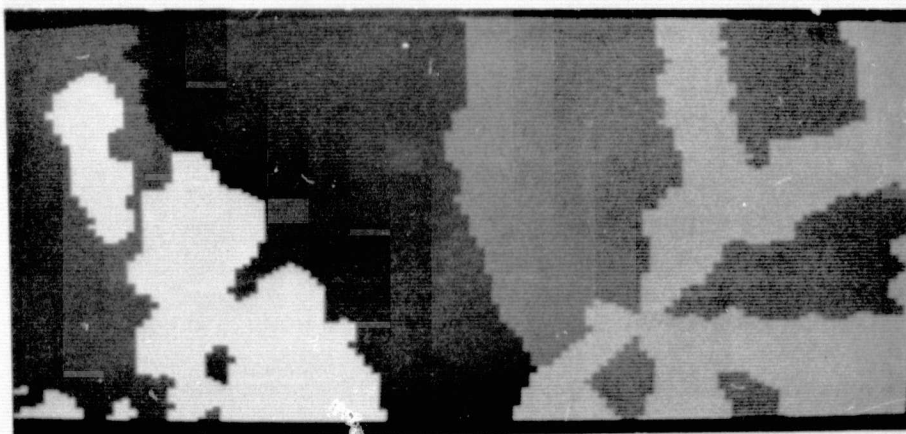


Figure X.8 The classified image of Figure X.6 after complete filling, 4-shrink and complete filling operations.

COL = ASSIGN CAT    ROW = TRUE CAT

	R DEC	1.3	1.4	2.3	2.4	2.5	2.6	7.2	TOTAL	#ERR	% ERR
UNKN	0	32498	17232	33984	0	26684	0	16623	127021	0	0
1.3	0	6956	0	0	0	0	0	0	6956	0	0
1.4	0	0	2499	140	0	31	0	0	2670	171	6
2.3	0	0	0	7717	0	10	0	0	7727	10	0
2.4	0	629	0	0	0	0	0	0	629	629	100
2.5	0	351	0	0	0	3683	0	0	4034	351	9
2.6	0	0	0	825	0	609	0	0	1434	1434	100
7.2	0	18	19	0	0	0	0	5588	5625	37	1
TOTAL	0	40452	19750	42666	0	31017	0	22211	156096	2632	30
#ERR	0	998	19	965	0	650	0	0	2632	*****	*****
% ERR	0	13	1	11	0	15	0	0	5	*****	*****

Table X.9 The contingency table of the best 2 band pairs for alpha - beta thresholds of .5 and .035 after 4-fill, 8-fill, 4-shrink, 8-shrink, and complete filling operations.

COL = ASSIGN CAT    ROW = TRUE CAT

	R DEC	1.3	1.4	2.3	2.4	2.5	2.6	7.2	TOTAL	#ERR	% ERR
UNKN	0	33077	18714	27493	229	32230	246	15032	127021	0	0
1.3	0	6849	53	24	0	15	0	15	6956	107	2
1.4	0	12	2498	47	0	112	0	1	2670	172	6
2.3	0	20	0	7431	3	260	13	0	7727	296	4
2.4	0	629	0	0	0	0	0	0	629	629	100
2.5	0	387	10	154	0	3483	0	0	4034	551	14
2.6	0	130	0	330	0	974	0	0	1434	1434	100
7.2	0	112	133	0	8	0	0	5372	5625	253	4
TOTAL	0	41216	21408	35479	240	37074	259	204201	156096	3442	32
#ERR	0	1290	196	555	11	1361	13	16	3442	*****	*****
% ERR	0	16	7	7	100	28	100	0	36	*****	*****

Table X.10 The contingency table of the best 2 band pairs for alpha - beta thresholds of .5 and .035 after 4-fill, 8-fill, 4-shrink, and complete filling operations.

ORIGINAL PAGE IS  
OF POOR QUALITY

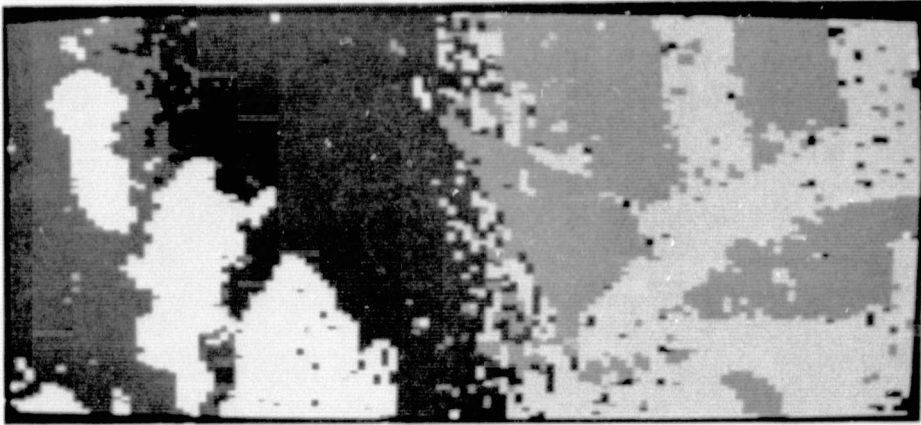


Figure X.9 The classified image of Figure X.6 after 4-fill, 8-fill, 4-shrink, 8-shrink, and complete filling operations.

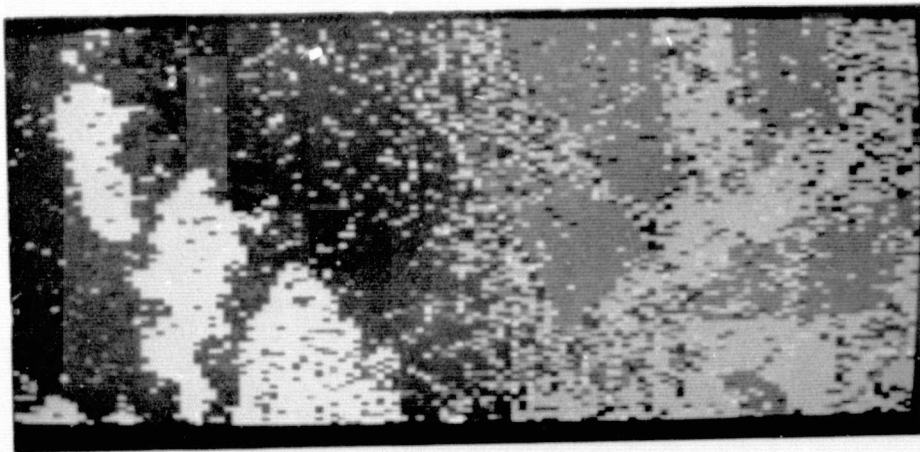


Figure X.10 The classified image of Figure X.6 after 4-fill, 8-fill, 4-shrink and complete filling operations.

CONTINGENCY TABLE FOR SAMH22GDT - 1 SAMH2BB04 - 1 SCALE FACTOR 10\*\* 0.

COL. = ASSIGN CAT      ROW = TRUE CAT

R DEC	1.3	1.4	2.3	2.4	2.5	2.6	7.2	TOTAL	ERR	ERR	
UNKWN	58517	15045	8859	14874	697	11310	8036	9683	127021	0	0
1.3	3126	3130	83	51	66	157	244	99	6956	700	18
1.4	917	62	1577	4	7	53	47	3	2670	176	10
2.3	2004	87	10	4918	14	278	374	42	7727	805	14
2.4	339	199	4	4	16	34	28	5	629	274	94
2.5	2367	217	14	91	12	1038	290	5	4034	629	38
2.6	781	53	7	93	1	242	241	16	1434	412	63
7.2	1428	255	209	42	18	5	9	3659	5625	538	13
TOTAL	69479	19048	10763	20077	831	13117	9260	13512	156096	3534	35
ERR	0	873	327	285	118	769	997	170	3534	*****	*****
ERR	0	22	17	5	88	43	80	4	37	*****	*****

Table X.11 The contingency table of the best 3 band pairs for alpha - beta thresholds of .7 and .049.

CONTINGENCY TABLE FOR SAMH22GDT - 1 SMH2F7R04 - 1 SCALE FACTOR 10\*\* 0

COL. = ASSIGN CAT      ROW = TRUE CAT

R DEC	1.3	1.4	2.3	2.4	2.5	2.6	7.2	TOTAL	ERR	ERR	
UNKWN	0	29197	16664	21977	1455	26104	17170	14454	127021	0	0
1.3	0	5589	162	96	128	310	470	201	6956	1367	20
1.4	0	125	2319	10	9	99	103	5	2670	351	13
2.3	0	141	21	6352	26	494	620	64	7727	1375	18
2.4	0	404	12	9	39	75	77	13	629	590	94
2.5	0	511	34	189	31	2556	706	7	4034	1478	37
2.6	0	15	19	169	1	644	471	25	1434	963	67
7.2	0	441	377	58	33	13	17	4686	5625	939	17
TOTAL	0	36513	19608	28860	1722	30295	19643	19455	156096	7063	38
ERR	0	1727	625	531	228	1635	2007	315	7063	*****	*****
ERR	0	24	21	8	85	39	81	6	37	*****	*****

Table X.12 The contingency table of the best 3 band pairs after a complete filling.

CONTINGENCY TABLE FOR SAMH22GDT - 1 SMH2F8B04 - 1 SCALE FACTOR 10\*\* 0

COL. = ASSIGN CAT      ROW = TRUE    CAT

R DEC	1.3	1.4	2.3	2.4	2.5	2.6	7.2	TOTAL	ERR	ERR
UNKN	0 2916	17790	24031	19	26491	14884	14646	127021	0	0
1.3	0 6739	23	0	0	22	60	112	6956	217	3
1.4	0 18	2481	0	0	36	135	0	2670	189	7
2.3	0 0	0	7155	0	276	296	0	7727	572	7
2.4	0 581	0	1	0	28	19	0	629	629	100
2.5	0 416	0	172	6	3172	268	0	4034	862	21
2.6	0 0	0	106	0	715	612	0	1434	821	57
7.2	0 279	196	0	0	0	0	5150	5625	475	8
TOTAL	0 37193	20490	31465	25	30740	16275	19908	156096	3765	29
ERR	0 1294	219	279	6	1077	778	112	3765	*****	*****
FRR	0 16	8	4	100	25	56	2	30	*****	*****

Table X.13 The contingency table of the best 3 band pairs after complete filling, 4-shrink, and complete filling operations.

CONTINGENCY TABLE FOR SAMH22GDT - 1 SMH2F9B04 - 1 SCALE FACTOR 10\*\* 0

COL. = ASSIGN CAT      ROW = TRUE    CAT

R DEC	1.3	1.4	2.3	2.4	2.5	2.6	7.2	TOTAL	ERR	ERR
UNKN	0 31125	16788	29548	0	26088	6792	16680	127021	0	0
1.3	0 6956	0	0	0	0	0	0	6956	0	0
1.4	0 0	2499	67	0	0	104	0	2670	171	6
2.3	0 0	0	7727	0	0	0	0	7727	0	0
2.4	0 629	0	0	0	0	0	0	629	629	100
2.5	0 351	0	0	0	3683	0	0	4034	311	9
2.6	0 1	0	2	0	609	822	0	1434	612	43
7.2	0 169	52	0	0	0	0	5404	5625	211	4
TOTAL	0 39231	19339	37344	0	30380	7718	22084	156096	1984	23
ERR	0 1150	52	69	0	609	104	0	1984	*****	*****
FRR	0 14	2	1	0	14	11	0	6	*****	*****

Table X.14 The contingency table of the best 3 band pairs after 4-fill, 8-fill, 4-shrink, 8-shrink and complete filling operations.

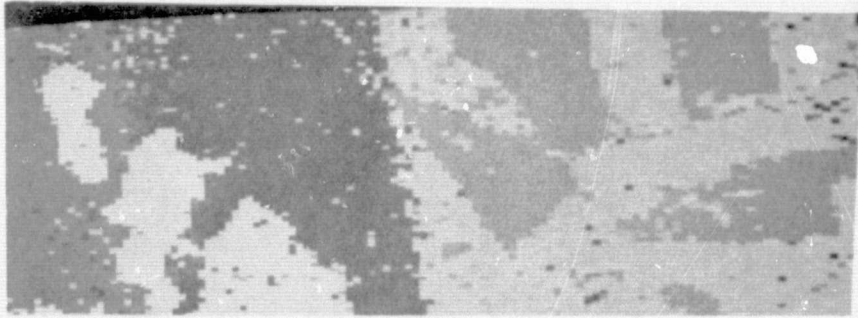


Figure X.11 The classification of the best 3 band pairs for alpha - beta thresholds of .7 and .049 after complete filling, 4-shrink, and complete filling operations.

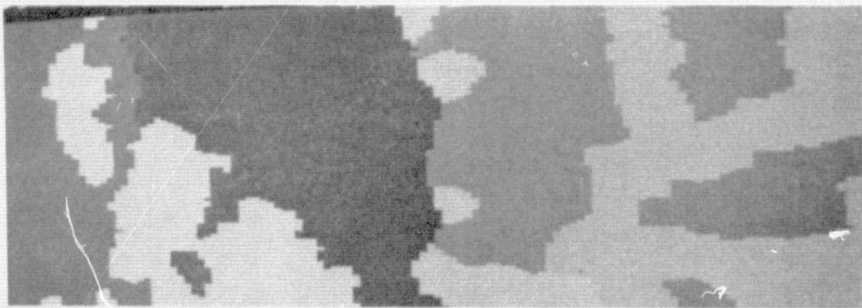


Figure X.12 The classification of the best 3 band pairs for alpha - beta thresholds of .7 and .049 after 4-fill, 8-fill, 4-shrink, 8-shrink, and complete filling operations.

CONTINGENCY TABLE FOR SAMH22GDT - 1 SMH2F3B04 - 1 SCALE FACTOR 10\*\* 0

COL. = ASSIGN CAT ROW = TRUE CAT

	R	DEC	1.3	1.4	2.3	2.4	2.5	2.6	7.2	TOTAL	ERR	ERR
UNKNOWN	0	28375	11135	47409	0	16118	0	23994	127021	0	0	0
1.3	0	6956	0	0	0	0	0	0	6956	0	0	0
1.4	0	0	2499	171	0	0	0	0	2670	171	6	6
2.3	0	0	0	7551	0	176	0	0	7727	176	2	2
2.4	0	629	0	0	0	0	0	0	629	629	100	100
2.5	0	245	0	2513	0	1276	0	0	4034	2758	68	68
2.6	0	0	0	825	0	609	0	0	1434	1434	100	100
7.2	0	0	87	0	0	0	0	5538	5625	87	2	2
TOTAL	0	36225	13691	58469	0	18179	0	29532	156096	5255	39	39
ERR	0	874	87	3509	0	785	0	0	5255	*****	*****	*****
FRR	0	11	3	32	0	38	0	0	12	*****	*****	*****

Table X.15 The contingency table of the best 3 band pairs after 4-fill, 8-fill, 4-shrink, 8-shrink, 4-shrink, 8-shrink, and complete filling operations.

## XI Spectral-Textural Analysis: Edit 9

With this edit we experimented to find the best texture transforms. The .82 - .88 micrometer band was chosen as the band having the most spatial information (Figure XI.1). Figure XI.2 is a 2x2 rectangular convolution of the .82 - .88 micrometer band and Figure XI.3 is a 3x3 rectangular convolution of the band. Each of these bands were used as inputs into the texture transform. The resulting textural transform images are shown in Figures XI.4, XI.5 and XI.6. Each of these were convoluted with a 2x2 window size (shown in Figures XI.7, XI.8, XI.9). Finally the textured transforms were convoluted with a 3x3 convolution window giving us 3 more texture images (Figures XI.10, XI.11 XI.12). Using our own visual discretion we chose the textural transform with a 3x3 rectangular convolution after and the 3x3 rectangular convolution before transforming with a 3x3 rectangular convolution after transforming as the two texture bands with the most information (these are shown in Figures XI.10 and XI.12).

We combined these 2 texture bands with the spectral bands and the feature selector chose band pairs .40 - .44 micrometers and the 3x3 rectangular convolution before and after the textured transform with .65 - .69 and 2.10 - 2.36 micrometers as the 2 best band pairs for classification. Band pair .72 - .76 and .981 - 1.045 micrometers was selected with the other two for the best 3 band pairs. Figure XI.13 and XI.14 show the graphs of the threshold alpha against the number of reserved decisions. For best 3 band pairs the best alpha threshold was .7 with a beta threshold of .049.

To check the choice of thresholds we checked several results using different thresholds. The best 3 band pairs classification with alpha, beta thresholds of .3 and .021 gave us a misidentification error rate of 20% and a false identification error rate of 20% (Table XI.1 and Figure XI.15). The error rate was low but the total number of reserved decisions 104,531 is high. Only 89 of these points were reserved due to more than one assignment, while 104,443 points were reserved because of no assignment. The largest cause of error was due to misidentification of category 2.6 as category 2.5, both subclasses of loblolly pine.

Post processing with a 4-shrink and then a complete filling we obtained misidentification and false identification error rates of 36% and 20%. Both category 2.6 and category 3.1, laurel oak, had misidentification error rates of 100% (Table XI.2 and Figure XI.16). Though the shrink operation usually reduces error, if a sparse category is assigned correctly, the shrink operation here tended to wipe out the category. Table XI.2 shows us that this happened to category 2.6 and category 3.1. If instead of a shrink we first did a 4-fill, then a 4-shrink and then a complete filling, the resulting contingency table is Table XI.3 (Figure XI.17). The misidentification error rate was 18% and the false identification error rate was 16%, but the misidentification error rate for category 2.6 was still high at 41%. The main cause of error is the confusion of 2.6 and 2.5. The only way left to eliminate the confusion is to change thresholds.

Values of .6 and .042 for the alpha, beta thresholds resulted in a misidentification error rate of 25% and a false identification error rate of 28% (Table XI.4). The misidentification error rate for categories 2.5 and 2.6 were 31% and 34%, respectively. If .7 and .049 are chosen for the alpha and beta thresholds we get error rates of 25% and 31%, but the misidentification error rate for category 2.6 is only 24% and the misidentification error rate of category 2.5 is 31% (Table XI.5). The number of reserved decisions is 71,919 with 43,045 points being reserved because of more than one assignment and 28,874 points reserved because of no assignment. With thresholds for alpha and beta of .8 and .063, the misidentification and false identification error rates were 28% and 32%, respectively (Table XI.6). Though the misidentification error rate for category 2.6 has been reduced to 19% and for category 2.5 it was reduced to 21%, the misidentification and false identification error rates for category 3.1 have grown to 62% and 62%, and for category 4.2 the rates have gone up to 52% and 45%. In addition the number of reserved decisions has risen to 121,716 indicating that the thresholds have gotten too high.

Since the error rates for Table XI.4 and Table XI.5 were almost the same, the results from the classification with thresholds of .7 and .049 should be better for post processing. The main cause of error had been with categories 2.5 and 2.5 and this classification showed lower error rates for these categories.

If we fill up the image with alternating 4-fill and 8-fills we get a misidentification error rate of 27% and a false identification error rate of 33% (Table XI.7). This is no improvement on the raw classification so the shrink operation is needed to eliminate incorrect assignments. Post processing with a 4-fill and an 8-fill so the shrink operations do not wipe out sparsely populated categories, then doing a 4-shrink and 8-shrink and finally a complete filling, we obtain a misidentification error rate of 8% and a false identification error rate of 11% (Table XI.8 and Figure XI.18). The misidentification error rate for category 2.6 was reduced to 0 and the confusion between category 3.1 and 4.2 was small. As was the case with the spectral analysis the misidentification of category 2.5 with 1.3 is the main cause of error. Though the texture analysis gives better overall results, it cannot overcome the inability of the decision rise to separate categories 2.5 and 1.3 in the lower right hand corner of the timber stand map.

The results of the best 2 band pairs classification were not as good. The contingency table resulting from alpha, beta thresholds of .3 and .021 resulted in a misidentification error rate of 25% and a false identification error rate of 31% (Table XI.9 and Figure XI.19). If we do a 4-fill, 4-shrink and fill up we get error rates of 23% and 29% (Table XI.10 and Figure XI.20). If we shrink first and then fill up, the results showed improvement with a misidentification error rate of 15% and a false identification error rate of 20% (Table XI.11 and Figure XI.21).

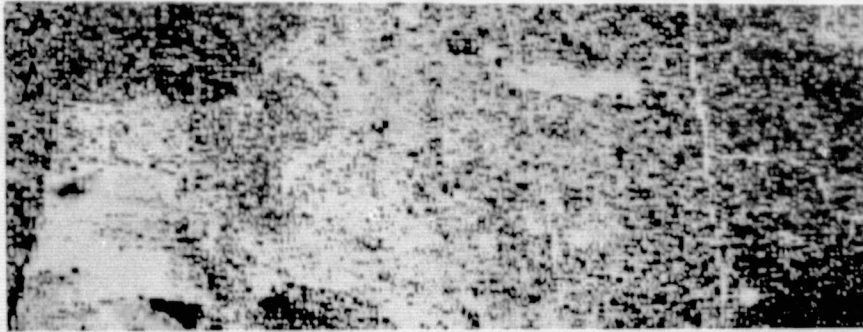


Figure XI.1 The .82 - .88 micrometer band used for the texture transform.

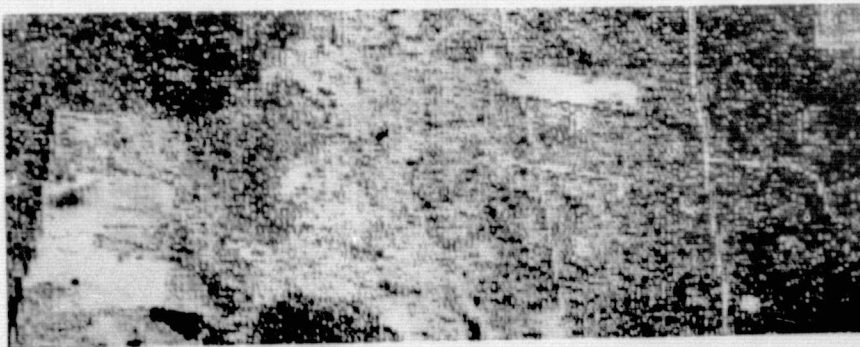


Figure XI.2 Shows Figure XI.1 after a 2x2 rectangular convolution.

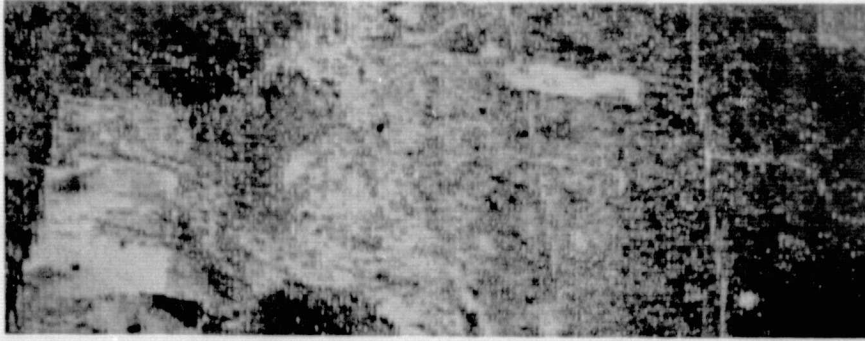


Figure XI.3 Shows Figure XI.1 after a 3x3 rectangular convolution.

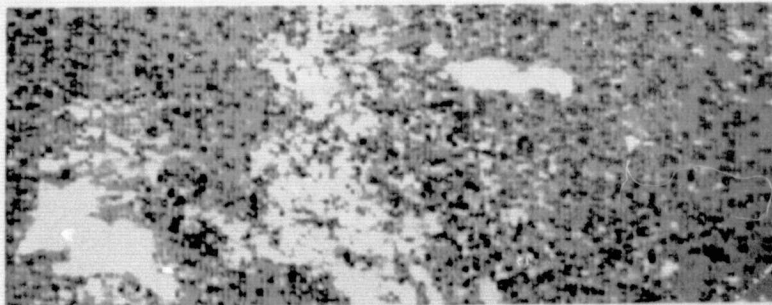


Figure XI.4 The texture transform of Figure XI.1.

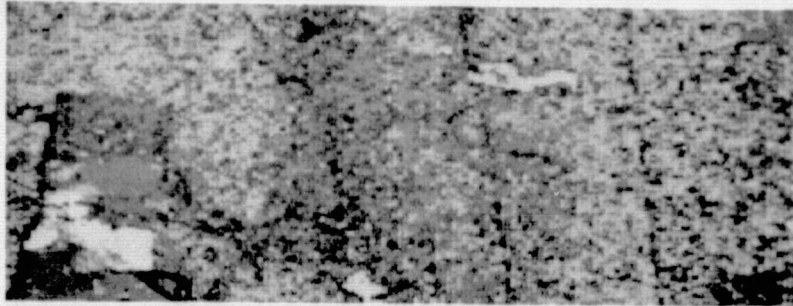


Figure XI.5 The texture transform of Figure XI.2.

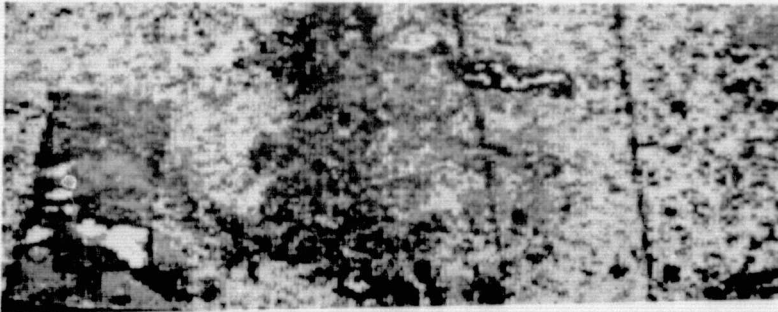


Figure XI.6 The texture transform of Figure XI.3.

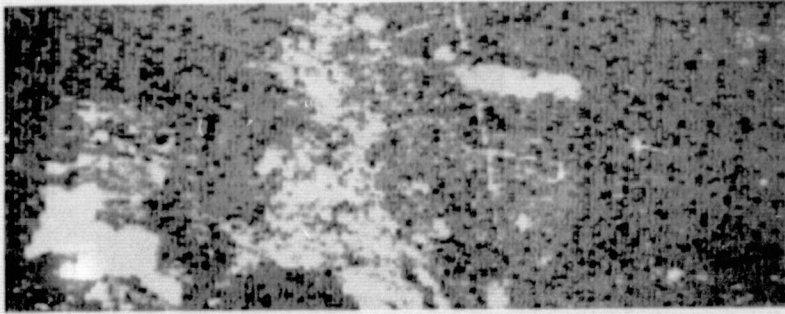


Figure XI.7 Shows Figure XI.4 after a 2x2 rectangular convolution.

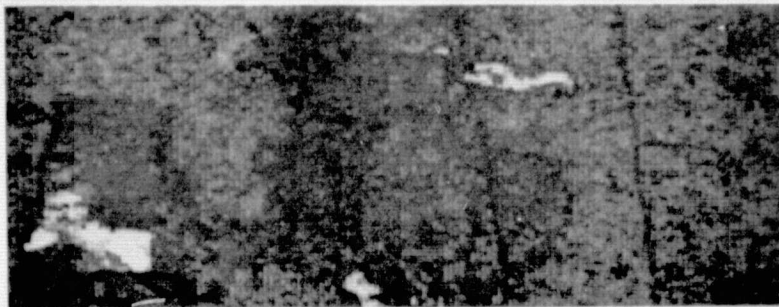


Figure XI.8 Shows Figure XI.5 after a 2x2 rectangular convolution.

ORIGINAL PAGE IS  
OF POOR QUALITY



Figure XI.9 Shows Figure XI.6 after a  $2 \times 2$  rectangular convolution.

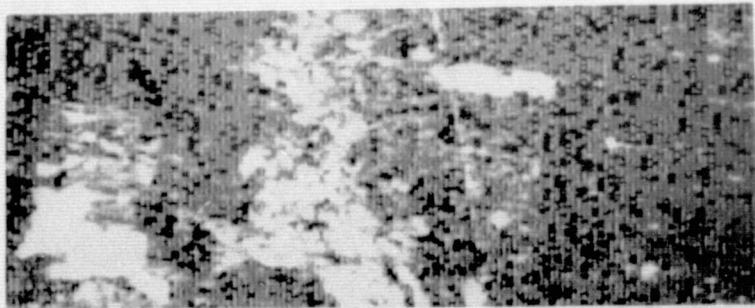


Figure XI.10 Shows Figure XI.4 after a  $3 \times 3$  rectangular convolution.

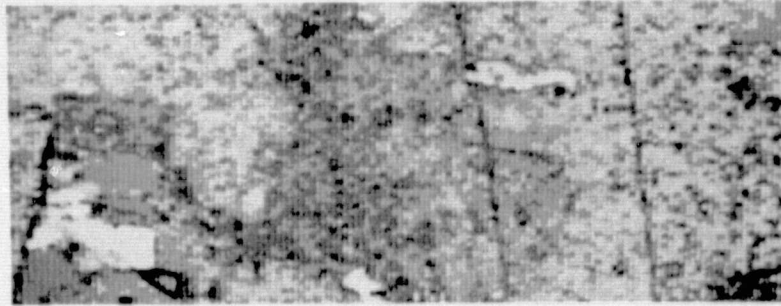


Figure XI.11 Shows Figure XI.5 after a 3x3 rectangular convolution.



Figure XI.12 Shows Figure XI.6 after a 3x3 rectangular convolution.

ORIGINAL PAGE IS  
OF POOR QUALITY

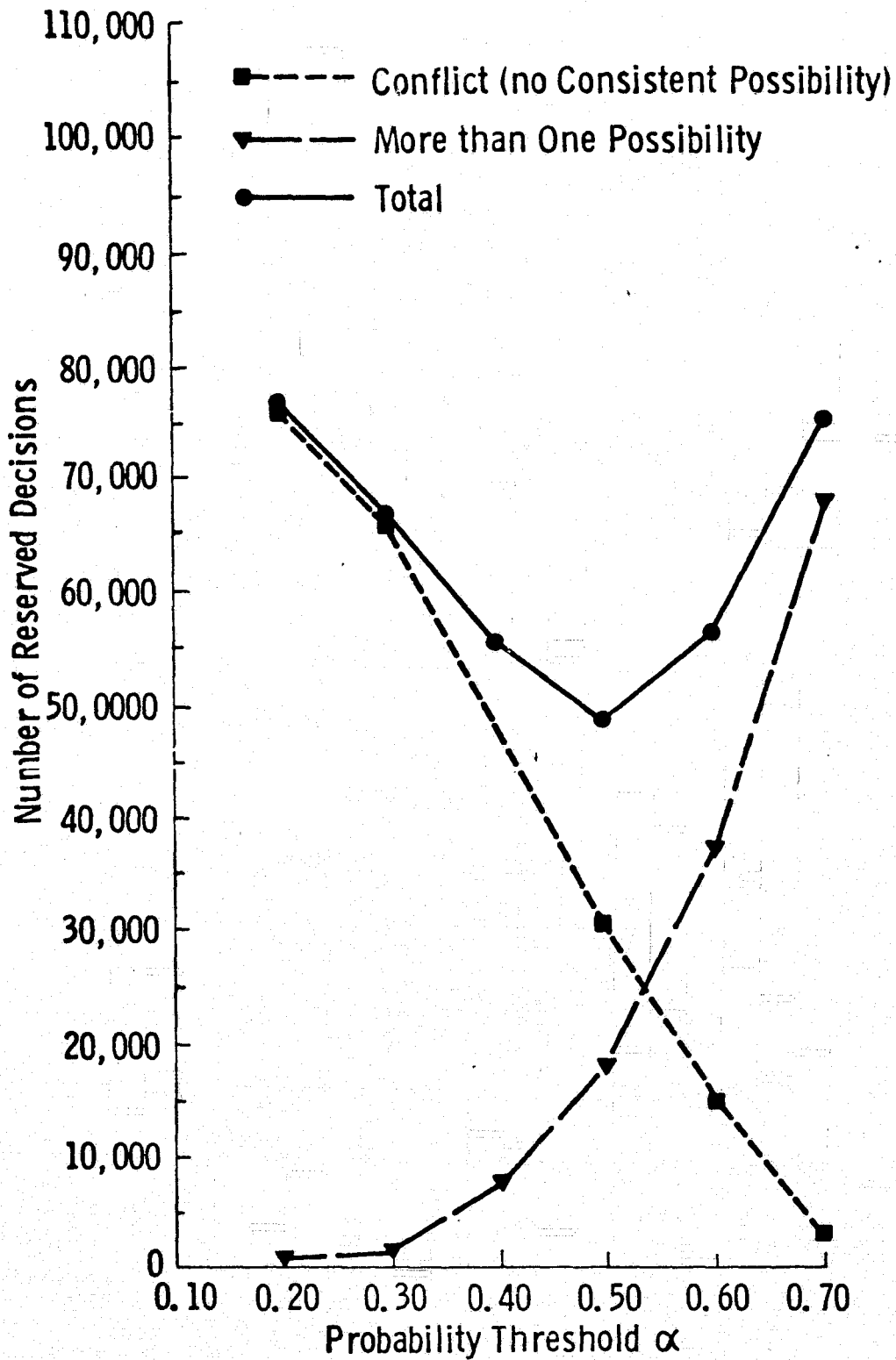


Figure XI.13 Number of reserved decisions as a function of probability threshold alpha for best 2 band pairs with texture for edit #9

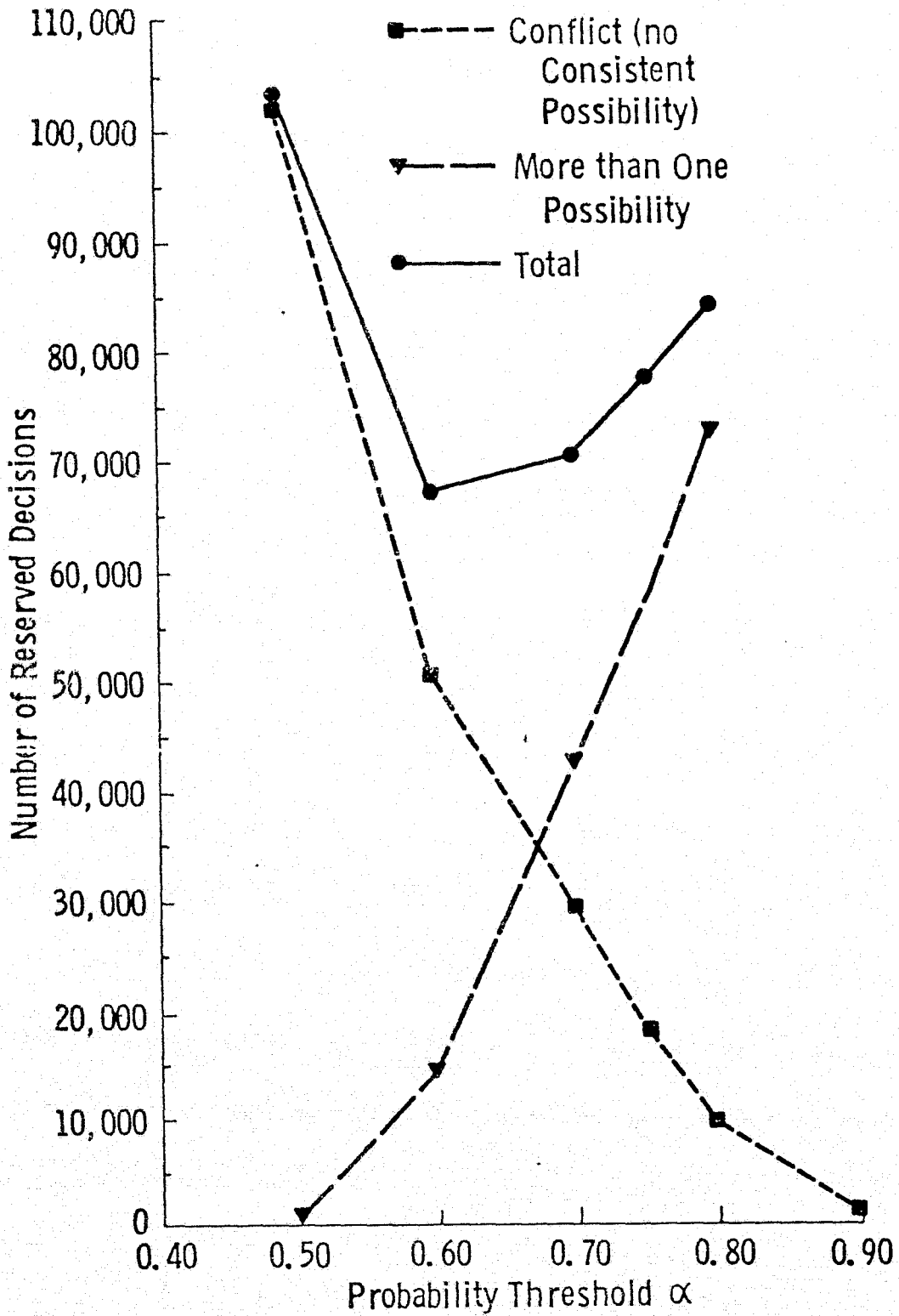


Figure XI.14 Number of reserved decisions as a function of probability threshold alpha for best 3 band pairs spectral only for edit #9

CONTINGENCY TABLE FOR SAMH33GTD - 1 - SAMH38B01 - 1

COL. = ASSIGN CAT    ROW = TRUE CAT

R DEC	1.3	2.3	2.5	2.6	3.1	4.2	7.2	TOTAL	ERR	ERR	
UNKWN	86919	9814	643	6838	1952	1028	1686	3979	112859	0	0
1.3	4281	4323	10	65	5	0	1	0	8685	81	2
2.3	695	7	212	1	4	0	0	6	925	18	8
2.5	7017	1101	8	3388	153	1	4	7	11679	1274	27
2.6	2251	1	7	167	205	1	10	3	2645	189	48
3.1	1249	0	0	0	1	207	61	9	1527	71	26
4.2	1407	0	0	6	9	62	209	8	1701	85	29
7.2	712	0	1	0	1	1	2	488	1205	5	1
TOTAL	104531	15246	881	10465	2330	1300	1973	4500	141226	1723	20
ERR	0	1109	26	239	173	65	78	33	1723	*****	*****
ERR	0	20	11	7	46	24	27	6	20	*****	*****

Table XI.1 The contingency table of the best 3 band pairs for alpha - beta thresholds of .3 and .021.

CONTINGENCY TABLE FOR SAMH33GTD - 1 - SMH3F3R01 - 1

COL. = ASSIGN CAT    ROW = TRUE CAT

R DEC	1.3	2.3	2.5	2.6	3.1	4.2	7.2	TOTAL	ERR	ERR	
UNKWN	30028	1405	32582	4508	0	3121	41215	112859	0	0	
1.3	0	8685	0	0	0	0	0	8685	0	0	
2.3	0	12	913	0	0	0	0	925	12	1	
2.5	0	4773	0	6906	0	0	0	11679	4773	41	
2.6	0	0	0	1160	0	0	0	1485	2645	100	
3.1	0	0	0	0	0	472	1055	1527	1527	100	
4.2	0	0	0	265	0	1436	0	1701	265	16	
7.2	0	0	0	0	0	0	1205	1205	0	0	
TOTAL	0	43498	2318	40913	4508	0	5020	44960	141226	9222	36
ERR	0	4785	0	1425	0	0	472	2540	9222	*****	*****
ERR	0	36	0	17	0	0	25	68	20	*****	*****

Table XI.2 The contingency table of the best 3 band pairs for alpha - beta thresholds of .3 and .021 after 4-shrink and complete filling operations.

ORIGINAL PAGE IS  
OF POOR QUALITY



Figure XI.15 The classification of the best 3 band pairs for alpha - beta thresholds of .3 and .021.



Figure XI.16 The classified image of Figure XI.15 after 4-shrink and complete filling operations.

CONTINGENCY TABLE FOR SAMH33GTD - 1 --- SMH3F5R01 - 1

COL. = ASSIGN CAT      ROW = TRUE    CAT

R DEC 1.3    2.3    2.5    2.6    3.1    4.2    7.2    TOTAL    ERR    ERR

UNKWN	0	24841	3096	29210	13581	7245	13346	21540	112859	0	0
1.3	0	8505	4	160	16	0	0	0	8685	180	2
2.3	0	37	865	0	5	0	0	18	925	60	6
2.5	0	3440	8	8071	116	0	2	42	11679	3608	31
2.6	0	14	62	870	1552	6	108	33	2645	1093	41
3.1	0	0	0	0	22	1099	338	68	1527	428	28
4.2	0	0	0	32	15	203	1405	46	1701	296	17
7.2	0	0	0	0	5	8	20	1172	1205	33	3
TOTAL	0	36837	4035	38343	15312	8561	15219	22919	141226	5698	18
ERR	0	3491	74	1062	179	217	468	207	5698	*****	*****
ERR	0	29	8	12	10	16	25	15	16	*****	*****

Table XI.3      The contingency table of the best 3 band pairs for alpha - beta thresholds of .3 and .021 after 4-fill, 4-shrink, and complete filling operations.

CONTINGENCY TABLE FOR SAMH33GTD - 1 --- SAMH3RR03 - 1

COL. = ASSIGN CAT      ROW = TRUE    CAT

R DEC 1.3    2.3    2.5    2.6    3.1    4.2    7.2    TOTAL    ERR    ERR

UNKWN	55612	14295	2026	12744	10575	7012	4262	6332	112859	0	0
1.3	2491	5764	39	314	63	1	2	11	8685	430	7
2.3	367	26	473	1	19	5	0	34	925	85	15
2.5	4178	1591	67	5200	605	8	12	18	11679	2301	31
2.6	1249	12	23	276	926	55	90	14	2645	470	34
3.1	806	0	1	1	25	522	151	21	1527	199	28
4.2	1013	0	0	11	47	271	350	9	1701	338	49
7.2	484	0	14	0	10	56	15	626	1205	95	13
TOTAL	66200	21688	2643	18547	12270	7930	4882	7065	141226	1518	25
ERR	0	1629	144	603	769	396	270	107	3918	*****	*****
ERR	0	22	23	10	45	43	44	15	28	*****	*****

Table XI.4      The contingency table of the best 3 band pairs for alpha - beta thresholds of .6 and .042.



Figure XI.17 The classified image of Figure XI.15 after 4-fill, 4-shrink and complete filling operations.



Figure XI.18 The classification of the best 3 band pairs for alpha - beta thresholds of .7 and .049 after 4-fill, 8-fill, 4-shrink, 8-shrink, and complete filling operations.

CONTINGENCY TABLE FOR SAMH33GTD - 1 --- SAMH3RB05 - 1

COL. = ASSIGN CAT      ROW = TRUE CAT

	R DEC	1.3	2.3	2.5	2.6	3.1	4.2	7.2	TOTAL	ERR	ERR
UNKN5568	0	1746	2292	13226	14103	6104	3455	6818	112859	0	0
1.3	1746	0	0	0	0	0	0	0	1746	0	12
2.3	35	23	477	4	33	9	9	30	925	98	17
2.5	5672	871	11	4166	861	12	20	17	11677	1881	31
2.6	1192	14	32	162	1137	61	64	22	2645	359	24
3.1	1245	0	1	1	37	31	11	20	1527	170	39
4.2	1235	0	0	5	58	138	255	10	1701	211	45
7.2	436	0	14	0	13	69	6	667	1205	102	13
TOTAL	71919	10250	2292	15066	16767	6672	4310	7502	141226	3446	25
ERR	0	968	223	574	1131	267	200	117	3446	*****	*****
ERR	0	16	32	12	50	48	45	15	31	*****	*****

Table XI.5 The contingency table of the best 3 band pairs for alpha - beta thresholds of .7 and .049.

CONTINGENCY TABLE FOR SAMH33GTD - 1 --- SAMH3RB08 - 1

COL. = ASSIGN CAT      ROW = TRUE CAT

	R DEC	1.3	2.3	2.5	2.6	3.1	4.2	7.2	TOTAL	ERR	ERR
UNKN97048	2878	549	3961	5003	503	468	2449	112859	5	0	
1.3	7457	1011	35	107	65	4	1	5	8685	217	18
2.3	778	7	112	1	23	2	0	2	925	35	24
2.5	10168	84	30	1188	196	7	4	2	11679	323	21
2.6	2151	0	8	62	402	7	7	8	2645	92	19
3.1	1480	0	0	2	14	18	8	5	1527	29	62
4.2	1647	0	0	2	11	5	26	10	1701	28	52
7.2	987	0	1	0	7	4	1	205	1205	13	6
TOTAL	121716	3985	735	5323	5721	550	516	2686	141226	737	28
ERR	0	91	74	174	316	29	21	32	737	*****	*****
ERR	0	8	40	13	44	62	45	14	32	*****	*****

Table XI.6 The contingency table of the best 3 band pairs for alpha - beta thresholds of .8 and .063.

ORIGINAL PAGE IS  
OF POOR QUALITY

CONTINGENCY TABLE FOR SAMH33GTD - 1 --- SMH3F4B05 - 1

	COL. = ASSIGN CAT							ROW = TRUE CAT			
	R DEC	1.3	2.3	2.5	2.6	3.1	4.2	7.2	TOTAL	ERR	ERR
UNKNOWN	0	18546	4509	20259	29258	16242	10331	13674	112859	0	0
1.3	0	7177	144	579	733	4	7	17	8573	1730	15
2.3	0	37	767	6	57	8	5	55	925	160	18
2.5	0	216	222	7268	2003	26	57	48	11679	441	38
2.6	0	70	51	291	1786	120	147	46	2645	650	25
3.1	0	0	3	1	126	716	479	57	1527	61	40
4.2	0	0	0	15	208	482	968	28	1701	730	43
7.2	0	0	24	0	27	140	11	1008	1205	190	15
TOTAL	0	20082	5719	28719	33093	17742	11920	14765	141226	8080	27
ERR	0	2117	444	1192	2649	784	620	265	8080	*****	*****
ERR	0	22	37	14	57	46	30	21	33	*****	*****

Table XI.7 The contingency table of the best 3 band pairs for alpha - beta thresholds of .7 and .049 after a complete filling.

CONTINGENCY TABLE FOR SAMH33GTD - 1 --- SMH3F3B05 - 1

	COL. = ASSIGN CAT							ROW = TRUE CAT			
	R DEC	1.3	2.3	2.5	2.6	3.1	4.2	7.2	TOTAL	ERR	ERR
UNKNOWN	0	20610	1986	22813	28848	15027	7507	16073	112859	0	0
1.3	0	8347	0	338	0	0	0	0	8685	338	4
2.3	0	0	925	0	0	0	0	0	925	0	0
2.5	0	2677	0	8105	663	234	0	0	11679	3574	31
2.6	0	0	0	0	2645	0	0	0	2645	0	0
3.1	0	0	0	0	0	1459	68	0	1527	68	4
4.2	0	0	0	0	0	184	1517	0	1701	184	11
7.2	0	0	0	0	0	74	0	1131	1205	74	6
TOTAL	0	31634	694	13312	256	22156	16978	9087	17204	141226	4238
ERR	0	2677	92	338	663	495	68	0	4238	*****	*****
ERR	0	24	0	4	20	25	4	0	11	*****	*****

Table XI.8 The contingency table of the best 3 band pairs for alpha - beta thresholds of .7 and .049 after 4-fill, 8-fill, 4-shrink, 8-shrink, and complete filling operations.

ORIGINAL PAGE IS OF POOR QUALITY

CONTINGENCY TABLE FOR SAMH33GTD - 1 --- SAMH3RC61 - 1

COL. = ASSIGN CAT ROW = TRIE CAT

	R DEC	1.3	2.3	2.5	2.6	3.1	4.2	7.2	TOTAL	FRR	ERR
UNKNWN	56293	14831	3549	7414	7759	5338	6717	10266	112859	0	0
1.3	233	641	1	188	76	10	21	9	8685	314	5
2.3	568	9	254	7	30	13	1	33	925	23	26
2.5	509	188	67	3694	809	4	116	19	11679	2895	44
2.6	1639	3	151	185	569	35	106	7	2645	437	43
3.1	735	2	6	3	11	631	115	24	1527	151	20
4.2	773	0	3	3	47	174	681	20	1701	247	27
7.2	256	0	32	0	2	60	5	850	1205	99	10
TOTAL	57684	22765	4032	11494	9393	6265	7755	11928	141226	4246	25
ERR	0	1894	219	386	975	296	364	112	4246	*****	*****
FRR	0	24	45	9	63	32	35	12	31	*****	*****

Table XI.9 The contingency table of the best 2 band pairs for alpha - beta thresholds of .3 and .021.

CONTINGENCY TABLE FOR SAMH33GTD - 1 --- SMH3F4C63 - 1

COL. = ASSIGN CAT ROW = TRIE CAT

	R DEC	1.3	2.3	2.5	2.6	3.1	4.2	7.2	TOTAL	ERR	ERR
UNKNWN	0	24365	8111	15641	19961	12645	15073	17063	112859	0	0
1.3	0	8255	9	246	114	2	21	38	8685	430	5
2.3	0	37	690	18	79	29	0	72	925	235	25
2.5	0	3371	113	6561	1357	0	234	43	11679	5118	44
2.6	0	8	238	340	1619	102	320	18	2645	1026	39
3.1	0	0	20	4	21	1299	150	24	1527	228	15
4.2	0	0	10	2	74	270	1313	32	1701	388	23
7.2	0	0	24	0	2	106	9	1064	1205	141	12
TOTAL	0	36036	9215	22812	23227	14453	17125	18354	141226	7566	23
ERR	0	3416	414	610	1647	509	743	227	7566	*****	*****
ERR	0	29	38	9	50	28	36	18	29	*****	*****

Table XI.10 The contingency table of the best 2 band pairs after 4-fill, 4-shrink, and complete filling operations.

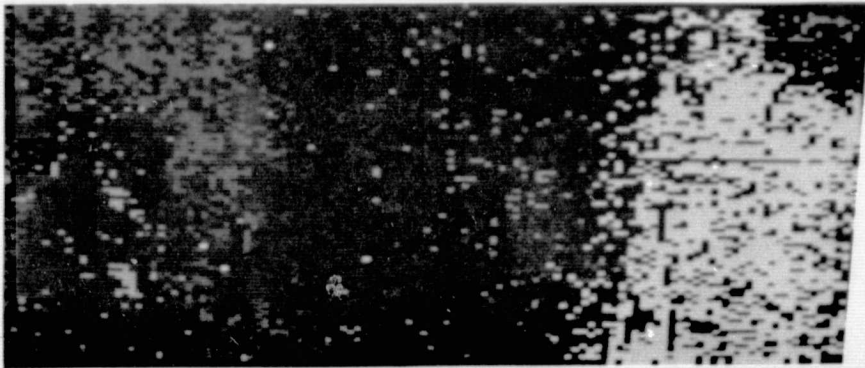


Figure XI.19 The classification of the best 2 band pairs for alpha - beta thresholds of .3 and .021.

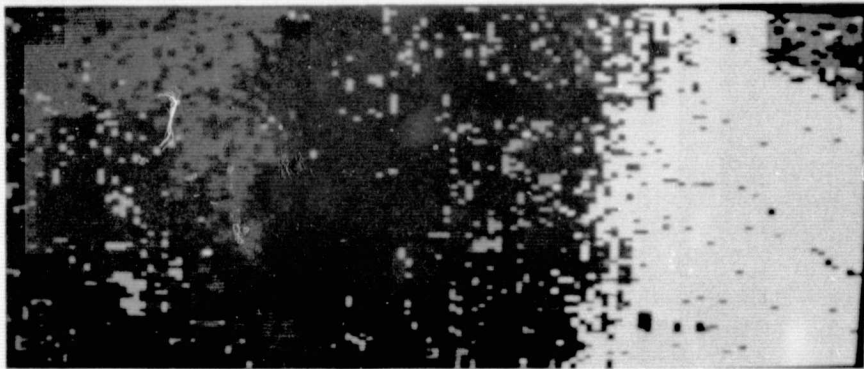


Figure XI.20 The classified image of Figure XI.19 after 4-fill, 4-shrink, and complete filling operations.

CONTINGENCY TABLE FOR CAN33010 - 1 --- CAN35043 - 1

CCL = ASSIGN CAT ROW = TRUE CAT

	R DEC	1.3	2.3	2.5	2.6	3.1	4.2	7.2	TOTAL	ERR	ERR
TOTAL	0	24725	7467	14855	20387	10580	14632	20203	112859	0	0
1.3	0	8551	0	84	22	0	0	29	8685	135	2
2.3	0	0	852	0	21	0	0	52	925	73	8
2.5	0	3819	81	6669	958	0	147	15	11679	5010	43
2.6	0	0	156	364	1942	47	136	0	2645	703	27
3.1	0	0	0	0	0	1436	86	5	1527	91	6
4.2	0	0	0	0	28	147	1498	28	1701	203	12
7.2	0	0	0	0	0	80	0	1125	1205	80	7
TOTAL	0	3784	8542	21275	23355	12222	16496	21462	141226	6295	15
ERP	0	3819	237	448	1025	274	360	129	6295	*****	*****
ERR	0	31	22	6	35	16	20	10	20	*****	*****

— Table XI.11 The contingency table of the best 2 band pairs after 4-shrink and complete filling operations.

ORIGINAL PAGE IS  
OF POOR QUALITY

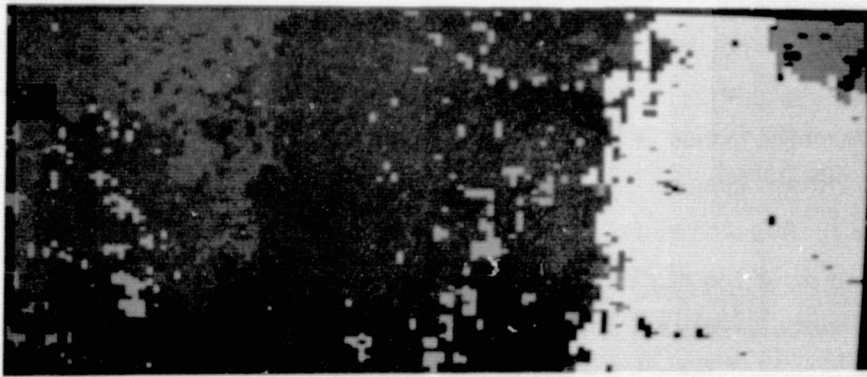


Figure XI.21 The classified image of Figure XI.19 after 4-shrink and complete filling operations

## XII Spectral-Textural Analysis: Edit 14

The spectral texture analysis of edit #14 began just like that of the other edits except the feature selection did not choose a texture band as one of the best 2 or best 3 band pairs. We, nevertheless, did an experiment with 2 band pairs.

We chose bands .40 - .44 and .72 - .76 with bands .72 - .76 and the texture transform image. The texture image was the result of a 3x3 convolution of the .82 - .88 micrometer band as input into the texture transform and a 3x3 convolution after the texture transform. The alpha and beta thresholds were .3 and .021, respectively. Figure XII.1 shows the .82 - .88 micrometer band used for the texture transform. The texture transformed image that was used for processing is shown in Figure XII.2. Figure XII.3 shows the texture transform result with no convolution before transforming and with a 3x3 convolution after. The feature selector did not choose this band and visually we can see that it has much less spatial information than the texture transform that was chosen.

The contingency table that resulted from the table look-up rule (Table XII.1) shows a 43% misidentification error rate and a 44% false identification error rate. This is not nearly as good as the spectral results. There were a large number of reserved decisions, 72,804, due to too low thresholds.

The main reason for the larger error was increased confusion between all categories and category 7.2, not site prepared. These errors were small on the spectral analysis.

Using the same spatial post processing that we used in the spectral analysis we reduced the error most of the time but not always. After a 4-fill, 8-fill, 4-shrink, 8-shrink, we eliminated almost all errors in the spectral analysis (Section VIII) but with this spectral-textural analysis (Table XII.2) we increase misidentification error on category 4.1 to 91%, and on category 2.3 it was about the same (59%) as before post processing.

The final filling of the image (Table XII.3) reduced the error rates to 35% and 31% but did not come close to the 85% classification accuracy of the 2-band spectral results. This might have been due to the texture function used or to the fact that there was little textural distribution between the categories in this image.

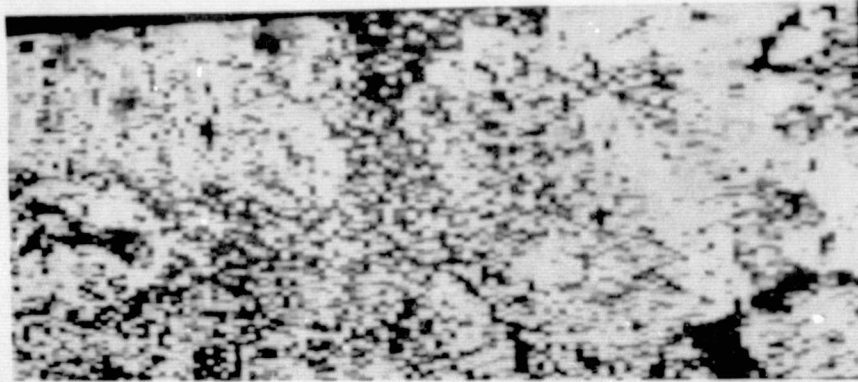


Figure XII.1 The .82 - .88 micrometer band used for the texture transform.

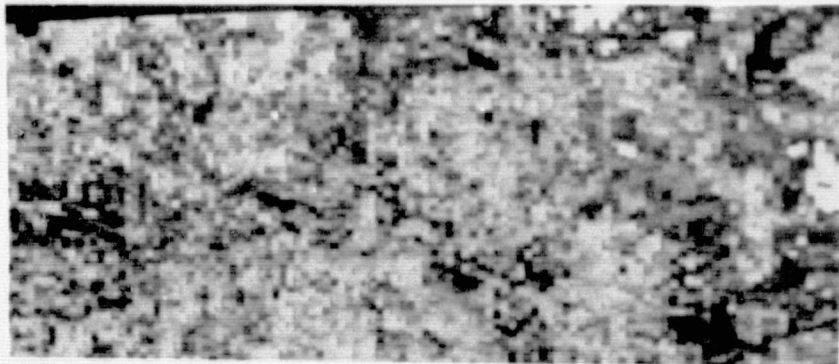


Figure XII.2 The texture transform of Figure XII.1 with a 3x3 rectangular convolution before the texture transform and a 3x3 rectangular convolution after.



Figure XII.3 The texture transform of Figure XII.1 with no rectangular convolution before the texture transform and a 3x3 rectangular convolution after.

CONTINGENCY TABLE FOR SAMH42GDT - 1 SAMH4 B03 - 1 SCALE FACTOR 10\*\*

R DEC	COL. = ASSIGN CAT				TOTAL	ROW = TRUE CAT			
	2.3	2.5	4.1	7.2		ERR	ERR	SD	
UNKNW65935	7345	13007	11622	22637	119946	0	0	0	
2.3	2816	1028	444	281	406	4975	1131	52	
2.5	2003	383	2445	115	30	4978	529	18	
4.1	1106	216	105	212	110	1749	431	67	
7.2	1542	229	133	112	898	2914	474	35	
TOTAL72804	9201	16134	12342	24081	134562	2564	43	0	
ERR	0	828	682	508	546	2564	*****	*****	
ERR	0	45	22	71	38	46	*****	*****	

Table XII.1 The contingency table of the best 2 band pairs for alpha - beta thresholds of .3 and .021.

CONTINGENCY TABLE FOR SAMH42GDT - 1 SMH4S4B03 - 1 SCALE FACTOR 10\*\* 0

R DEC	COL. = ASSIGN CAT				TOTAL	ROW = TRUE CAT			
	2.3	2.5	4.1	7.2		ERR	ERR	SD	
UNKNW*****	569	3254	2962	10390	119946	0	0	0	
2.3	4720	104	18	4	129	4975	151	59	
2.5	3667	18	1293	0	0	4978	18	1	
4.1	1696	33	3	5	12	1749	48	91	
7.2	2405	37	19	0	453	2914	56	11	
TOTAL*****	761	4587	2971	10984	134562	271	40	0	
ERR	0	88	40	4	141	273	*****	*****	
ERR	0	46	3	44	24	29	*****	*****	

Table XII.2 The contingency table of the best 2 band pairs after 4-fill, 8-fill, 4-shrink, and 8-shrink operations.

ORIGINAL PAGE IS  
OF POOR QUALITY

	COL. = ASSIGN CAT	ROW = TRUE	CAT						
	R DEC 2.3	2.5	4.1	7.2	TOTAL	ERP	ERR	SD	
UNKWN	0 15273	27797	24138	52738	119946	n	0	0	
2.3	0 3234	407	322	1012	4975	1741	35	0	
2.5	0 373	4605	0	0	4978	372	7	0	
4.1	0 824	159	538	228	1749	1211	69	1	
7.2	0 490	411	0	2013	2914	901	31	0	
TOTAL	0 20194	33379	24998	55991	134562	4226	35	0	
ERR	0 1687	977	322	1240	4226	*****	*****	*****	
ERR	0 34	18	37	38	31	*****	*****	*****	

Table XII.3 The contingency table of the best 2 band pairs after 4-fill, 8-fill, 4-shrink, 8-shrink and complete filling operations.

### XIII Spectral-Textural Analysis: Edit 3

In addition to the six spectral bands, we provided the feature selector with two textural transform bands. The texture bands were created from the .82 - .88 micrometer spectral bands as before. We used a 3x3 convolution before and after textural transform and no convolution before and 3x3 convolution after textural transform. The feature selector chose bands .40 - .44 and .588 - .643 micrometers with .40 - .44 micrometers and no convolution before and 3x3 convolution after texture bands for the best 2 band pairs. Figure XIII.1 shows how the alpha and beta thresholds were chosen in an attempt to minimize the total number of reserved decisions and to equalize the number of reserved decisions due to no assignment and the number of reserved decisions due to multiple assignments.

For the best 2 band pairs the alpha threshold was set at .5 and the beta threshold at .035. Table XIII.1 shows the resulting contingency table for the best 2 band pairs. There are 49,130 reserved decisions with 18,083 due to no assignment and 31,047 due to multiple assignment. The misidentification error rate was 42% and the false identification error rate was 43%. The largest cause of error was the misidentification error rate (90%) of category 1.3, shortleaf pine, mostly caused by assigning category 1.2, another subclass of shortleaf pine. Post processing with a 4-fill, 8-fill, 4-shrink, 8-shrink and a complete filling results in a misidentification error rate of 34% and a false identification error rate of 20% (Table XIII.2).

The band pairs used for the best 2 along with the .588 - .643 and .65 - .69 micrometer band pair were chosen by the feature selector as the best 3 band pairs. Figure XIII.2 shows the graph of the threshold alpha against the number of reserved decisions. For the best 3 band pairs the alpha threshold was set at .6 and the beta threshold was set at .042. It is interesting to note, that the number of reserved decisions due to no assignment was 25,878, and the number of reserved decisions due to more than one assignment was 26,566 which are very close indicating good thresholds.

Table XIII.3 shows the resulting contingency table for the best 3 band pairs. The misidentification error rate was 38% and the false identification

error rate was 41%. The greatest cause of confusion is the misidentification of category 1.3 and the false identification of category 1.3, a subclass of shortleaf pine. As with the spectral analysis of edit #3 (Chapter IX), the confusion is mostly within class types. Confusion between category 1.2 and category 1.3, subclasses of shortleaf pine, and confusion between category 2.4 and category 2.6 cause most of the error. Figure XIII.3 shows the best 3 band pairs classification.

Post processing with a 4-fill and an 8-fill (Table XIII.4 and Figure XII.4) did not really change the error rates. The misidentification error rate is 40% and the false identification error rate is 44%. A 4-shrink (Table XIII.5 and Figure XIII.5) and an 8-shrink (Table XIII.6) eliminate almost all of the confusion between class types, but the error within class type 1 is still high. This confusion within class type 1 was also present in the spectral analysis (Chapter IX). The final post processing, a complete filling, resulted in a contingency table (Table XIII.7 and Figure XIII.6) having a misidentification error rate of 25% and a false identification error rate of 29%.

Note that the results of 4-fill, 8-fill, 4-shrink, 8-shrink, and complete filling operations for the best 3 band pairs (Table XIII.7 and Figure XIII.6) and the results of 4-fill, 8-fill, 4-shrink, 8-shrink and complete filling operations for best 3 band pairs using the spectral analysis (Chapter IX, Table IX.7 and Figure IX.8) shows less error in the spectral results. Yet, comparison of Figure XIII.6 and Figure IX.8 show that the figure from the texture analysis is actually truer to the timber stand and compartment map for edit #3 than the spectral figure. It seems this is due to the area covered by the ground truth overlay (Figure IX.2), so that more ground truth would have resulted in better classification accuracy for the texture analysis.

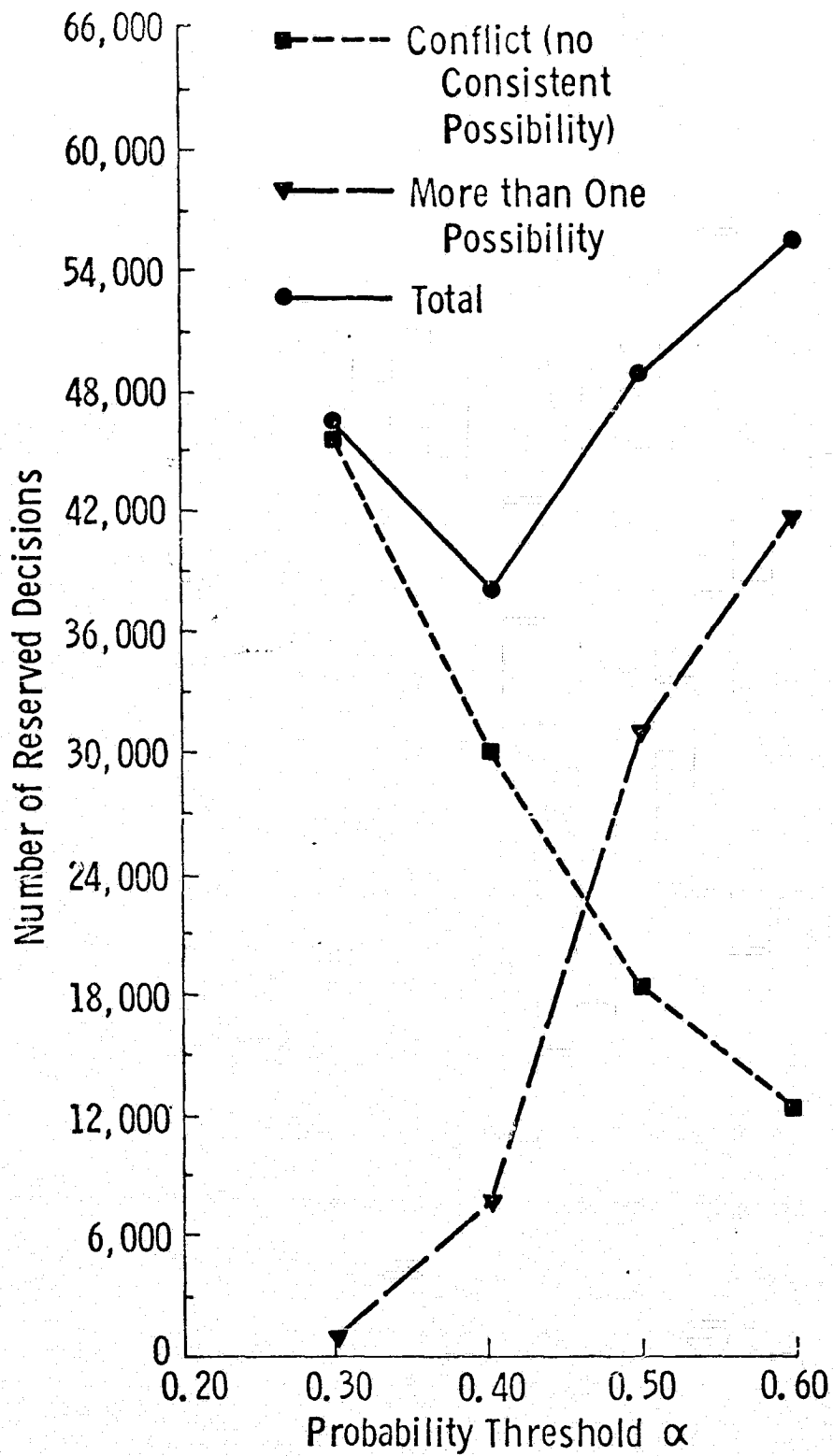


Figure XIII.1 Number of reserved decisions as a function of probability threshold alpha for best 2 band pairs with texture for edit #3

CONTINGENCY TABLE FOR SAMH12GDT - 1 SAMH1 R23 - 1 SCALE FACTOR 10\*\* 0

COL. = ASSIGN CAT      ROW = TRUE CAT

R DEC	1.2	1.3	2.4	2.6	7.1	TOTAL	FRR	FBR	SD	
UNKNWN	2645	7452	1245	10200	7426	8658	67633	0	0	0
1.2	6200	2411	227	579	1040	447	12003	2312	60	0
1.3	1177	423	67	17	179	0	1863	619	90	1
2.4	5681	567	150	2583	723	263	2972	1703	40	0
2.6	3211	552	58	452	2043	82	6405	1151	36	0
7.1	216	1	5	153	58	3597	4020	217	0	0
TOTAL	42133	12413	1762	1479	11476	13047	101896	6002	42	0
FRR	0	155	450	1201	2000	792	6002	*****	*****	*****
FBR	0	31	87	22	50	18	42	*****	*****	*****

Table XIII.1 The contingency table of the best 2 band pairs for alpha - beta thresholds of .5 and .035.

CONTINGENCY TABLE FOR SAMH12GDT - 1 SMH1F3B03 - 1 SCALE FACTOR 10\*\*

COL. = ASSIGN CAT      ROW = TRUE CAT

R DEC	1.2	1.3	2.4	2.6	7.1	TOTAL	#ERR	% ERR	% SD	
UNKNWN	0	17749	0	19587	14981	15316	67633	0	0	0
1.2	0	8152	0	1323	1692	836	12003	3851	32	0
1.3	0	1418	0	0	445	0	1863	1863	100	0
2.4	0	261	0	6553	2919	239	9972	3419	34	0
2.6	0	281	0	0	6124	0	6405	281	4	0
7.1	0	0	0	0	4020	4020	0	0	0	0
TOTAL	0	27861	0	27463	26161	20411	101896	9414	34	0
#ERR	0	1960	0	1323	5056	1075	9414	*****	*****	*****
% ERR	0	19	0	17	45	21	20	*****	*****	*****

Table XIII.2 The contingency table of the best 2 band pairs after 4-fill, 8-fill, 4-shrink, 8-shrink and complete filling operations.

ORIGINAL PAGE IS  
OF POOR QUALITY

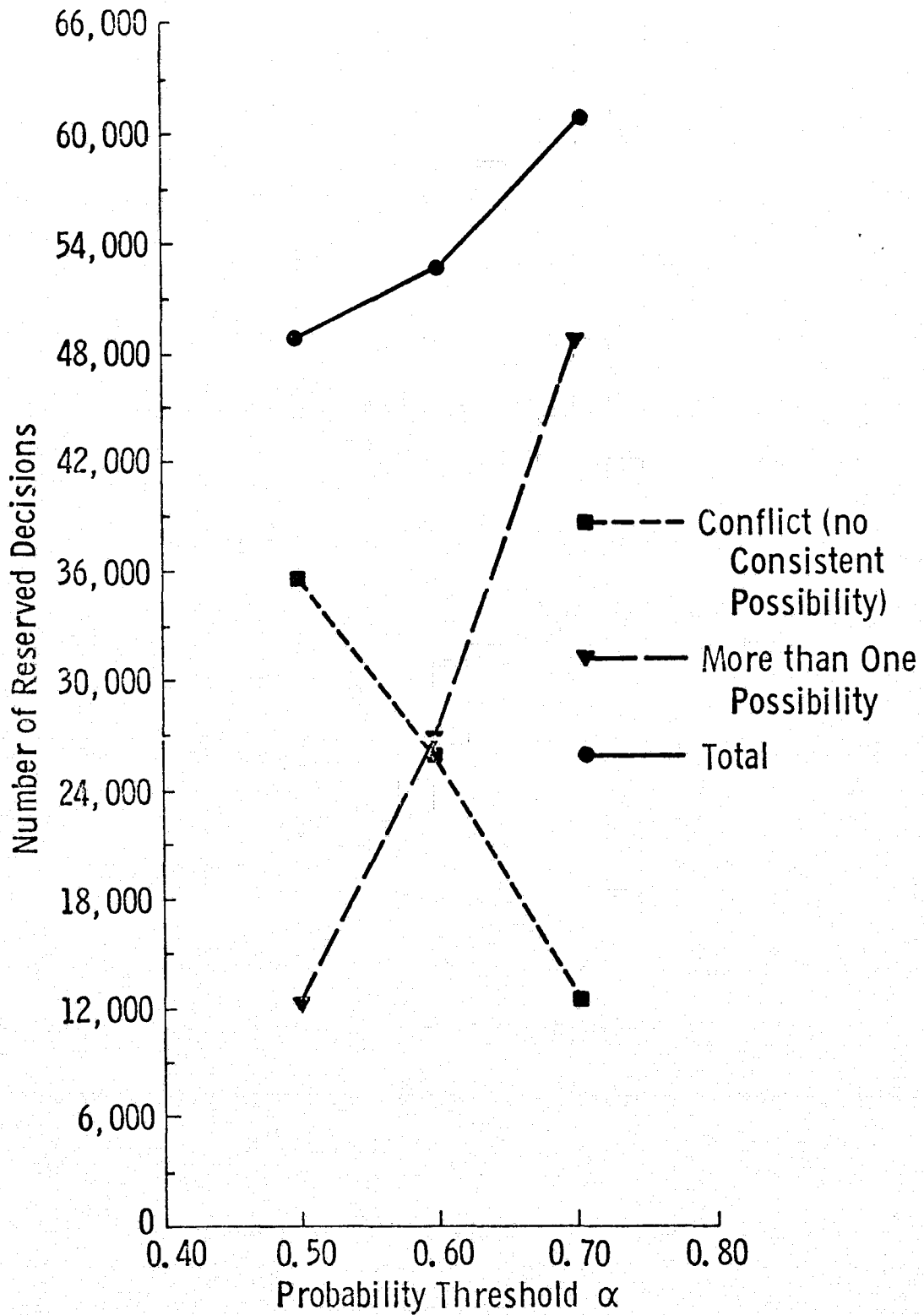


Figure XIII.2 Number of reserved decisions as a function of probability threshold alpha for best 3 band pairs with texture for edit #3

CONTINGENCY TABLE FOR SAMH12GDT - 1 SAMH1 P14 - 1 SCALE FACTOR 10\*\*

COL. = ASSIGN CAT      ROW = TRUE CAT

R DEC	1.2	1.3	2.4	2.6	7.1	TOTAL	ERR	FRP	SD
UNKNW	6660	4221	2364	7324	8403	8471	67633	0	0
1.2	6658	2862	656	548	870	422	12003	2476	46
1.3	1497	362	285	26	113	0	1863	481	63
2.4	5882	411	155	2265	893	281	4275	1825	45
2.6	3394	669	55	600	274	51	6405	285	33
7.1	362	6	207	23	3642	4020	236	6	0
TOTAL	52444	14668	3221	1077	12226	12657	101896	6003	38
ERR	132	872	1181	1224	744	6003	*****	*****	*****
FRP	21	75	36	48	18	41	*****	*****	*****

Table XIII.3 The contingency table of the best 3 band pairs for alpha - beta thresholds of .6 and .042.

CONTINGENCY TABLE FOR SAMH12GDT - 1 SMH1F2B04 - 1 SCALE FACTOR 10\*\*

COL. = ASSIGN CAT      ROW = TRUE CAT

R DEC	1.2	1.3	2.4	2.6	7.1	TOTAL	#ERR	% ERR	% SD
UNKNW	96	14781	5624	16474	19209	11449	67633	0	0
1.2	5	6241	1873	1326	1976	582	12003	5757	48
1.3	2	907	666	68	220	0	1863	1195	64
2.4	13	1420	340	5281	2453	465	9972	4678	47
2.6	0	1075	117	808	4270	135	6405	2135	33
7.1	0	0	8	324	44	3644	4020	376	9
TOTAL	116	24424	8628	24281	28172	16275	101896	14141	40
#ERR	0	3402	2338	2526	4693	1182	14141	*****	*****
% ERR	0	35	78	32	52	24	44	*****	*****

Table XIII.4 The contingency table of the best 3 band pairs after 4-fill and 8-fill operations.

ORIGINAL PAGE IS  
OF POOR QUALITY

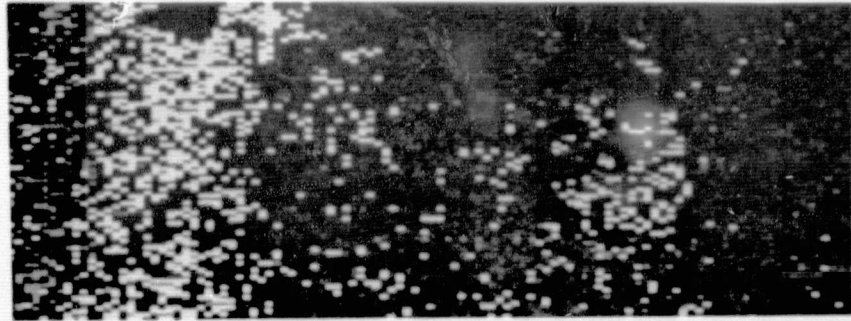


Figure XIII.3 The classification of the three best band pairs for alpha - beta thresholds of .6 and .042.

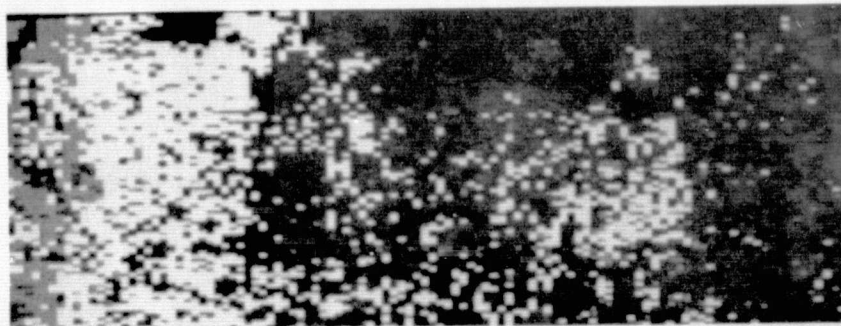


Figure XIII.4 The classified image of Figure XIII.3 after 4-fill and 8-fill operations.

CONTINGENCY TABLE FOR SAMH12GDT - 1 SMH1S1B04 - 1 SCALE FACTOR 10\*\* C

COL. = ASSIGN CAT      ROW = TRUE    CAT

R DEC	1. 2	1. 3	2. 4	2. 6	7. 1	TOTAL	#ERR	% ERR	% SD	
UNKWN45873	5089	1607	3613	4983	6468	67633	0	0	0	
1. 2	7181	3264	633	378	318	229	12003	1558	32	0
1. 3	1189	362	301	1	10	0	1863	373	55	0
2. 4	7242	210	8	2017	408	87	9972	713	26	0
2. 6	4393	173	1	23	1813	2	6405	199	10	0
7. 1	640	0	0	73	0	3307	4020	73	2	0
TOTAL66518	9098	2550	6105	7532	10093	101896	2916	25	0	
#ERR	0	745	642	475	736	318	2916	*****	*****	*****
% ERR	0	19	68	19	29	9	28	*****	*****	*****

Table XIII.5 The contingency table of the best 3 band pairs after 4-fill, 8-fill, and 4-shrink operations.

CONTINGENCY TABLE FOR SAMH12GDT - 1 SMH1S2B04 - 1 SCALE FACTOR 10\*\* 0

COL. = ASSIGN CAT      ROW = TRUE    CAT

R DEC	1. 2	1. 3	2. 4	2. 6	7. 1	TOTAL	#ERR	% ERR	% SD	
UNKWN62426	910	299	287	440	3271	67633	0	0	0	
1. 2	10897	805	185	24	13	79	12003	301	27	0
1. 3	1732	66	65	0	0	0	1863	66	50	0
2. 4	9622	5	0	341	3	1	9972	9	3	0
2. 6	6181	13	0	0	211	0	6405	13	6	0
7. 1	1140	0	0	10	0	2870	4020	10	0	0
TOTAL91998	1799	549	662	667	6221	101896	399	17	0	
#ERR	0	84	185	34	16	80	399	*****	*****	*****
% ERR	0	9	74	9	7	3	20	*****	*****	*****

Table XIII.6 The contingency table of the best 3 band pairs after 4-fill, 8-fill, 4-shrink and 8-shrink operations.

CONTINGENCY TABLE FOR SAMH12GDT - 1 SMH1F3B04 - 1 SCALE FACTOR 10\*\*

	COL. = ASSIGN CAT	ROW = TRUE CAT								
	R DEC	1. 2	1. 3	2. 4	2. 6	7. 1	TOTAL	#ERR	% ERR	% SD
UNKWN	0	15644	5385	13505	16484	16615	67633	0	0	0
1. 2	0	7887	1238	1274	697	907	12003	4116	34	0
1. 3	0	1262	512	0	69	0	1863	1351	73	1
2. 4	0	144	0	8704	821	303	9972	1268	13	0
2. 6	0	379	0	0	6026	0	6405	379	6	0
7. 1	0	0	0	109	0	3911	4020	109	3	0
TOTAL	0	25336	7135	23592	24097	21736	101896	7223	25	0
#ERR	0	1805	1238	1383	1587	1210	7223	*****	*****	*****
% ERR	0	19	71	14	21	24	29	*****	*****	*****

Table XIII.7 The contingency table of the best 3 band pairs after 4-fill, 8-fill, 4-shrink, 8-shrink and complete filling operations.

ORIGINAL PAGE IS  
OF POOR QUALITY

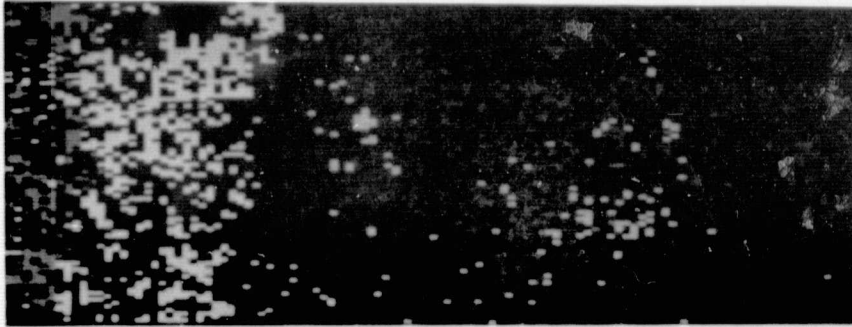


Figure XIII.5 The classified image of Figure XIII.3 after 4-fill, 8-fill and 4-shrink operations.

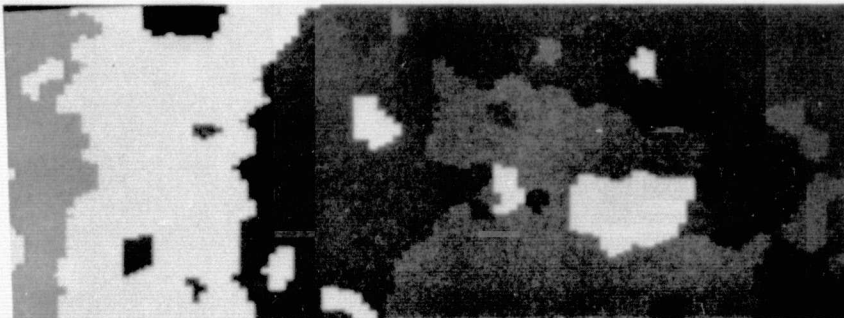


Figure XIII.6 The classified image of Figure XIII.3 after 4-fill, 8-fill, 4-shrink, 8-shrink, and complete filling operations.

#### XIV Conclusions

Use of textural features and spatial post processing has been shown to cut the average classification error to less than half its initial value while tending to increase and equalize the equally weighted average misidentification error and equally weighted false identification error. The classified images resulting from spatial and textural processing have a more cartographic map-like quality than the typically salt and pepper classified images using no textural features or spatial post-processing.

The simultaneous decrease in average classification error and increase in both equally weighted average misidentification error and false identification error means that more pixels whose true category identification is of a frequently occurring category get reassigned correctly by the spatial post-processing than of an infrequently occurring category. This is a natural consequence of the fact that the spatial processing is more of a syntactic operation than a semantic one. Spatial processing operations which use category labels instead of just sameness or difference of category labels could be designed which do not favor the larger categories over the smaller categories.

Because of the strong interaction between average error, average misidentification error, average false identification error, and classified image appearance and complexity, it is clear that further work can bear much fruit by analysis of these interaction effects. In particular, we recommend that textural and spatial post-processing concepts be developed using classified image's local neighborhood contexts as the independent variable and classification error as the dependent variable.

## REFERENCES

- Ashby, R. W., "Constraint Analysis of Many-Dimensional Relations," Yearbook for the Society of General System's Research, Vol. 9, 1964, pp. 99-105.
- Brooner, W. G., R. M. Haralick, and I. Dinstein, "Spectral Parameters Affecting Automated Image Interpretation Using Bayesian Probability Techniques," Proceedings of the Seventh International Symposium on Remote Sensing of Environment, University of Michigan, Ann Arbor, Michigan, May 17-21, 1971, pp. 1929-1949.
- Eppler, W. G., "An Improved Version of the Table Look-up Algorithm for Pattern Recognition," Proceedings of the Ninth International Symposium on Remote Sensing of Environment, Environmental Research Institute of Michigan, Ann Arbor, Michigan, April 1974, pp. 793-812.
- Eppler, W. G., C. A. Hemke, and R. H. Evans, "Table Look-up Approach to Pattern Recognition," Proceedings of the Seventh International Symposium on Remote Sensing of Environment, University of Michigan, Ann Arbor, Michigan, May 17-21, 1971, pp. 1415-1425.
- Lewis, A. J., "Geomorphic Evaluation of Radar Imagery of Southeastern Panama and Northwestern Columbia," CRES Technical Report No. 133-18, University of Kansas Center for Research, Inc., Lawrence, Kansas, February 1971.
- Kaizer, H., "A Quantification of Textures on Aerial Photographs," Boston University Research Laboratories, Technical Note 121, 1955, AD69484.
- Landaris, G. G. and G. L. Stanley, "Diffraction-Pattern Sampling for Automatic Pattern Recognition," Proceedings of the IEEE, Vol. 58, no. 2, February 1970, pp. 198-216.
- Gramenopoulos, N., "Terrain Type Recognition Using ERTS-1 MSS Images," Symposium on Significant Results Obtained from the Earth Resources Technology Satellite, NASA SP-327, March 1973, pp. 1229-1241.
- Hornung, R. J. and J. A. Smith, "Application of Fourier Analysis to Multispectral/Spatial Recognition," Management and Utilization of Remote Sensing Data ASP Symposium, Sioux Falls, South Dakota, October 1973.
- Kirvida, L. and G. Johnson, "Automatic Interpretation of Earth Resources Technology Satellite Data for Forest Management," Symposium on Significant Results Obtained from the Earth Resources Technology Satellite, NASA SP-327, March 1973, pp. 1076-1082.
- Rosenfeld, A. and M. Thurston, "Edge and Curve Detection for Visual Scene Analysis," IEEE Transactions on Computers, Vol. C-20, No. 5, May 1971, pp. 562-569.

Matheron, G., Elements Pour Une Theorie des Milieux Poreux, Masson, Paris, 1967.

Serra, J. and G. Verchery, "Mathematical Morphology Applied to Fibre Composite Materials," Film Science and Technology, Vol. 6, 1973, pp. 141-158.

Haralick, R. M., K. Shanmugam, and I. Dinstein, "Textural Features for Image Classification," IEEE Transactions on Systems, Man and Cybernetics, Vol. SMC-3, No. 6, November 1973, pp. 610-621.

O'Neill, E., "Spatial Filtering in Optics," IRE Transactions on Information Theory, June 1956, pp. 56-65.

Cutrona, L. J., E. N. Leith, C. J. Palermo, and L. J. Porcello, "Optical Data Processing and Filtering Systems," IRE Transaction on Information Theory, Vol. 6 No. 3, June 1960, pp. 386-400.

Goodman, J. W., Introduction to Fourier Optics, McGraw-Hill, New York, 1968.

Preston, K., Coherent Optical Computers, McGraw-Hill, New York, 1972.

Shulman, A. R., Optical Data Processing, John Wiley & Sons, Inc., New York, 1970.

Jensen, N., "High-Speed Image Analysis Techniques," Photogrammetric Engineering, Vol. XXXIX, No. 12, December 1973, pp. 1321-1328.

Swanlund, G., "Honeywell's Automatic Tree Species Classifier," Honeywell Systems and Research Division, Report 90-G-24, December 31, 1969.

Triendl, E. E., "Automatic Terrain Mapping by Texture Recognition," Proceedings of the Eighth International Symposium on Remote Sensing of Environment, Environmental Research Institute of Michigan, Ann Arbor, Michigan, October 1972, pp. 771-776.

Sutton, R. and E. Hall, "Texture Measures for Automatic Classification of Pulmonary Disease," IEEE Transactions on Computers, Vol. C-21, No. 7, July 1972, pp. 667-676.

Maurer, H., "Texture Analysis with Fourier Series," Proceedings of the Ninth International Symposium on Remote Sensing of Environment, Environmental Research Institute of Michigan, Ann Arbor, April 1974, pp. 1411-1420.

Darling, E. M. and R. D. Joseph, "Pattern Recognition from Satellite Altitudes," IEEE Transactions on Systems, Man, and Cybernetics, Vol. SSC-4, March 1968, pp. 38-47.

Read, J. S. and S. N. Jayaramamurthy, "Automatic Generation of Texture Feature Detectors," IEEE Transactions on Computers, Vol. C-21, No. 7, July 1972, pp. 803-812.

Haralick, R. M., "A Texture-Context Feature Extraction Algorithm for Remotely Sensed Imagery," Proceedings 1971 IEEE Decision and Control Conference, Gainesville, Florida, December 15-17, 1971, pp. 650-657.

Haralick, R. M., K. Shanmugam, and I. Dinstein, "On Some Quickly Computable Features for Texture," Proceedings of the 1972 Symposium on Computer Image Processing and Recognition, University of Missouri, Vol. 2, August 1972, pp. 12-2-1, 12-2-10.

## APPENDIX 1

### Textural Transform Programs

## PROGRAM DESCRIPTION

### Table of Contents

- I. User Interaction
- II. Internal Program Description
- III. Non-Standard Subroutines
- IV. Subroutine Documentations
- V. Listing

## 1. User Interaction

User parameters are input by the routine TXINPT which asks for parameters by name:

NFUNC = 1            use subroutine FUNC 1

NFUNC = 2            use subroutine FUNC 2

NFUNC = 3            use subroutine FUNC 3

NFUNC = 4            use subroutine FUNC 4

NFUNC = 5            use subroutine FUNC 5

NDIS = distance between spaces of neighboring cells

IBOUT = logical unit number to output error messages

PCLCT = percent of point to count in FPLXIT

FILNMP = input filename

FILNMQ = output filename

ORIGINAL PAGE IS  
OF POOR QUALITY

## 11. Internal Program Description

The texture programs are set up so that after the call to TXINPT at the beginning of execution the user does not interact anymore with the computer.

The user must know which function he wants to use. The user inputs 1, 2, 3, 4, or 5 corresponding to FUNC1, FUNC2, FUNC3, FUNC4, and FUNC5 respectively; where:

- FUNC1 - computes the sum probability feature of the image
- FUNC2 - computes the gradient entropy feature of the image
- FUNC3 - computes the entropy feature of the image
- FUNC4 - computes the gradient feature of the image
- FUNC5 - prepares normalized lex arrays which have been equal probability quantized according to their diagonal elements.

The parameter NDIS is the distance between spaces of neighboring cells. The texture transform works on the co-occurrence of grey levels on neighboring cells. Each cell has a 0° neighbor, a 90° neighbor, a 135° neighbor, and a 45° neighbor. This covers all the cells, since a cell's 180° neighbor has that cell as a 0° neighbor. Thus, for each grey level, there is a count of the co-occurrences of grey levels as one of the four specified neighbors. The parameter NDIS is the distance the algorithm gives to look for the neighboring cells. If the user wants to perform the texture transform using all co-occurrence counts, then the parameter PCLCT should be 1.00. If the user only wants to count 80% of the cells, the PCLCT should be set to 0.80, and so on.

The mainline TXJDM calls the ASCII I/O routine TXINPT for input parameters. The TXJDM transfers control to TXTMN. This routine sets up the work area, allocating core to those arrays that need it. FPLXIT is then called to compute the lex arrays where:

- LEX1 - array containing count over all grey levels of vertically adjacent (90-degree) neighbor;
- LEX2 - array containing count over all grey levels of horizontally adjacent (0-degree) neighbor;
- LEX3 - array containing count over all grey levels of left diagonally adjacent (135-degree) neighbor;
- LEX4 - array containing count over all grey levels of right diagonally adjacent (45-degree) neighbor.

When these counts have finished, control is returned to TXTMN, which transfers control to the appropriate function as specified by the user. The FUNC array which is passed as an argument to the FUNC routines is equivalenced to the lex arrays. For example:

```

FUNC (1,1) = LEX1 (1)
FUNC (1,2) = LEX2 (1)
FUNC (1,3) = LEX3 (1)
FUNC (1,4) = LEX4 (1)

```

After the appropriate function has been applied, control is again returned to TXTMN. TXTMN then calls in PLXIT. PLXIT reads in the image data and determines the corresponding eight neighbors and applies the texture transform.

Let  $Z_r \times Z_c$  be the set of resolution cells of an image  $I$  (by row-column coordinates). Let  $G$  be the set of grey tones possible to appear on image  $I$ . Then  $I: Z_r \times Z_c \rightarrow G$ . Let  $R$  be a binary relation on  $Z_r \times Z_c$  pairing together all those resolution cells in the desired spatial relation. The co-occurrence matrix  $P$ ,  $P: G \times G \rightarrow [0,1]$ , for image  $I$  and binary relation  $R$  is defined by

$$P(i,j) = \frac{\# \{((a,b),(c,d)) \in R \mid I(a,b) = i \text{ and } I(c,d) = j\}}{\#R}$$

The textural transform  $J, J: Z_r \times Z_c (-\infty, \infty)$ , of image  $I$  relative to function  $f$ , is defined by

$$J(y,x) = \frac{1}{\#R(y,x)} \sum_{(a,b) \in R(y,x)} f[P(I(y,x), I(a,b))]$$

Assuming  $f$  to be the identity function, the meaning of  $J(y,x)$  is as follows. The set  $R(y,x)$  is the set of all those resolution cells in  $Z_r \times Z_c$  in the desired spatial relation to resolution cell  $(y,x)$ . For any resolution cell  $(a,b) \in R(y,x)$ ,  $P(I(y,x), I(a,b))$  is the relative frequency by which the grey tone  $I(y,x)$ , appearing at resolution cell  $(y,x)$ , and the grey tone  $I(a,b)$ , appearing at resolution cell  $(a,b)$ , co-occur together in the desired spatial relation on the entire image. The sum

$$\sum_{(a,b) \in R(y,x)} P(I(y,x), I(a,b))$$

is just the sum of the relative frequencies of grey tone co-occurrence over

all resolution cells in the specified relation to resolution cell (y,x).

The factor  $\frac{1}{\#R(y,x)}$ , the reciprocal of the number of resolution cells in the desired spatial relation to (y,x) is just a normalizing factor.

These data values are then written out in the corresponding place on the output texture transformed image. When PLXIT exits, the texture transform has been created. Control goes to TXTMN, which exits back to the mainline TXTDM. This program returns to the beginning and brings back the ASCII I/O routines to get the parameters for the next texture transform. If none are desired, a carriage return will terminate the processing.

All ASCII I/O on our PDP-15 is 5/7 ASCII in double integer words. The PDP-15 has 36 bits in one double integer word.

See Figure 1 for the program flow.

### III. Non-Standard Subroutines

ADJ1

ADJ2 Dynamic core allocation routines

ADJ3

The program can allocate memory by performing what essentially amounts to a dynamic Fortran equivalence and dimension

KDPUSH - ignore (delete)

Error stack processing used in KANDIDATES.

SDKINL - KANDIDATS sequential file opener

Opens files for KANDIDATS routines. Uses Seek and Enter (STANDARD Fortran routines) and can be modified to fit your file structure.

SKPDSC - skip descriptor records

KANDIDATS creates descriptor records, containing processing history information, before the image data. Since the file is sequential, these must be skipped. If the user has random access on images, this can be ignored. If not, be sure that image record numbers are advanced to first image data record.

IMTRXP - Matrix print-out routine

Any standard Matrix print routine will work.

SREAD - sequential read (uses Fortran reads)

SWRITE - sequential write (uses Fortran write)

Starting on the next page is an explanation of the "ADJ routines and several ideas on how to get around them.

The included program segment may be compared to the following example:

1. INTEGER ARRAY (500), X(1)
2. REAL Y(1)
3. INTEGER XSIZE, YSIZE, YSTART, TTLSZE
4. READ (5, 100) XSIZE, YSIZE
5. TTLSZE = XSIZE + YSIZE
6. IF (TTLSZE .GT. 500) CALL ERROR
7. YSTART = XSIZE + 1
8. CALL ADJ1 (X, ARRAY (1))
9. CALL ADJ1 (Y, ARRAY (YSTART))
10. . . . TASK CODE
11. STOP
12. END

Within the task code, X and Y may be referenced as vectors with respective types, integer and real. In addition references to X will access the first XSIZE elements of ARRAY and references to Y will access the last YSIZE elements of ARRAY.

If X and Y are used only in contexts that functions may be used in, then the program segment may be recoded using statement functions. (Check your particular implementation of FORTRAN for applicability.)

1. INTEGER ARRAY (500)
2. REAL RL
3. INTEGER XSIZE, YSIZE, TTLSIZE
4. X(I) = ARRAY (I)
5. Y(I) = RL(ARRAY (I + XSIZE))
6. READ (5, 100) XSIZE, YSIZE
7. TTLSIZE = XSIZE + YSIZE
8. IF (TTLSIZE .GT. 500) CALL ERROR
9. . . . TASK CODE
10. STOP
11. END

Where the function RL is coded as follows.

1. REAL FUNCTION RL(ARG)
2. REAL ARG
3. RL = ARG
4. RETURN
5. END

Within the task code, X and Y will have respective types integer and real and will access those specified locations of ARRAY.

However, X and Y may only be used as functions.

In the context of subroutine calls, adjustable dimensions is a standard feature of FORTRAN as in the following example:

1. INTEGER ARRAY (500)
2. INTEGER XSIZE, YSIZE, YSTART, TTLSIZE
3. READ (5, 100) XSIZE, YSIZE
4. TTLSIZE = XSIZE + YSIZE
5. IF (TTLSIZE .GT. 500) CALL ERROR
6. YSTART = XSIZE + 1
7. CALL SUB (ARRAY(1), ARRAY (YSTART), XSIZE, YSIZE)
8. STOP
9. END

Where SUB is coded as follows:

1. SUBROUTINE SUB (X, Y, XSIZE, YSIZE)
2. INTEGER XSIZE, YSIZE
3. INTEGER X(XSIZE)
4. REAL Y(YSIZE)
5. . . . TASK CODE
6. RETURN

This approach necessitates a division of storage allocation code and task code.

Alternatively X and Y may be dimensioned independently and given a reasonable but sufficient size.

1. INTEGER X (250)
2. REAL Y(250)
3. READ (5, 100) XSIZE, YSIZE
4. IF (XSIZE .GT. 250). OR.
5. (YSIZE .GT. 250) CALL ERROR
6. . . . TASK CODE
7. STOP
8. END

Check the output of the FORTRAN compiler being used.

If the compiler generates and uses dope vectors it would be possible to produce user written ADJ routines.

Keep in mind that all recoding must preserve the size, shape, type and usage of the involved data elements.

IV. Subroutine Documentations

ORIGINAL PAGE IS  
OF POOR QUALITY

## GENERAL MATRIX PRINTOUT PROGRAM

PROGRAM TITLE: SUBROUTINE IMTRXP  
DATE OF LISTING: February 13, 1973  
PROGRAMMER: Dinesh Goel  
DOCUMENTED BY: Dinesh Goel  
PROGRAM LANGUAGE: FORTRAN IV  
COMPUTER REQUIRED: PDP 15/20  
PURPOSE:

This subroutine divides an integer matrix into sections suitable for printer output and prints the matrix with matrix title, column designation, row designation, and column and row labels.

### CALLING SEQUENCE:

CALL IMTRXP (IA, NROW, NCOL, NRWDIM, TTL1, TTL2, TTL3, CLBL, RLBL, ISTR)

### INPUT ARGUMENTS:

IA Input array of matrix to be printed out.  
NROW Number of rows in the printed matrix.  
NCOL Number of columns in the printed matrix.  
NRWDIM Row dimension of the entire matrix which is stored by columns.  
TTL1 Matrix title of 13 words.  
TTL2 Column title of 2 words.  
TTL3 Row title of 2 words.  
CLBL Array of column labels.  
RLBL Array of row labels.  
ISTR This is an option  
if 1, matrix will be printed as such.  
if 2, transposed matrix will be printed out.  
if 3, matrix is assumed to be symmetric having long to short storage in IA.

if 4, matrix is assumed to be symmetric having short to long storage in IA.

**OUTPUT ARGUMENTS:**

None.

**OTHER PARAMETERS AND ARRAYS:**

IROW      Array for any one row of matrix as finally printed out.

**COMMENTS:**

If the printed matrix has large number of columns which can not fit on one page of printer output, it will be separated into blocks, each of which is small enough to fit on one page. The rows are printed in the blocks of 5. This program takes only the integer numbers, for real numbers RMTRXP can be used. File code 17 octal has been used for printing the matrix which must be assigned to teletype or IBM printer in the beginning as desired.

## Sequential Read

PROGRAM TITLE: SREAD  
VERSION: B  
DATE: June 22, 1973  
UPDATE: April 29, 1975  
AUTHOR: Robert M. Haralick  
DOCUMENTED BY: Robert M. Haralick  
PROGRAM LANGUAGE: FORTRAN IV  
IMPLEMENTED ON: PDP 15/20  
PURPOSE:

This subroutine reads a set of lines on a file of single image data stored in standard bit compacted form. SREAD assumes that SDKINL has already been called to open the file on IDAT.

### ENTRY POINT:

SPREAD (IDAT, IARRAY, IDY, IDENT, IEV, ERRRET)

### ARGUMENT LIST:

IDAT	the file code on which the image resides
IARRAY	2-dimensional array (row x column) which subimage is returned in
IDY	number of records in subimage. The number of rows and columns for a record will be taken from IDENT (14) and IDENT (13), respectively
IDENT	identification array of 20 words.
IEV	integer event variable
	IEV = 1 success
	IEV = -2001 illegal file code
	IEV = -2006/IO/too small
	IEV = -2007 EOF
	IEV = -2009 READ ERROR
	IEV = 2012 illegal data mode

ERRRET

alternate return taken if an error occurs

SUBROUTING REQUIRED:

ADJ1

KDPOP

KDPUSH

UNPACK

COMMENTS:

IARRAY must be a two dimensional array

IDENT (13)\* IDENT (14) must not be greater than 256

unless the user has a block data program to allocate more  
memory to labeled common area /IO/.

## Skip Descriptor Records

PROGRAM TITLE: SKPDSC  
VERSION: A  
DATE: July 10, 1973  
UPDATE: October 15, 1974  
AUTHOR: Robert M. Haralick  
DOCUMENTED BY: Robert M. Haralick  
PROGRAM LANGUAGE: FORTRAN IV  
IMPLEMENTED ON: PDP 15/20  
PURPOSE:

This program skips the descriptor records of images stored in standard bit compacted form. SKPDSC assumes that SDKINL has been called previously.

### ENTRY POINT:

SKPDSC (IDATP, IDENT, IEV, ERRRET)

### ARGUMENT LIST:

IDATP	file code on which the image resides.
IDENT	identification array of 20 words for the image.
IEV	= 1 success = -2001 illegal file code = -2007 EOF = -2009 read error
ERRRET	Alternate return taken if error occurs

### SUBROUTINES REQUIRED:

KDPOP  
KDPUSH

## Sequential Disc Initializer

PROGRAM TITLE: SDKINL  
VERSION: B  
DATE: June 30, 1973  
UPDATE: October 15, 1974  
AUTHOR: Robert M. Haralick  
DOCUMENTED BY: Robert M. Haralick  
PROGRAM LANGUAGE: FORTRAN IV  
IMPLEMENTED ON: PDP 15/20  
PURPOSE:

This subroutine initializes a PDP 15/20 sequential disc file for input or output. The file is used to store image data in standard bit compacted form. The number of data words will be written in a logical record of at least 20 and the number of bits per data word should not be more than 18.

### ENTRY POINT:

SDKINL: (IDAT, FILNM, IDENT, IRDWRT, IEV, ERRRET)

### ARGUMENT LIST:

IDAT	file code on which file resides.
FILNM	array containing the fil name.
IDENT	identification array of 20 words.
IRDWRT	read/write indicator. IRDWRT =1 initialize as input file. IRDWRT =2 initialize as output file
IEV	integer event variable. = 1 Success = -2001 Illegal file code = -2002 Number of bits per point has a illegal value = -2003 Frame coordinate and image dimension information not specified in-Ident-array = -2004 Illegal request

= -2005 file does not exist

= -2011 illegal min/max/NZL/nbits combination

= -2012 illegal data mode

ERRRET

ALTERNATE RETURN TAKEN IF A ERROR OCCURS

SUBROUTINES REQUIRED:

ENTER

FSTAT

ICEIL

KDPOP

KDPUSH

MAXØ

SEEK

## Sequential Write

PROGRAM TITLE:            WRITE  
VERSION:                    C  
DATE:                      June 22, 1973  
UPDATE:                    October 15, 1974  
AUTHOR:                    Robert M. Haralick  
DOCUMENTED BY:            Robert M. Haralick  
IMPLEMENTED ON:            PDP 15/20  
PURPOSE:

This program writes a set of lines or a file of single image data stored in standard bit compacted format. SWRITE assumes that SDKINL has also been called to initialize the file on IDAT.

### ENTRY POINT:

SWRITE (IDAT, IARRAY, IDY, IDENT, IEV, ERRRET)

### ARGUMENT LIST:

IDAT	file code on which 1 image resides.
IARRAY	2-dimensional array (row x column) in which subimage is transferred to program.
IDY	number of records for subimage. The number of rows and columns for a record will be taken from IDENT (13) and IDENT (14).
IDENT	identification array of 20 words.
IEV	integer event variable IEV = 1 success IEV = -2001 illegal file code IEV = -2006 /10/ too small IEV = -2007 EOF IEV = -2008 WRITE ERROR IEV = -2012 illegal data mode
ERRRET	ATTENATE RETURN TAKEN IF ERROR OCCURS

SUBROUTINE REQUIRED:

ADJ1  
KDPOP

KDPUSH  
PACK

COMMENTS:

IARRAY must be a two dimensional array.  
IDENT (13)\* IDENT (14) must not be greater than 256  
unless the user has a block data program to allocate more  
memory to labeled common area /10/.

V. Listing

ORIGINAL PAGE IS  
OF POOR QUALITY

CERROR

E-R-R-O-R

ASCII ERROR I/O FOR TEXTURE PROGRAM

PROGRAM TITLE ERROR  
VERSION A  
AUTHOR CHIN-HUANG CHEN  
DATE FEBRUARY 1975  
UPDATE  
PROGRAM LANGUAGE FORTRAN IV  
IMPLEMENTED ON PDP 15  
DOCUMENTED BY CHIN-HUANG CHEN  
PURPOSE

THIS ROUTINE TELLS THE USER EITHER LSTID OR TXTMN IS  
IN ERROR ON .DAT SLOT IOU<sup>T</sup> OR IBOUT  
ENTRY POINT ERROR(IERR, IEV, IOU<sup>T</sup>, IBOUT)  
ARGUMENT LIST  
IERR PARAMETER USED TO DETERMINE EITHER LSTID  
OR TXTMN IS IN ERROR  
IEV INTEGER EVENT VARIABLE  
IOU<sup>T</sup> ERROR MESSAGE OUTPUT .DAT SLOT  
IBOUT ALTERNATE ERROR MESSAGE OUTPUT .DAT SLOT

SUBROUTINE ERROR(IERR, IEV, IOU<sup>T</sup>, IBOUT)  
DOUBLE INTEGER FDATE(3)

GO TO (304, 310), IERR  
CALL ADATE(FDATE)  
WRITE(IOU<sup>T</sup>, 405) FDATE  
405 FORMAT(1X, 3A5)  
IF(IBOUT.NE. IOU<sup>T</sup>)WRITE(IBOUT, 405) FDATE  
GO TO 200  
304 WRITE(IOU<sup>T</sup>, 305) IEV  
IF(IOU<sup>T</sup>.NE. IBOUT) WRITE(IBOUT, 305) IEV  
305 FORMAT(' LSTID ERROR', I5)  
GO TO 400  
310 WRITE(IBOUT, 311) IEV  
IF(IBOUT.NE. IOU<sup>T</sup>) WRITE(IBOUT, 311) IEV  
311 FORMAT(' TXTMN ERROR IEV=', I5)  
400 CALL CLOSE(IBOUT)  
200 RETURN  
END

ORIGINAL PAGE IS  
OF POOR QUALITY



```

C     PARAMETERS      NUMLIN      NUMBER OF LINES IN THE IMAGE
C     NUMPPL          NUMBER OF POINTS PER LINE IN THE IMAGE
C     IMAX            LARGEST GRAY TONE
C     IMIN            LEAST GRAY TONE
C     LEAST1          =IMIN-1.  LEAST1 IS USED FOR NORMALISING
C                     THE GRAY TONES.
C     NOBL            NUMBER OF GRAY TONES
C                     NOBL=IMAX-IMIN+1
C     NBUBL           SIZE OF A LEX ARRAY
C                     NBUBL=NOBL*(NOBL+1)/2
C
C     INPUT AND       IMAGE READ IN FROM FILE (02).
C     OUTPUT
C
C     RETURNS         NORMAL AND ALTERNATE ERROR RETURNS
C
C     SUBPROGRAMS     INDEX
C     REQUIRED
C
C     CALLED BY       TXTMN
C
C     COMMENTS        FPLXIT WORKS FOR ALL SPATIAL DISTANCES.  IT DOES THIS
C                     BY HAVING NDIS+1 LINES OF IDATA IN CORE, WHERE NDIS
C                     IS THE SPATIAL DISTANCE PARAMETER.

```

```

C     SUBROUTINE FPLXIT(IDATI, IDATA, LEX1, LEX2, LEX3, LEX4, IPT,
1 IDENT, MM1, IMGNO, POLCT, IARRAY, IEV, IERR1)
C     DOUBLE INTEGER INT, LEX1, LEX2, LEX3, LEX4
C     DIMENSION IDATA(1, 1), LEX1(1), LEX2(1), LEX3(1), LEX4(1), IPT(1)
C     DIMENSION IDENT(20), IARRAY(1, 1, 1)

```

```

C     IDATA(NUMPPL, MM1), IPT(MM1)

```

```

C         STACK SUBROUTINE NAME IN ERROR STACK

```

```

C     CALL KDPUSH('FPLXI', 'T')

```

```

C         SET PARAMETERS

```

```

C     NUMPPL=IDENT(6)
C     NUMLIN=IDENT(7)
C     IMIN=IDENT(15)
C     IMAX=IDENT(16)
C     LEAST1=IMIN-1
C     NOBL=IMAX-LEAST1
C     NBUBL=NOBL*(NOBL+1)/2

```

```

C         INITIALISE THE LEX ARRAYS TO ZERO

```

```

C     DO 14 I=1, NBUBL

```

```
LEX1(I)=0
LEX2(I)=0
LEX3(I)=0
14 LEX4(I)=0
```

```
C
C
C CHECK IF SIZE OF IMAGE IS TOO SMALL,
C RELATIVE TO THE DISTANCE PARAMETER MM
C
```

```
MM=MM1-1
MM2=MM*2
IEV=-5011
IF(NUMPPL.LT.MM2.OR.NUMLIN.LT.MM2) GO TO 9999
```

```
C
C
C NUMPMM=NUMPPL-MM
C NUMLMM=NUMLIN-MM
```

```
C
C READ IN THE FIRST MM1 LINES OF THE IMAGE
C AND SET UP POINTERS
C
```

```
DO 110 IY=1,MM1
IPT(IY)=IY
CALL RREAD(IDATI,IARRAY,IMGNO,IY,1,IDENT,IEV,ERR1)
DO 111 LY=1,NUMPPL
111 IDATA(LY,IY)=IARRAY(1,1,LY)
110 CONTINUE
```

```
C
C
C SETTING UP POINTERS FOR THE FIRST AND
C LAST ROWS OF THE IMAGE ARRAYS
C
```

```
IST=IPT(1)
LST=IPT(MM1)
```

```
C
C GO THROUGH ALL BUT MM ROWS OF IMAGE
```

```
NOVFLO=131017
INT=3856347531
```

```
C
C NEXT=MM1+1
```

```
DO 105 LCNT = NEXT,NUMLIN
IF(RCM(INT).GT.PCLCT) GO TO 105
```

```
C
C SKIP LINES RANDOMLY BY USING RANDOM NUMBER
C GENERATOR RCM EXTERNAL FUNCTION
C
C
C
```

```
C
C GO THROUGH EACH ROW MM TIMES. THE FIRST
C SET OF MM COLUMNS ARE HANDLED SEPARATELY
C
```

```
DO 120 IRW=1,MM
```

ORIGINAL PAGE IS  
OF POOR QUALITY

IRM=IRW+MM

SET I, L, J AND K EQUAL TO THE  
(NORMALISED) VALUES OF GRAY TONES OF  
RESOLUTION CELLS IN POSITIONS A, B, C  
AND D AS IN THE DIAGRAM --

A C  
B D

WHERE A INITIALLY IS THE UPPER LEFT  
CORNER CELL. THE CELLS ARE A DISTANCE  
MM APART.

I=IDATA(IRW,IST)-LEAST1  
L=IDATA(IRW,LST)-LEAST1  
K=IDATA(IRM,LST)-LEAST1  
J=IDATA(IRM,IST)-LEAST1

PUT THE TWO DIMENSIONAL INFORMATION  
INTO ONE DIMENSIONAL FORM. THE FUNCTION  
NEEDED TO CONVERT A DOUBLE SUBSCRIBED  
ARRAY, IMM(X,Y), INTO A SINGLE  
SUBSCRIBED ARRAY, IMM(Z), IS OF THE  
FORM  $G(X) + F(Y)$ , WHERE  $G(X) = (X-1)*X/2$   
AND  $F(Y) = Y$ . THEREFORE

$$Z = (X-1)*X/2 + Y$$

THIS IS DONE IN THE PROGRAM BY THE  
EXTERNAL FUNCTION INDEX(X,Y).

SINCE THE ORDER OF OCCURRENCE OF THE  
GRAY TONES BELONGING TO A RESOLUTION  
CELL PAIR IS IMMATERIAL, THE ARRAYS ARE  
SYMMETRIC. WE LET THE LARGER OF THE TWO  
HAVE THE FIRST SUBSCRIPT, I. E., THE ARRAY  
IS STORED IN LOWER TRIANGULAR FORM. THE  
ORDER OF THE SUBSCRIPTING IS AS FOLLOWS --

IMM(1,1) = IMM(1),  
IMM(2,1) = IMM(2),  
IMM(2,2) = IMM(3),  
IMM(3,1) = IMM(4),

IMM(NOBL,NOBL) = IMM(NBUBL).

THE SCANNING PROCEDURE, THAT IS THE  
METHOD BY WHICH THE PAIRWISE COMPARISONS  
ARE MADE, IS DESCRIBED BELOW FOR THE  
GENERAL CASE.  
CONSIDER A RESOLUTION CELL WITH SPATIAL  
COORDINATES (M,N), AND CALL THIS CELL I.  
THE SCANNING OPERATION BEGINS IN THE  
UPPER LEFT HAND CORNER OF THE IMAGE AND  
IT THEN PROCEEDS BY COMPARING THE GRAY

TONE OF &I& WITH AT MOST FOUR GRAY TONES  
 OF ITS NEIGHBOURING RESOLUTION CELLS.  
 THAT &I& NEVER NEEDS TO CONSIDER MORE  
 THAN FOUR NEIGHBOURS CAN BE SEEN FROM  
 THE DIAGRAM OF THE SEARCH PATTERN SHOWN  
 BELOW --

```

      I J
      M L K
  
```

ON A GIVEN ITERATION, &I& WILL LOOK FIRST  
 AT ITS VERTICAL NEIGHBOUR (&L&), NEXT  
 AT ITS HORIZONTAL NEIGHBOUR (&J&), THIRD  
 AT ITS LOWER RIGHT NEIGHBOUR (&K&) AND  
 FOURTH AT ITS LOWER LEFT DIAGONAL  
 NEIGHBOUR (&M&). &I& THEN MOVES INTO  
 THE POSITION OF THE RIGHT RESOLUTION  
 CELL OF THE PREVIOUSLY SCANNED FIRST  
 ROW (THE POSITION OCCUPIED BY &J&).  
 THE OPERATION IS REPEATED UNTIL ALL  
 NEIGHBOURING PAIRS OF RESOLUTION CELLS  
 HAVE BEEN EXAMINED. THE PROCEDURE IS  
 FURTHER REPEATED FOR CELLS SKIPPED OVER  
 IF THE SPATIAL DISTANCE IS GREATER THAN  
 ONE, TILL ALL CELLS HAVE BEEN EXHAUSTED.

```

IL=INDEX(I, L)
  
```

COUNT VERTICALLY ADJACENT (90-DEGREE)  
 NEIGHBOUR

```

LEX1(IL)=LEX1(IL)+1
  
```

```

IJ=INDEX(I, J)
  
```

COUNT HORIZONTALLY ADJACENT (0-DEGREE)  
 NEIGHBOUR

```

LEX2(IJ)=LEX2(IJ)+1
  
```

```

IK=INDEX(I, K)
  
```

COUNT LEFT DIAGONALLY ADJACENT  
 (135-DEGREE) NEIGHBOUR

```

LEX3(IK)=LEX3(IK)+1
  
```

NOW ITERATE DOWN THE ROW

```

DO 130 N=IRM, NUMPMM, MM
  
```

```

NMM=N+MM
I=J
  
```

M=L  
L=K

J=IDATA(NMM, IST)-LEAST1  
K=IDATA(NMM, LST)-LEAST1

IL=INDEX(I, L)

COUNT VERTICALLY ADJACENT (90-DEGREE)  
NEIGHBOUR

LEX1(IL)=LEX1(IL)+1

IJ=INDEX(I, J)

COUNT HORIZONTALLY ADJACENT (0-DEGREE)  
NEIGHBOUR

LEX2(IJ)=LEX2(IJ)+1

IK=INDEX(I, K)

COUNT LEFT DIAGONALLY ADJACENT  
(135-DEGREE) NEIGHBOUR

LEX3(IK)=LEX3(IK)+1

IM=INDEX(I, M)

COUNT RIGHT DIAGONALLY ADJACENT  
(45-DEGREE) NEIGHBOUR

LEX4(IM)=LEX4(IM)+1

130 CONTINUE

COMPUTE THE LAST SET OF MM COLUMNS  
SEPARATELY

I=J  
M=L  
L=K

IL=INDEX(I, L)

COUNT VERTICALLY ADJACENT (90-DEGREE)  
NEIGHBOUR

LEX1(IL)=LEX1(IL)+1

IM=INDEX(I, M)

COUNT RIGHT DIAGONALLY ADJACENT  
(45-DEGREE) NEIGHBOUR

```

      LEX4(IM)=LEX4(IM)+1
C
120 CONTINUE
C
C
C      SHIFT THE POINTERS FOR THE TWO ARRAYS.
C      THIS IS DONE BY A CYCLIC ROTATION.
C      THE POINTER ARRAY IPT IS SUCH THAT AT ANY
C      TIME THE ITH LOCATION OF IPT CONTAINS
C      THE POINTER TO THE ITH POSITION OF THE
C      LINE IN IDATA OR JDATA ARRAY.  FOR
C      EXAMPLE, IF IPT(2)=4 THEN THE FOURTH LINE
C      OF THE PHYSICAL JDATA ARRAY IS ACTUALLY
C      THE SECOND LINE, AT THAT MOMENT.
C
      IF(LCNT.EQ.NUMLIN) GO TO 105
C
C      ROTATE IN A CYCLIC MANNER
C
      ITEMP=IPT(1)
      DO 135 IB=1,MM
135  IPT(IB)=IPT(IB+1)
      IPT(MM1)=ITEMP
C
C      SET UP THE POINTERS TO THE FIRST AND
C      LAST ROWS OF THE TWO IMAGE ARRAYS
C
      IST=IPT(1)
      LST=IPT(MM1)
C
C      READ IN A NEW LINE INTO THE IDATA ARRAY
C
      CALL RREAD(IDATA,IARRAY,IMGNO,LCNT,1,IDENT,IEV,ERR1)
      DO 112 LY=1,NUMPFL
112  IDATA(LY,LST)=IARRAY(1,1,LY)
      IF(LEX1(IL).GT.NOVFLO) GO TO 106
      IF(LEX2(IJ).GT.NOVFLO) GO TO 106
      IF(LEX3(IK).GT.NOVFLO) GO TO 106
      IF(LEX4(IM).GT.NOVFLO) GO TO 106
C
105 CONTINUE
      GO TO 108
106 IEV=-5010
      RETURN IERR1
C
C      THE LAST MM ROWS ARE COMPUTED SEPARATELY
C      DO LOOP TO GO THROUGH THE MM ROWS
108 DO 140 LR=1,MM
      ISR=IPT(LR+1)
C
C      DO LOOP TO GO THROUGH EACH ROW MM TIMES
      DO 142 IRW=1,MM
C
      I=IDATA(IRW,ISR)-LEAST1

```

ORIGINAL PAGE IS  
OF POOR QUALITY

```
DO LOOP TO WORK DOWN A ROW, COMPUTING  
THE 0-DEGREE NEIGHBOUR ONLY
```

```
DO 144 N=IRW, NUMPMM, MM  
NMM=N+MM  
J=IDATA(NMM, ISR)-LEAST1
```

```
IJ=INDEX(I, J)
```

```
COUNT HORIZONTALLY ADJACENT (0-DEGREE)  
NEIGHBOUR
```

```
LEX2(IJ)=LEX2(IJ)+1
```

```
144 I=J  
142 CONTINUE  
140 CONTINUE
```

```
DOUBLE THE DIAGONAL TO MAKE EVERYTHING  
COME OUT RIGHT
```

```
NOBL=IMAX-IMIN+1  
DO 12 I=1, NOBL
```

```
II=INDEX(I, I)
```

```
LEX1(II)=LEX1(II)*2  
LEX2(II)=LEX2(II)*2  
LEX3(II)=LEX3(II)*2  
12 LEX4(II)=LEX4(II)*2
```

```
CALL CLOSE(IDATI)  
CALL KDPOP  
RETURN
```

```
ERROR
```

```
9999 CALL CLOSE(IDATI)  
RETURN IERR1
```

```
END
```



C SUBPROGRAMS INDEX  
C REQUIRED

C CALLED BY TXTMN  
C

C SUBROUTINE FUNC1(LEX1, LEX2, LEX3, LEX4, FUNC, NBUBL, NOBL)  
C DOUBLE INTEGER FUNC, LEX1, LEX2, LEX3, LEX4

C DIMENSION LEX1(1), LEX2(1), LEX3(1), LEX4(1), FUNC(1, 4)

C FUNC(NBUBL, 4)

C NOW COMPUTE FUNC

C TO DETERMINE THE TOTAL NUMBER OF PAIRS IN A GIVEN DIRECTION  
C

C R1=0.  
C R2=0.  
C R3=0.  
C R4=0.

C DO 5 I=1, NOBL  
C DO 5 J=1, NOBL  
C IJ=INDEX(I, J)  
C TEMP=LEX1(IJ)  
C R1=R1+TEMP  
C TEMP=LEX2(IJ)  
C R2=R2+TEMP  
C TEMP=LEX3(IJ)  
C R3=R3+TEMP  
C TEMP=LEX4(IJ)  
C R4=R4+TEMP  
5 CONTINUE

C TO COMPUTE AVERAGE

C AVG1=0.  
C AVG2=0.  
C AVG3=0.  
C AVG4=0.

C DO 6 I=1, NOBL  
C DO 6 J=1, NOBL  
C IJ=INDEX(I, J)

C TEMP=LEX1(IJ)  
C AVG1=AVG1+TEMP\*TEMP  
C TEMP=LEX2(IJ)  
C AVG2=AVG2+TEMP\*TEMP  
C TEMP=LEX3(IJ)  
C AVG3=AVG3+TEMP\*TEMP

```
TEMP=LEX4(I,J)
AVG4=AVG4+TEMP*TEMP
CONTINUE
```

```
AVG1=AVG1/R1
AVG2=AVG2/R2
AVG3=AVG3/R3
AVG4=AVG4/R4
```

```
DO 7 I=1,NOBL
DO 7 J=I,NOBL
IJ=INDEX(I,J)
```

```
TEMP=LEX1(IJ)
FUNC(IJ,1)=(TEMP-AVG1)*1000./R1
TEMP=LEX2(IJ)
FUNC(IJ,2)=(TEMP-AVG2)*1000./R2
TEMP=LEX3(IJ)
FUNC(IJ,3)=(TEMP-AVG3)*1000./R3
TEMP=LEX4(IJ)
FUNC(IJ,4)=(TEMP-AVG4)*1000./R4
CONTINUE
```

```
RETURN
END
```

ORIGINAL PAGE IS  
OF POOR QUALITY

```

C
C
C PROGRAM          SUBROUTINE FUNC2
C TITLE
C
C PROGRAMMER      A. SINGH  OCTOBER 1972
C UPDATE         ROBERT M HARALICK  FEBRUARY 1974
C               GE MONAGHAN        OCTOBER 1974
C               CHIN-HUANG CHEN    FEBRUARY 22, 1975
C
C DOCUMENTEN-    A. SINGH
C TATION
C
C COMPUTER       ANY
C REQUIRED
C
C PROGRAM        FORTRAN IV
C LANGUAGE
C
C PURPOSE        FUNC2 COMPUTES THE GRADIENT ENTROPY FEATURE OF THE
C               IMAGE.
C
C METHOD          FUNC2 FIRST COMPUTES THE TOTAL NUMBER OF PAIRS FOR
C               EACH DIRECTION. THE GRADIENT ENTROPY COMPONENT IS
C                $\text{ALOG}(1. + \text{ABS}(I-J)) * \text{ALOG}(P(I, J))$ , WHERE THE PROBABILITY
C               IS  $P(I, J) = \text{LEXK}(IJ) / (\text{TOTAL NUMBER OF PAIRS FOR THE}$ 
C                $K \text{ LEX ARRAY})$ .  $IJ = \text{INDEX}(I, J)$ .
C
C CALLING        CALL FUNC2(LEX1, LEX2, LEX3, LEX4, FUNC, NBUBL)
C SEQUENCE
C
C ARGUMENTS      LEX1, LEX2, LEX3 AND LEX4 ARE THE FOUR TRIANGULAR
C               GRAY TONE MATRICES.
C               FUNC THIS IS A TWO DIMENSIONAL ARRAY WHERE THE
C               RESULTS OF SUBROUTINE FUNC2 ARE STORED.
C               THESE ARE STORED IN TRIANGULAR FORM LIKE
C               THE LEX ARRAYS. THE SECOND SUBSCRIPT
C               CORRESPONDS TO THE DIRECTION (K=1, 2, 3 OR 4
C               IS 90, 0, 135 OR 45 DEGREES RESPECTIVELY),
C               WHILE THE FIRST SUBSCRIPT,  $IJ = \text{INDEX}(I, J)$ ,
C               IS THE LOCATION OF THE GRAY TONE PAIR (I, J)
C               AS IN THE LEX ARRAYS.
C               NBUBL SIZE OF A LEX ARRAY
C                $\text{NBUBL} = \text{NOBL} * (\text{NOBL} + 1) / 2$ 
C
C PARAMETERS    NOBL NUMBER OF GRAY TONES
C AND ARRAYS    R1, R2, R3, R4 ARE THE RECIPRICAL OF THE TOTAL NUMBER
C               OF GRAY TONE PAIRS FOR EACH OF THE FOUR
C               DIRECTIONS.
C               RL1, 2, 3, 4 ARE THE PROBABILITIES  $P(I, J)$ , FOR THE
C               FOUR DIRECTIONS, FOR GRAY TONE I TO OCCUR
C               NEXT TO GRAY TONE J IN A PARTICULAR
C               DIRECTION.
C

```

```

C INPUT AND NONE
C OUTPUT
C RETURNS NO ERROR RETURNS
C SUBPROGRAMS INDEX
C REQUIRED
C CALLED BY TXTMN

```

```

C SUBROUTINE FUNC2(LEX1, LEX2, LEX3, LEX4, FUNC, NBUBL, NOBL)

```

```

C DOUBLE INTEGER FUNC, LEX1, LEX2, LEX3, LEX4
C DIMENSION LEX1(1), LEX2(1), LEX3(1), LEX4(1), FUNC(1, 4)

```

```

C FUNC(NBUBL, 4)

```

```

C NOW COMPUTE FUNC

```

```

C TO DETERMINE THE TOTAL NUMBER OF PAIRS IN A GIVEN DIRECTION

```

```

C R1=0
C R2=0
C R3=0
C R4=0

```

```

C DO 5 I=1, NOBL
C DO 5 J=1, NOBL
C IJ=INDEX(I, J)

```

```

C TEMP=LEX1(IJ)
C R1=R1+TEMP
C TEMP=LEX2(IJ)
C R2=R2+TEMP
C TEMP=LEX3(IJ)
C R3=R3+TEMP
C TEMP=LEX4(IJ)
C R4=R4+TEMP

```

```

C 5 CONTINUE

```

```

C TO GET R1, R2, R3, R4 TO SAVE DIVISIONS

```

```

C R1=1./R1
C R2=1./R2
C R3=1./R3
C R4=1./R4

```

TO COMPUTE ANGULAR MOMENTUM COMPONENT

```

C
C
C
C
DO 2 I=1,NOBL
DO 2 J =I,NOBL
IJ=INDEX(I,J)
TEMP=LEX1(IJ)
RL1=TEMP*R1
TEMP=LEX2(IJ)
RL2=TEMP*R2
TEMP=LEX3(IJ)
RL3=TEMP*R3
TEMP=LEX4(IJ)
RL4=TEMP*R4
FUNC(IJ,1)=ALOG(1.+ABS(FLOAT(I-J)))*ALOG(1.E-9+RL1)*200.
FUNC(IJ,2)=ALOG(1.+ABS(FLOAT(I-J)))*ALOG(1.E-9+RL2)*200.
FUNC(IJ,3)=ALOG(1.+ABS(FLOAT(I-J)))*ALOG(1.E-9+RL3)*200.
FUNC(IJ,4)=ALOG(1.+ABS(FLOAT(I-J)))*ALOG(1.E-9+RL4)*200.
C
2 CONTINUE
C
RETURN
END

```

CFUNC3

F-U-N-C-3

C  
C  
C PROGRAM SUPROUTINE FUNC3  
C TITLE  
C  
C PROGRAMMER A. SINGH OCTOBER 1972  
C UPDATE ROBERT M HARALICK FEBRUARY 1974  
C GE MONAGHAN OCTOBER 1974  
C CHIN-HUANG CHEN FEBRUARY 22, 1975  
C  
C DOCUMENTEN- A. SINGH  
C TATION  
C  
C COMPUTER ANY  
C REQUIRED  
C  
C PROGRAM FORTRAN IV  
C LANGUAGE  
C  
C PURPOSE FUNC3 COMPUTES THE ENTROPY FEATURE OF THE IMAGE.  
C  
C METHOD FUNC3 FIRST COMPUTES THE TOTAL NUMBER OF PAIRS FOR  
C EACH DIRECTION. THE ENTROPY COMPONENT IS THEN  
C  $-P(I, J) * \text{ALOG}(P(I, J))$ , WHERE THE PROBABILITY  $P(I, J)$   
C IS  $P(I, J) = \text{LEXK}(IJ) / (\text{TOTAL NUMBER OF PAIRS FOR}$   
C  $\text{THE K LEX ARRAY})$ .  $IJ = \text{INDEX}(I, J)$ .  
C  
C CALLING CALL FUNC3(LEX1, LEX2, LEX3, LEX4, FUNC, NBUBL)  
C SEQUENCE  
C  
C ARGUMENTS LEX1, LEX2, LEX3 AND LEX4 ARE THE FOUR TRIANGULAR  
C GRAY TONE MATRICES.  
C FUNC THIS IS A TWO DIMENSIONAL ARRAY WHERE THE  
C RESULTS OF SUBROUTINE FUNC3 ARE STORED.  
C THESE ARE STORED IN TRIANGULAR FORM LIKE  
C THE LEX ARRAYS. THE SECOND SUBSCRIPT  
C CORRESPONDS TO THE DIRECTION (K=1, 2, 3 OR 4  
C IS 90, 0, 135 OR 45 DEGREES RESPECTIVELY),  
C WHILE THE FIRST SUBSCRIPT,  $IJ = \text{INDEX}(I, J)$ ,  
C IS THE LOCATION OF THE GRAY TONE PAIR (I, J)  
C AS IN THE LEX ARRAYS.  
C NBUBL SIZE OF A LEX ARRAY  
C  $\text{NBUBL} = \text{NOBL} * (\text{NOBL} + 1) / 2$   
C  
C PARAMETERS NOBL NUMBER OF GRAY TONES  
C AND ARRAYS R1, R2, R3, R4 ARE THE RECIPRICAL THE TOTAL NUMBER  
C OF GRAY TONE PAIRS FOR EACH OF THE FOUR  
C DIRECTIONS.  
C R1, 2, 3, 4 ARE THE PROBABILITIES  $P(I, J)$ , FOR THE  
C FOUR DIRECTIONS, FOR GRAY TONE I TO OCCUR  
C NEXT TO GRAY TONE J IN A PARTICULAR  
C DIRECTION.  
C  
C INPUT AND NONE

ORIGINAL PAGE IS  
OF POOR QUALITY



```
TEMP=LEX1(IJ)
RL1 = TEMP*R1
TEMP=LEX2(IJ)
RL2 = TEMP*R2
TEMP=LEX3(IJ)
RL3 = TEMP*R3
TEMP=LEX4(IJ)
RL4 = TEMP*R4
```

C

```
IF(RL1.LT.0.000001) GO TO 31
FUNC(I,J,1) = (-RL1*ALOG(RL1))*200.
31 IF(RL2.LT.0.000001) GO TO 32
FUNC(I,J,2) = (-RL2*ALOG(RL2))*200.
32 IF(RL3.LT.0.000001) GO TO 33
FUNC(I,J,3) = (-RL3*ALOG(RL3))*200.
33 IF(RL4.LT.0.000001) GO TO 2
FUNC(I,J,4) = (-RL4*ALOG(RL4))*200.
2 CONTINUE
```

C

```
RETURN
END
```

ORIGINAL PAGE IS  
OF POOR QUALITY



```

C      INPUT AND      NONE
C      OUTPUT
C
C      RETURNS        NO ERROR RETURNS
C
C      SUBPROGRAMS    INDEX
C      REQUIRED
C
C      CALLED BY      TXTMN
C
C
C      SUBROUTINE FUNC4(LEX1, LEX2, LEX3, LEX4, FUNC, NBUBL, NOBL)
C      DOUBLE INTEGER FUNC, LEX1, LEX2, LEX3, LEX4
C
C      DIMENSION LEX1(1), LEX2(1), LEX3(1), LEX4(1), FUNC(1, 4)
C
C      FUNC(NBUBL, 4)
C
C      AF=1. /FLQAT(NBUBL)
C
C
C      NOW COMPUTE FUNC
C
C      TO DETERMINE THE TOTAL NUMBER OF PAIRS IN A GIVEN DIRECTION
C
C      R1=0.
C      R2=0.
C      R3=0.
C      R4=0.
C      DO 5 I=1, NOBL
C      DO 5 J=1, NOBL
C      IJ=INDEX(I, J)
C      TEMP=LEX1(IJ)
C      R1=R1+TEMP
C      TEMP=LEX2(IJ)
C      R2=R2+TEMP
C      TEMP=LEX3(IJ)
C      R3=R3+TEMP
C      TEMP=LEX4(IJ)
C      R4=R4+TEMP
C 5     CONTINUE
C
C      TO GET R1, R2, R3, R4 TO SAVE DIVISIONS
C
C      R1=1. /R1
C      R2=1. /R2
C      R3=1. /R3
C      R4=1. /R4
C
C      TO COMPUTE ANGULAR MOMENTUM COMPONENT
C
C      DO 2 I=1, NOBL
C      DO 2 J =I, NOBL
C      IJ=INDEX(I, J)

```

```
TEMP=LEX1(IJ)
TEMP=LEX2(IJ)
FUNC(IJ,1)=(ABS(FLOAT(I-J))/(AF+TEMP*R1))*200.
TEMP=LEX3(IJ)
FUNC(IJ,2)=(ABS(FLOAT(I-J))/(AF+TEMP*R2))*200.
TEMP=LEX4(IJ)
FUNC(IJ,3)=(ABS(FLOAT(I-J))/(AF+TEMP*R3))*200.
```

C

```
FUNC(IJ,4)=(ABS(FLOAT(I-J))/(AF+TEMP*R4))*200.
```

```
2 CONTINUE
```

C

```
RETURN
END
```

CFUNC5

F-U-N-C-5

PLEXIT QUANTIZING FUNCTION

PROGRAM TITLE: FUNC5  
VERSION: A  
DATE: NOVEMBER 23, 1973  
AUTHOR: ROBERT M HARALICK  
UPDATE: CHIN-HUANG CHEN 2/22/75  
DOCUMENTED BY: ROBERT M HARALICK  
IMPLEMENTED ON: PDF 15  
LANGUAGE: FORTRAN  
PURPOSE:

THIS SUBROUTINE PREPARES NORMALIZED LEX  
ARRAYS WHICH HAVE BEEN EQUAL PROBABILITY QUANTIZED ACCORDING  
TO THEIR DIAGONAL ELEMENTS AND PUTS THE RESULTS IN FUNC ARRAY.

ENTRY POINT: FUNC5(LEX1, LEX2, LEX3, LEX4, FUNC, NBUBL)

ARGUMENT LIST:

LEX1 IS VERTICAL CO-OCCURENCE MATRIX  
LEX2 IS HORIZONTAL CO-OCCURENCE MATRIX  
LEX3 IS 135 DEGREE CO-OCCURENCE MATRIX  
LEX4 IS 45 DEGREE CO-OCCURENCE MATRIX  
FUNC IS THE NORMALIZED AND QUANTIZED  
CO-OCCURENCE MATRICES  
FUNC(NBUBL, 4)  
NBUBL IS THE SIZE OF THE LEX ARRAYS

SUBROUTINE FUNC5(LEX1, LEX2, LEX3, LEX4, FUNC, NBUBL, NOBL)  
DOUBLE INTEGER FUNC, LEX1, LEX2, LEX3, LEX4, F

DIMENSION LEX1(1), LEX2(1), LEX3(1), LEX4(1), FUNC(1, 4), F(1)  
DATA INTVD /8/

CALL ADJ1(F, FUNC(1, 1))

CALL LEXEQP(LEX4, NOBL, INTVD, F)

DO 12 I=1, NBUBL  
12 FUNC(I, 4)=F(I)

CALL LEXEQP(LEX3, NOBL, INTVD, F)

DO 13 I=1, NBUBL  
13 FUNC(I, 3)=F(I)

CALL LEXEQP(LEX2, NOBL, INTVD, F)

DO 14 I=1, NBUBL  
14 FUNC(I, 2)=F(I)

CALL LEXEQP(LEX1, NOBL, INTVD, F)

RETURN  
DO 15 I=1, NBUBL

ORIGINAL PAGE IS  
OF POOR QUALITY

15    FUNC(I, 1)=F(I)  
      END

**ORIGINAL PAGE IS  
OF POOR QUALITY**

CLEXEQF

L-E-X-E-Q-F

EQUAL PROBABILITY QUANTIZE THE DIAGONAL OF THE LEX ARRAY

PROGRAM TITLE: LEXEQF  
VERSION: A  
DATE: NOVEMBER 23, 1973  
AUTHOR: ROBERT M HARALICK  
UPDATE CHIN-HUANG CHEN 2/22/75  
DOCUMENTED BY: ROBERT M HARALICK  
LANGUAGE: FORTRAN IV  
PURPOSE:

THIS SUBROUTINE EQUAL PROBABILITY QUANTIZES  
THE LEX ARRAY ON THE BASIS OF THE DIAGONAL ELEMENTS.

ENTRY POINT: LEXEQF(LEX, NOBL, INTVD, FUNC)

ARGUMENT LIST:

LEX IS THE LEX ARRAY  
NOBL IS THE NUMBER OF BRIGHTNESS LEVELS  
INTVD IS THE NUMBER OF DESIRED QUANTIZED  
LEVELS  
FUNC IS THE NORMALIZED AND QUANTIZED LEX  
ARRAY.

SUBROUTINE LEXEQF(LEX, NOBL, INTVD, FUNC)  
DOUBLE INTEGER FUNC, LEX

DIMENSION LEX(1), FUNC(1)  
COMMON /IO/NSIZE, F(16), FLQ(16), MEX(136), IT(176)

PUT CUMULATIVE DISTRIBUTION OF  
DIAGONAL ELEMENTS OF LEX ARRAY INTO F.

IF(INTVD.GT.16) INTVD=16

NSIZE=1024

NBUBL=NOBL\*(NOBL+1)/2

S=0

DO 1 I=1, NOBL

II=INDEX(I, I)

TEMP=LEX(II)

1 S=S+TEMP

S=1./S

TEMP=LEX(1)

F(1)=TEMP\*S

DO 2 I=2, NOBL

J=INDEX(I, I)

TEMP=LEX(J)

2 F(I)=F(I-1)+TEMP\*S



```
11 CONTINUE  
   FUNC(N)=TEMP*S*1000.  
   RETURN  
   END
```

**ORIGINAL PAGE IS  
OF POOR QUALITY**

CPLXIT

P-L-X-I-T

C

C

C

PROGRAM           SUBROUTINE PLXIT  
TITLE

C

C

PROGRAMMER        A. SINGH    NOVEMBER 872  
MODIFIED           5/14/73 ROBERT M HARALICK  
                   7/10/73  
                   2/2/74  
                   8/10/74 GE MONAGHAN  
                   10/10/74 RM HARALICK  
                   2/22/75 CHIN-HUANG CHEN

C

C

DOCUMENTATION     A. SINGH

C

C

COMPUTER           PDF 15  
REQUIRED

C

C

PROGRAM           FORTRAN IV  
LANGUAGE

C

C

PURPOSE           PLXIT COMPUTES THE JDATA IMAGE

C

C

METHOD           PLXIT COMPUTES THE JDATA IMAGE UTILISING THE RESULTS  
OF FPLXIT AND FUNC. LET G(I,J) BE THE GRAY LEVEL OF  
THE JTH RESOLUTION CELL IN THE ITH LINE OF THE  
CONSIDERED IMAGE (IDATA), AND LET V(I,J) BE THE JTH  
RESOLUTION CELL IN THE ITH LINE OF THE JDATA IMAGE.  
THEN --

C

C

$$V(I, J) = \text{FUNC}(G(I, J+L), G(I-L, J+L), G(I-L, J), G(I-L, J-L), \\ G(I, J-L), G(I+L, J-L), G(I+L, J), G(I+L, J+L)),$$

C

C

WHERE FUNC IS A FUNCTION (SUCH AS FUNC1, FUNC2 OR  
FUNC3) PROVIDED BY THE USER.

C

C

L = 1, 2, 3, ... IS THE  
SEPARATION BETWEEN CELLS. L=1, MEANS NEAREST  
NEIGHBOUR, L=2, MEANS NEXT TO NEAREST NEIGHBOUR ETC.  
PLXIT WORKS FOR ALL POSITIVE L.

C

C

ENTRY POINT        PLXIT(IDATI, IDATJ, IDATA, JDATA, IDENT, FUNC, IPT  
                   NBUBL, MM1, NXMIN, NXMAX, JIDENT, IEV, IERR1)

C

C

ARGUMENTS         IDATI        DAT SLOT WHERE ORIGINAL IMAGE RESIDES  
                   IDATJ        DAT SLOT FOR JDATA IMAGE  
                   IDATA        SCRATCH ARRAY WHERE THE ORIGINAL IMAGE IS  
                                  READ IN.  
                   JDATA        INTEGER ARRAY WHERE THE JDATA IMAGE IS  
                                  GENERATED AND STORED BEFORE BEING WRITTEN  
                                  ONTO THE TAPE (03).  
                   IDENT        IDENTIFICATION ARRAY OF IDATA  
                   JIDENT       IDENTIFICATION ARRAY OF JDATA  
                   FUNC         A TWO DIMENSION ARRAY CONTAINING THE

C

RESULTS OF THE EXTERNAL FUNCTION PROGRAM.  
 THE SECOND INDEX DETERMINES THE DIRECTION,  
 WHILE THE FIRST ONE CORRESPONDS TO THE  
 ELEMENT IN THE ASSOCIATED LEX ARRAY.  
 IPT ARRAY WHICH CONTAINS THE POINTERS FOR  
 THE IDATA AND THE JDATA ARRAYS  
 NBUBL SIZE OF A LEX ARRAY  
 NBUBL=NOBL\*(NOBL+1)/2, WHERE NOBL IS THE  
 NUMBER OF GRAY TONES.  
 MM1 SPATIAL DISTANCE + 1  
 NXMIN MINIMUM JDATA VALUE  
 NXMAX MAXIMUM JDATA VALUE  
 IEV INTEGER EVENT VARIABLE  
 IEV=-5011 IF NUMPPL OR NUMLIN IS LESS THAN  
 TWICE MM.

PARAMETERS NUMLIN NUMBER OF LINES IN THE IMAGE  
 AND ARRAYS NUMPPL NUMBER OF POINTS PER LINE IN THE INPUT IMAGE  
 IMAX LARGEST GRAY TONE ON INPUT FILE  
 IMIN LEAST GRAY TONE ON INPUT FILE  
 LEAST1 =IMIN-1. LEAST1 IS USED FOR NORMALIZING  
 THE GRAY TONES.  
 NOBL NUMBER OF GRAY TONES  
 NOBL=IMAX-IMIN+1

RETURNS NO ERROR RETURNS

SUBPROGRAMS INDEX  
 REQUIRED

CALLED BY TXTMN

COMMENTS PLXIT WORKS FOR ALL SPATIAL DISTANCES. IT DOES  
 THIS BY HAVING MM + 1 LINES OF IDATA IN THE CORE,  
 WHERE MM IS THE SPATIAL DISTANCE PARAMETER.

SUBROUTINE PLXIT(IDATI, IDATJ, IDATA, JDATA, IDENT, FUNC, IPT, NBUBL, MM1,  
 1 IMGNO, NXMIN, NXMAX, JDENT, IARRAY, IEV, IERR1)

DOUBLE INTEGER FUNC  
 DIMENSION IDATA(1, 1), JDATA(1, 1), FUNC(1, 1), IPT(1), IDENT(20)  
 DIMENSION JDENT(20), IARRAY(1, 1, 1)

IDATA(NUMPPL, MM1), JDATA(NUMPPL, MM1), FUNC(NBUBL, 4), IPT(MM1)

STACK SUBROUTINE NAME IN ERROR STACK

CALL KDPUSH('PLXIT', '')

SET PARAMETERS

ORIGINAL PAGE IS  
 OF POOR QUALITY



SET OF MM COLUMNS ARE HANDLED SEPARATELY

DO 120 IRW=1, MM

IRM=IRW+MM

SET I, L, J AND K EQUAL TO THE (NORMALISED) VALUES OF GRAY TONES OF RESOLUTION CELLS IN POSITIONS A, B, C AND D AS IN THE DIAGRAM --

A C  
B D

WHERE A INITIALLY IS THE UPPER LEFT CORNER CELL. THE CELLS ARE A DISTANCE MM APART.

I=IDATA(IRW, IST)-LEAST1  
L=IDATA(IRW, LST)-LEAST1  
K=IDATA(IRM, LST)-LEAST1  
J=IDATA(IRM, IST)-LEAST1

PUT THE TWO DIMENSIONAL INFORMATION INTO ONE DIMENSIONAL FORM. THE FUNCTION NEEDED TO CONVERT A DOUBLE SUBSCRIBED ARRAY, IMM(X,Y), INTO A SINGLE SUBSCRIBED ARRAY, IMM(Z), IS OF THE FORM  $G(X) + F(Y)$ , WHERE  $G(X) = (X-1)*X/2$  AND  $F(Y) = Y$ . THEREFORE  $Z = (X-1)*X/2 + Y$ .

THIS IS DONE IN THE PROGRAM BY THE EXTERNAL FUNCTION INDEX(X,Y).

SINCE THE ORDER OF OCCURRENCE OF THE GRAY TONES BELONGING TO A RESOLUTION CELL PAIR IS IMMATERIAL, THE ARRAYS ARE SYMMETRIC. WE LET THE LARGER OF THE TWO HAVE THE FIRST SUBSCRIPT, I. E., THE ARRAY IS STORED IN LOWER TRIANGULAR FORM. THE ORDER OF THE SUBSCRIPTING IS AS FOLLOWS -

IMM(1,1) = IMM(1),  
IMM(2,1) = IMM(2),  
IMM(2,2) = IMM(3),  
IMM(3,1) = IMM(4),

IMM(NOBL, NOBL) = IMM(NBUBL).

THE SCANNING PROCEDURE, THAT IS THE METHOD BY WHICH THE PAIRWISE COMPARISONS ARE MADE, IS DESCRIBED BELOW FOR THE GENERAL CASE.

CONSIDER A RESOLUTION CELL WITH SPATIAL

ORIGINAL PAGE IS  
OF POOR QUALITY

COORDINATES (M,N), AND CALL THIS CELL I. THE SCANNING OPERATION BEGINS IN THE UPPER LEFT HAND CORNER OF THE IMAGE AND IT THEN PROCEEDS BY COMPARING THE GRAY TONE OF &I& WITH AT MOST FOUR GRAY TONES OF ITS NEIGHBOURING RESOLUTION CELLS. THAT &I& NEVER NEEDS TO CONSIDER MORE THAN FOUR NEIGHBOURS CAN BE SEEN FROM THE DIAGRAM OF THE SEARCH PATTERN SHOWN BELOW --

```

      I J
      M L K
  
```

ON A GIVEN ITERATION, &I& WILL LOOK FIRST AT ITS VERTICAL NEIGHBOUR (&L&), NEXT AT ITS HORIZONTAL NEIGHBOUR (&J&), THIRD AT ITS LOWER RIGHT NEIGHBOUR (&K&) AND FOURTH AT ITS LOWER LEFT DIAGONAL NEIGHBOUR (&M&). &I& THEN MOVES INTO THE POSITION OF THE LEFT-MOST RESOLUTION CELL OF THE PREVIOUSLY SCANNED SECOND ROW (THE POSITION OCCUPIED BY &M&). THE OPERATION IS REPEATED UNTIL ALL NEIGHBOURING PAIRS OF RESOLUTION CELLS HAVE BEEN EXAMINED. THE PROCEDURE IS FURTHER REPEATED FOR CELLS SKIPPED OVER IF THE SPATIAL DISTANCE IS GREATER THAN ONE, TILL ALL CELLS HAVE BEEN EXHAUSTED.

IL=INDEX(I, L)

ADD FUNC(IL, 1) TO CENTER CELL AND  
90-DEGREE NEIGHBOUR

JDATA(IRW, IST) = JDATA(IRW, IST) + FUNC(IL, 1)  
JDATA(IRW, LST) = JDATA(IRW, LST) + FUNC(IL, 1)

IJ=INDEX(I, J)

ADD FUNC(IJ, 2) TO CENTER CELL AND  
0-DEGREE NEIGHBOUR

JDATA(IRW, IST) = JDATA(IRW, IST) + FUNC(IJ, 2)  
JDATA(IRM, IST) = JDATA(IRM, IST) + FUNC(IJ, 2)

IK=INDEX(I, K)

ADD FUNC(IK, 3) TO CENTER CELL AND  
135-DEGREE NEIGHBOUR

JDATA(IRW, IST) = JDATA(IRW, IST) + FUNC(IK, 3)  
JDATA(IRM, LST) = JDATA(IRM, LST) + FUNC(IK, 3)



L=K

IL=INDEX(I, L)

ADD FUNC(IL, 1) TO CENTER CELL AND  
90-DEGREE NEIGHBOUR

JDATA(NIM, IST) = JDATA(NIM, IST) + FUNC(IL, 1)

JDATA(NIM, LST) = JDATA(NIM, LST) + FUNC(IL, 1)

IM=INDEX(I, M)

ADD FUNC(IM, 4) TO CENTER CELL AND  
45-DEGREE NEIGHBOUR

JDATA(NIM, IST) = JDATA(NIM, IST) + FUNC(IM, 4)

JDATA(NI, LST) = JDATA(NI, LST) + FUNC(IM, 4)

120 CONTINUE

TO WRITE OUT THE COMPLETED LINE OF THE  
JDATA IMAGE

DO 699 J=1, MM

IXM=NUMPPL-J+1

JDATA(J, IST)=(JDATA(J, IST)\*8)/5

JDATA(IXM, IST)=(JDATA(IXM, IST)\*8)/5

699 CONTINUE

IF(LCNT.NE.1) GO TO 695

DO 694 J=1, NUMPPL

IARRAY(1, 1, J)=(JDATA(J, IST)\*5)/3

694 CONTINUE

GO TO 798

695 CONTINUE

DO 797 J=1, NUMPPL

IARRAY(1, 1, J)=JDATA(J, IST)

797 CONTINUE

798 CONTINUE

LINE=LCNT-MM1

CALL RWRITE(IDATJ, IARRAY, 1, LINE, 1, JDENT, IEV, ERR1)

DO 700 IXM=1, NUMPMM

IF(JDATA(IXM, IST).LT.NXMIN) NXMIN=JDATA(IXM, IST)

IF(JDATA(IXM, IST).GT.NXMAX) NXMAX=JDATA(IXM, IST)

700 CONTINUE

SHIFT THE POINTERS FOR THE TWO ARRAYS.  
THIS IS DONE BY A CYCLIC ROTATION.  
THE POINTER ARRAY IPT IS SUCH THAT AT ANY  
TIME THE ITH LOCATION OF IPT CONTAINS  
THE POINTER TO THE ITH POSITION OF THE

C LINE IN IDATA OR JDATA ARRAY. FOR  
C EXAMPLE, IF IPT(2)=4 THEN THE FOURTH LINE  
C OF THE PHYSICAL JDATA ARRAY IS ACTUALLY  
C THE SECOND LINE, AT THAT MOMENT.  
C

C IF(LCNT EQ. NUMLIN) GO TO 105  
C

C ROTATE IN A CYCLIC MANNER  
C

C ITEMP=IPT(1)  
C DO 135 IB=1,MM  
C 135 IPT(IB)=IPT(IB+1)  
C IPT(MM1)=ITEMP  
C

C SET UP THE POINTERS TO THE FIRST AND  
C LAST ROWS OF THE TWO IMAGE ARRAYS  
C

C IST=IPT(1)  
C LST=IPT(MM1)  
C

C READ IN A NEW LINE INTO THE IDATA ARRAY  
C

C CALL RREAD(IDATI, IARRAY, IMGNO, LCNT, 1, IDENT, IEV, ERR1)  
C DO 112 LY=1, NUMPFL  
C 112 IDATA(LY, LST)=IARRAY(1, 1, LY)  
C

C ZERO OUT THE LAST LINE OF THE JDATA ARRAY  
C

C DO 145 JJ=1, NUMPFL  
C 145 JDATA(JJ, LST)=0  
C

C 105 CONTINUE  
C

C THE LAST MM ROWS ARE COMPUTED SEPARATELY  
C

C DO LOOP TO GO THROUGH THE MM ROWS  
C

C ILINE=LINE  
C DO 140 LR=1,MM  
C 140 ISR=IPT(LR+1)  
C

C DO LOOP TO GO THROUGH EACH ROW MM TIMES  
C

C DO 142 IRW=1,MM  
C

C I=IDATA(IRW, ISR)-LEAST1  
C

C DO LOOP TO WORK DOWN A ROW, COMPUTING  
C THE 0-DEGREE NEIGHBOUR ONLY  
C

C DO 144 N=IRW, NUMPMM, MM  
C NMM=N+MM  
C J=IDATA(NMM, ISR)-LEAST1  
C

C I,J=INDEX(I, J)  
C



RETURN TERRI  
END

ORIGINAL PAGE IS  
OF POOR QUALITY



405 IF(IBOUT.NE.IOUT)WRITE(IBOUT,405) FDATE  
FORMAT(1X,3A5)  
RETURN  
END

ORIGINAL PAGE IS  
OF POOR QUALITY

CTXJDM

T-X-J-D-M

TEXTURE JDATA MAINLINE

PROGRAM TITLE: TXJDM  
 VERSION: A  
 AUTHOR: ROBERT M HARALICK  
 DATE: NOVEMBER 1974  
 UPDATE: FEBRUARY 1975  
 CHIN-HUANG CHEN  
 PROGRAM LANGUAGE: FORTRAN IV  
 IMPLEMENTED ON: PDP 15  
 PURPOSE:

THIS ROUTINE IS THE MAIN LINE FOR THE JDATA GENERATION  
 DISPLAY. INPUT PARAMETERS ARE FUNCTION TYPE, SPATIAL DISTANCE  
 RELATIONSHIP, ERROR MESSAGE OUTPUT, DAT SLOT, PERCENT OF LINES  
 COUNTED IN GENERATING THE FOUR NEIGHBOR GRAY TONE MATRICES,  
 INPUT FILE NAME, AND OUTPUT FILE NAME.

SUBROUTINES CALLED:

- TXINPT
- ERROR
- TXTMN
- SDKINL
- SKPDSC
- FPLXIT
- SREAD
- INDEX
- FUNC1
- FUNC2
- FUNC3
- FUNC4
- FUNC5
- EQPINT
- LEXEQP
- PLXIT
- INDEX
- SREAD

DOUBLE INTEGER NPPCAL, NTOTAL, FILNMP, FILNMQ  
 DIMENSION FILNMQ(2), FILNMP(2)  
 COMMON IWORK(8000), IWRK(7000)  
 COMMON /DFA/ NG, F(50)  
 COMMON /DFB/ AMEAN, VAR, NPPCAL, NTOTAL, START, END, NCALL, NNTERS, DANGE  
 COMMON /ID/ NSIZE, IDUM(2048)  
 COMMON /TXT/ ITXT(10)  
 DATA IOUT, IDATK, IDATQ, NDIM/6, 2, 1, 15000/  
 NSIZE = 1024

200 CONTINUE

GET INPUT PARAMETERS



CTXTMN

T-X-T-M-N

C

C PROGRAM SUBROUTINE TXTMN  
C TITLE

C

C PROGRAMMER MODIFIED BY A. SINGH, OCTOBER &72  
C MODIFIED FOR FDP BY ROBERT M HARALICK 5/1/73  
C 7/10/73  
C 2/2/74  
C 6/30/74  
C GE MONAGHAN 9/20/74  
C RM HARALICK 10/10/74  
C UPDATE CHIN-HUANG CHEN 2/22/75

C

C DOCUMENTATION A. SINGH, OCTOBER &72

C

C COMPUTER REQUIRED FDP-15

C

C PROGRAM LANGUAGE FORTRAN IV

C

C PURPOSE TXTMN IS THE MAINLINE SUBROUTINE FOR THE TEXTURE  
C ROUTINE PACKAGE TO COMPUTE THE JDATA IMAGE.

C

C METHOD TXTMN DOES THE FOLLOWING -  
C TAKES IN LABELS AND PARAMETERS FROM ARGUMENT LIST,  
C READS IN THE IMAGE FROM FILE (02),  
C SETS THE MAXIMUM AND MINIMUM GRAY LEVELS,  
C SETS UP DYNAMIC ALLOCATION OF PARAMETERS AND  
C CALLS THE REST OF THE SUBROUTINES.

C

C ENTRY POINT CALL TXTMN(IWORK,NDIM,S,T,NDIS,IFUNC,  
C NXMIN,NXMAX,PCLCT,IEV,ERR1)

C

C ARGUMENTS IWORK SCRATCH ARRAY WHERE THE IMAGE IS READ IN  
C AND THEN LATER IT IS USED FOR DYNAMIC  
C ALLOCATION.  
C NDIM SIZE OF SCRATCH ARRAY. NDIM SHOULD BE  
C EITHER NUMPPL\*NUMLIN OR  
C  $2*(M*(A+1)+1)+4*B*(B+1)$ , WHICH EVER ONE  
C IS LARGER.  
C A IS THE NUMBER OF POINTS/LINE IN THE  
C IMAGE, B IS THE MAXIMUM NUMBER OF GRAY  
C LEVELS POSSIBLE AND M IS THE LARGEST  
C REDUCTION DISTANCE THE PROGRAM WILL RUN  
C WITH.  
C S NAME OF FILE THE IMAGE IS ON  
C T NAME OF FILE WHERE THE JDATA IMAGE IS CREATED  
C NDIS SPACING BETWEEN NEIGHBORLY RESOLUTION CELLS  
C IFUNC PARAMETER USED TO DETERMINE WHICH FUNCTION  
C COMPUTES THE JDATA IMAGE.  
C IFUNC=1 FOR SUM PROBABILITY  
C IFUNC=2 FOR ANGULAR MOMENTUM FEATURE

IFUNC=3 FOR ENTROPY FEATURE  
 IFUNC=4 FOR GRADIENT FEATURE OF THE IMAGE  
 IFUNC=5 FOR NORMALIZED LEX ARRAY WHICH HAS BEEN  
 EQUAL PROBABILITY QUANTIZED  
 NXMIN IS THE MINIMUM ON THE JDATA IMAGE  
 NXMAX IS THE MAXIMUM ON THE JDATA IMAGE  
 PCLCT IS THE PERCENT OF LINES COUNTED  
 IEV INTEGER EVENT VARIABLE  
 ERR1 ALTERNATE ERROR RETURN

PARAMETERS  
AND ARRAYS

NUMLIN NUMBER OF LINES IN THE INPUT IMAGE  
 NUMPFL NUMBER OF POINTS PER LINE IN THE INPUT IMAGE  
 IMAX MAXIMUM GRAY LEVEL  
 IMIN MINIMUM GRAY LEVEL  
 LEAST1 =IMIN-1  
 NOBL NUMBER OF GRAY LEVELS  
 NBUBL =NOBL\*(NOBL+1)/2 IS THE SIZE OF A LEX ARRAY  
 NIDATA, NJDATA, NLEX1, 2, 3, 4, NFUNC AND NTOT ARE POINTERS  
 FOR DYNAMIC ALLOCATION IN IWORK.

INPUT AND OUTPUT

READ IN FROM FILE (OZ)  
 ERROR FOR INCORRECT SIZE OF IWORK,  
 ERROR IF PARAMETER IFUNC HAS BEEN  
 INITIALIZED INCORRECTLY.  
 INPUT IMAGE ON FILE CODE IDATI.  
 WRITES JDATA IMAGE ON FILE CODE IDATJ.

SUBPROGRAMS FPLXIT, FLXIT, INDEX, FUNC1, FUNC2, FUNC3, FUNC4, FUNC5  
 SEEK SYSTEM LIBRARY  
 CLOSE SYSTEM LIBRARY

REQUIRED

RETURNS NORMAL AND ALTERNATE  
 PROGRAM TERMINATED FOR INCORRECT  
 SIZE OF IWORK, ERROR IF IFUNC  
 INITIALISED INCORRECTLY.

CALLED BY MAIN LINE PROGRAM TXJDM

SUBROUTINE TXTMN(IWORK, NDIM, S, T, NDIS, IFUNC, NXMIN,  
 ZNXMAX, PCLCT, IEV, ERR1)

INTEGER ERR1  
 DOUBLE INTEGER FUNC  
 DOUBLE INTEGER FDATE, S, T, A, B  
 DOUBLE INTEGER LEX, C1, R1, CC1, RR1

DIMENSION IWORK(1), LEX1(1), LEX2(1), LEX3(1), LEX4(1), IDATA(1, 1), T(2)

ORIGINAL SOURCE  
 FILE NO. 4-177

```

DIMENSION IDENT(20), S(2), JDENT(20), FDATE(3)
DIMENSION JDATA(1, 1), IPT(1), FUNC(1, 1)
  DIMENSION CC1(8), RR1(8), LEX(13), C1(2), R1(2)

```

```

  IDATA(NUMPFL, MM1), JDATA(NUMPFL, MM1), LEX1(NBUBL), LEX2(NBUBL),
  LEX3(NBUBL), LEX4(NBUBL), IPT(MMAX), FUNCT(NBUBL, 4)

```

```

COMMON /TXT/ IMAX, IMIN, NUMPFL, NUMLIN, NBUBL, NOBL, LEAST1
DATA A, B, IZ, IONE, ITWO/'TXTMN', /, /, /, 0, 1, 2/
DATA IDATI, IDATJ/2, 3/
DATA LEX/'LEX ', 'ARRAY', 11*' / /
DATA C1, R1/'COL ', ' ', 'ROW ', ' / /
DATA CC1/'C1', 'C2', 'C3', 'C4', 'C5', 'C6', 'C7', 'C8' /
DATA RR1/'R1', 'R2', 'R3', 'R4', 'R5', 'R6', 'R7', 'R8' /

```

```

CALL KDPUSH(A, B)
CALL SDKINL(IDATI, S, IDENT, 1, IEV, ERR1)
NUMPFL=IDENT(6)
NUMLIN=IDENT(7)
IMIN=IDENT(15)
IMAX=IDENT(16)

```

```

LEAST1=IMIN-1
NOBL=IMAX-LEAST1
NBUBL=NOBL*(NOBL+1)/2

```

```

      SET DYNAMIC ALLOCATION PARAMETERS

```

```

      SINCE THE SIZE OF IDATA, JDATA AND IPT ARE DIFFERENT FOR DIFFERENT
      REDUCTIONS, THE MAXIMUM SPACE THEY WILL REQUIRE HAS TO BE
      RESERVED. IDATA AND JDATA THIS WILL BE (NDIS+1)*NUMPFL, AND FOR
      IPT JUST NDIS+1.

```

```

MM1=NDIS+1
NIDATA=1
NJDATA=NIDATA+NUMPFL*MM1
NLEX1=NJDATA+NUMPFL*MM1
NLEX2=NLEX1+NBUBL
NLEX3=NLEX2+NBUBL
NLEX4=NLEX3+NBUBL
NFUNC=NLEX1
NIPT=(NLEX4+NBUBL)*2
NTOT=NIPT+MM1

```

```

      CHECKING IF THE SIZE OF IWORK IS ENOUGH

```

```

IF(NTOT.GT.NDIM)GO TO 78
NBIG=NDIM-NTOT

```

ADJUST THE DIMENSIONS

```

CALL ADJ2(IDATA, IWORK(NIDATA), NUMPPL)
CALL ADJ2(JDATA, IWORK(NJDATA), NUMPPL)
CALL ADJ1(LEX1, IWORK(NLEX1))
CALL ADJ1(LEX2, IWORK(NLEX2))
CALL ADJ1(LEX3, IWORK(NLEX3))
CALL ADJ1(LEX4, IWORK(NLEX4))
CALL ADJ2(FUNC, IWORK(NFUNC), NBUBL)
CALL ADJ1(IPT, IWORK(NIPT))

```

ZERO OUT THE SCRATCH AREA

```

DO 30 JLK=1, NDIM
30 IWORK(JLK)=0

```

SKIP THE DESCRIPTOR RECORDS

```

CALL SKPDSC(IDATI, IDENT, IEV, ERR1)

```

COMPUTE THE FOUR LEX ARRAYS

```

CALL FPLXIT(IDATI, IDATA, LEX1, LEX2, LEX3, LEX4, IPT, IDENT, MM1,
ZPCLCT, IEV, ERR1)

```

WRITE OUT THE LEX ARRAYS

```

CALL IMTRXP(LEX1, 8, 8, 8, LEX, C1, R1, CC1, RR1, 4)
CALL IMTRXP(LEX2, 8, 8, 8, LEX, C1, R1, CC1, RR1, 4)
CALL IMTRXP(LEX3, 8, 8, 8, LEX, C1, R1, CC1, RR1, 4)
CALL IMTRXP(LEX4, 8, 8, 8, LEX, C1, R1, CC1, RR1, 4)

```

CALL PROPER FUNCTION SUBPROGRAM

```

IEV=-5011
IF(IFUNC.EQ.1) CALL FUNC1(LEX1, LEX2, LEX3, LEX4, FUNC, NBUBL)
IF(IFUNC.EQ.2) CALL FUNC2(LEX1, LEX2, LEX3, LEX4, FUNC, NBUBL)
IF(IFUNC.EQ.3) CALL FUNC3(LEX1, LEX2, LEX3, LEX4, FUNC, NBUBL)
IF(IFUNC.EQ.4) CALL FUNC4(LEX1, LEX2, LEX3, LEX4, FUNC, NBUBL)
IF(IFUNC.EQ.5) CALL FUNC5(LEX1, LEX2, LEX3, LEX4, FUNC, NBUBL)
IF(IFUNC.LE.0.OR.IFUNC.GE.6) RETURN ERR1
DO 79 I=1, 20
JDENT(I)=IDENT(I)
CONTINUE

```

```

JDENT(5)=10
JDENT(19)=1

```

```
JDENT(10)=3
JDENT(11)=512
JDENT(15)=-256
JDENT(16)=255
CALL CPYDSC(IDATI, S, IDATJ, T, JDENT, IEV, ERR1)
CALL ADATE(FDATE)
NW=JDENT(12)*2
WRITE(IDATJ) A, B, FDATE, S, (IZ, I=15, NW)
WRITE(IDATJ) IONE, (IZ, I=2, NW)
WRITE(IDATJ) ITWO, IFUNC, NDIS, (IZ, I=3, NW)
```

C

```
CALL PLXIT(IDATI, IDATJ, IDATA, JDATA, IDENT, FUNC, IPT, NBUBL, MM1,
2NXMIN, NXMAX, JDENT, IEV, ERR1)
```

```
4 CONTINUE
CALL KDPOP
RETURN
```

C

C

```
ERROR RETURN FOR NOT ENOUGH WORK SPACE
```

C

```
78 IEV=-5010
RETURN ERR1
```

C

```
END
```